Sand Dune Systems in Iran - Distribution and Activity.

Wind Regimes, Spatial and Temporal Variations of the Aeolian Sediment Transport in Sistan Plain (East Iran)

Dissertation Thesis

Submitted for obtaining the degree of

Doctor of Natural Science

(Dr. rer. nat.)

to the

Fachbereich Geographie

Philipps-Universität Marburg

by

M.Sc. Hamidreza Abbasi

Marburg, December 2019

Supervisor: Prof. Dr. Christian Opp

Physical Geography

Faculty of Geography

Phillipps-Universität Marburg

To my wife

and my son (Hamoun)

۱٤٥ - نقش : کتیبه ای با خط پهلوی متعلق به دوره ساسانی که قسمت روی آن کنده شده و در حال نابودی است.
محل : غرقاب گلپایگان عکاس : محمد ناصری فرد تاریخ : زمستان ۸۳
ترجمه توسط دکتر رسول بشاش رئیس پژوهشکده خط و گویش میراث فرهنگی - سه چیز را پاس بدارید . آب ، آتش و خاک

A picture of the rock painting in the Golpayegan Mountains, my city in Isfahan province of Iran, it is written in the Sassanid Pahlavi line about 2000 years ago:

"Preserve three things; water, fire, and soil"

Translated by: Prof. Dr. Rasoul Bashash, Photo: Mohammad Naserifard, winter 2004.

Declaration by the Author

I declared that this thesis is composed of my original work, and contains no material previously published or written by another person except where due reference has been made in the text. I have clearly stated the contribution by others to jointly-authored works that I have included in my thesis.

Hamidreza Abbasi

List of Contents

Abstract 1

1. General Introduction 7

1.1 Introduction and justification 7

1.2 Wind erosion in Iran 9

1.3 Problem statement 12

1.4 Thesis Aims and Objectives 13

1.5 Thesis structure 14

1.6 References 16

2. Physical Setting 19

2.1 Study area 19

2.2 Iran deserts 19

2.2.1 Climate 19

2.2.2 Deserts and sand dunes in Iran 21

2.3 Sistan Plain 25

2.3.1 Location 25

2.3.2 Climate 26

2.3.3 Geological setting 26

2.3.4 Sand transport and dunes 27

2.4 References 30

3. Methodology 33

3.1 Data and methods 33

3.2 Sand dunes activity 33

3.2.1 Climatic data 33

3.2.2 Sand transport calculations 34

3.3 Sand dunes activity 37

3.3.1 Sand dunes distribution 37

3.3.2 Sand dunes activity 37
3.4 Wind regime and sand transport in Sistan and Registan 42
3.5 Spatial and temporal variations of the aeolian transport in Sistan 43
3.6 Geostatistical analysis 45
3.7 References 47
4. Assessment of the Distribution and Activity of Dunes in Iran based on Mobility Indices and Ground Data 49
4.1 Introduction 50
4.2 Material and methods 55
4.3 Results 56
4.3.1 Spatial variability of sand drift potential 56
4.3.2 Lancaster mobility index 58
4.3.3 Tsoar mobility index 62
4.3.4 Yizhaq mobility index (YMI) 64
4.3.5 Comparison of the three models and development of a new model 66
4.4 Conclusions 72
4.5 References 74
5. Wind regime and sand transport in the Sistan and Registan regions (Iran/Afghanistan) 81
5.1 Introduction 82
5.2 Study area 83
5.3 Materials and methods 85
5.4 Results and discussion 86
5.4.1 Wind velocity 86
5.4.2 Wind direction 89
5.5 Spatial variability of Sand transport 91
5.6 Temporal variability of Sand transport 93
5.7 Morphology of dunes 96
5.8 Conclusion 98
5.9 References 100
6. Spatial and temporal variation of the aeolian sediment transport in the ephemeral Baringak Lake (Sistan Plain, Iran) using field measurements and geostatistical analyses 104

6.1 Introduction 105
6.2 Research Area 106
6.3 Material and methods 108
6.4 Results and discussion 110
6.4.1 Wind data analysis and wind erosion events 110
6.4.2 Aeolian sediment transport.....113
6.4.3 Geostatistical analysis.....113
6.4.4 Mapping of the aeolian sediment transport 116
6.5 Conclusion 117
6.6 References.....119
7. Final conclusion.....123
7.1 Conclusion 123
7.2 References.....130
Appendix A: 133

List of Tables

Table 2.1 Size and distribution of Iran and the world's arid lands 20
Table 2.2 Distribution of sand dunes in Iran's provinces 21
Table 2.3 Distribution and artificial fixation sand dunes in Sistan.....28
Table 3.1 Frequency of wind in different directions and wind speed classes in Zabol Station 34
Table 3.2 Derivation of weighting factors for relative rate of sand transport.....35
Table 3.3 The classification of wind energy environments.....36
Table 4.1 Important sand seas and dune fields in Iran 51
Table 4.2 Sand Dune Mobility Models 53
Table 4.3 Comparison of the three sand dune activity models 67
Table 4.4 A summary of present conditions of dune activity in Iran 70
Table 5.1 The classification of wind energy environments using drift potential 86
Table 5.2 A summary of the wind velocity parameters from Sistan and Registan desert 88
Table 5.3 A summary of annual percentage of the two main wind direction. 90
Table 5.4 Summary of annual mean of sand drift parameters in Sistan and Registan desert.....91
Table 6.1 Area, average depth and location of the six Sistan Plain Lakes.....106
Table 6.2 General characteristics of wind erosion events 112
Table 6.3 Summary statistics of the average transport rates in the Baringak study area 113
Table 6.4 Results of the cross variogram analysis and the fitted models for sediment.....114
Table 6.5 Validation of the kriging interpolation for the sediment transport rates.....116

List of Figures

Fig. 1.1 A schematic of the modes of sediment transport by the wind 8
Fig. 1.2 The distribution of dust storms (visibility <1000 meters) in south-west Asia 10
Fig. 1.3 Numbers of days with sand and dust storms in Abadan Khuzestan and Sistan 10
Fig. 1.4 The PM_{10} and $PM_{2.5}$ concentrations in the most polluted cities in the world 11
Fig. 1.5 A dusty day in Zabol city, Sistan, Iran 11
Fig. 1.6 Flow chart of the thesis structure 14
Fig. 2.1 climate zoning in Iran 19
Fig. 2.2 Distribution of sand dunes and weather stations in Iran 23
Fig. 2.3 Impressions of the sand dunes in Iran 24
Fig. 2.4 Hirmand Basin and Hamouns complex Lakes 25
Fig. 2.5 The location of six ephemeral Lakes; Hydrology systems; Erosive corridors 27
Fig. 2.6 Active sand dunes in Sistan region and Lut desert 28
Fig. 2.7 Shifting dunes impacts in Sistan 29
Fig. 3.1 Sand rose of Zahedan climatological station 37
Fig. 3.2 Sand dune mobility classification graph Lancaster's index 39
Fig. 3.3 Sand dune mobility classification graph Tsoar index 40
Fig. 3.4 A key of sand dune mobility classification graph Yizhaq model 42
Fig. 3.5 Morphological Classification of Dunes 43
Fig. 3.6 The location of study area, erosion pins and sand transport direction 44
Fig. 3.7 The general view of the dried bed Hamoun-e Baringak Lake and erosion pin 45
Fig. 3.8 An example of typical variogram and its important parameters 46
Fig. 4.1 Sand dunes distribution and location of meteorological stations used in this study 54
Fig. 4.2 Annual drift potential at selected meteorological stations near sand dunes in Iran 57
Fig. 4.3 Spatial variations of sand drift potential in Iran's deserts 58
Fig. 4.4 Sand dune activity in Iran's deserts based on Lancaster's mobility index 60
Fig. 4.5 Dune field mobility in Iran's deserts based on Lancaster's index 61

Fig. 4.6 Dune field mobility in Iran’s deserts based on Tsoar's index.....62
Fig. 4.7 Sand dune activity in Iran’s deserts based on Tsoar's index.....63
Fig. 4.8 Dune field mobility index values in Iran’s deserts based on Yizhaq model 64
Fig. 4.9 Sand dune activity in Iran based on the Yizhaq model 65
Fig. 4.10 Relation between sand drift potential and the percent time wind above transport.....69
Fig. 4.11 Dune mobility index values based on the Modified Lancaster Index in Iran 71
Fig. 4.12 Sand dune activity in Iran based on the Modified Lancaster Index 72
Fig. 5.1 the location of Sistan and Registan desert 84
Fig. 5.2 Map of the annual mean wind velocities in the Sistan and Registan deserts.....87
Fig. 5.3 Monthly average of mean wind velocity in Sistan and Registan 88
Fig. 5.4 Annual wind roses in Sadobist Roozeh wind domain.....90
Fig. 5.5 Sand roses for the Sadobist Roozeh wind domain 92
Fig. 5.6 The spatial distribution of DP in the Sadobist Roozeh wind domain 93
Fig. 5.7 Temporal variability of Sand transport characteristics in study area.....95
Fig. 5.8 Average monthly of DP, RDD, RDP and RDP/DP in the study area.....97
Fig. 5.9 Map of dune types in Sistan and Registan Sand Sea.....98
Fig. 6.1 Location of the Hamouns (ephemeral lakes) in the Sistan plain 107
Fig. 6.2 NDVI for the Sistan Region derived from Landsat-8 ETM + images 109
Fig. 6.3 Graduated erosion pin and indicators of the wind energy in the Baringak Lake 110
Fig. 6.4 Annual and seasonal wind roses for the Zabol Meteorological Station.....111
Fig. 6.5 Maximum daily wind speed at the Zabol meteorological station in 2013.....112
Fig. 6.6 Aeolian sediment transport rate variograms.....115
Fig. 6.7 Erosion pin locations and sediment transport rate.....117

Acknowledgment

Firstly, I especially would like to express my deepest gratitude and appreciation to my supervisor, Prof. Christian Opp for his invaluable help, dedicated efforts, guidance and patience throughout this study.

I am particularly grateful to Dr. Michael Groll for his kind assistance, knowledge and advice in Marburg University.

Many thanks also, to my friends for their moral support and most of all, their invaluable friendship in Research Institute Forests and Ranglands, Iran.

Finally, I would like to express my deepest love and gratitude to my family members for their unending prayers, support and encouragement during the course of this study.

Published Works by the Author Incorporated into the Thesis

Papers:

Publication 1: Included as Chapter 4

Abbasi H.R., Opp C., Groll M., Rohipour H., Gohardoust A., 2019. Sand Dunes System in Iran; Distribution and Activity, Aeolian research 41, December 2019, 100539 (in print).

https://doi.org/10.1016/j.aeolia.2019.07.005

Publication 2: Included as Chapter 5

Abbasi H.R., Opp C., Groll M., Gohardoust A., 2018. Wind regime and sand transport in the Sistan and Registan regions (Iran/Afghanistan), Zeitschrift für Geomorphologie, 62(Suppl.1), 041-057.

Publication 3: Included as Chapter 6

Abbasi H.R., Opp C., Groll M., Rohipour H., Khosroshahi M., Khaksarian F., Gohardoust A., 2018. Spatial and temporal variations of the aeolian sediment transport in the ephemeral Baringak Lake (Sistan Plain, Iran) using field measurements and geostatistical analyses, Zeitschrift für Geomorphologie, 61/4: 315-326.

Conference Contribution:

Abbasi H.R, Opp C., Groll M., Rouhipoor H., Gohardoost A., 2018. A comparison of general models of activity of sand dunes in Iran, the tenth International Conference on Aeolian Research (ICAR-X), 25-29 June, Bordeaux, France.

Abbasi H.R, Opp C., Groll M., Rouhipoor H., Gohardoost A., 2016. Wind regime and sand transport in Sistan and Registan desert, Oral presentation, Marin desert conference, 2-3 February, Rauischholzhausen, Germany.

Abbasi H.R, Opp C., Akavan R., Khaksarian F, Gohardoost A., 2015. Temporal and spatial variability of wind erosion in Sistan's Baringak Hamoun Lake, oral presentation, Marin desert conference, 12-13 February, Rauischholzhausen, Germany.

Abbasi H.R., Opp C., Khosroshahi M., Rouhipoor H., Bandage schafi S, Seyed Akhlaghi S.J., 2015. Wind regime and sand transport in Iran's sand sea systems, Poster presentation, Marin desert conference, 12-13 February, Rauischholzhausen, Germany.

Abbasi H.R, Opp C., 2014. Identification of the sensitivity areas to wind erosion in the Sistan Province (Hamouns Lakes), oral presentation, the Eight International Conference on Aeolian Research (ICAR-IIX), 21-25 July, Lanzhou, China.

Abbasi H.R., Opp C., Khosroshahi M., Rouhipoor H., Kashki M.T., Dashtakian k.,2014. Investigation of dune systems in Iran for a digital database and atlas of sand seas and dune fields, The Eight International Conference on Aeolian Research (ICAR-IIX), 21-25 July, Lanzhou, China.

Abbasi H.R., Opp C., Khosroshahi M, Gohardoost A.,2014, The role of playas for sand dunes formation in Iran, International Symposium on Losses, Soil and climate Change in Southern Eurasia,15-19 October, Gorgan, Iran.

Abbreviation:

No.	Abbreviation	Meaning
1	SDS	Sand and dust storms
2	DP	Sand drift potential
3	RDD	The resultant drift direction
4	RDP	The resultant drift potential
5	%W	The percentage of winds above threshold
6	M or MI	Mobility index
7	LMI	Lancaster mobility index
8	TMI	Tsoar mobility index
9	YMI	Yizhaq mobility index
10	MLI	Modified Lancaster index
11	PET	The annual potential evapotranspiration
12	P	Precipitation
13	LLJ	Low level jets
14	NDVI	Normalized difference vegetation index
15	DEM	Digital elevation models
16	IRNA	Islamic Republic News Agency
17	bln	Billion
18	VU	Vector unit
19	A	Active dunes
20	S.A	Stabilized and active
21	A.I.S	Active dunes, interdunes stabilizes
22	C.A	Crest active
23	S	Inactive and stabilized dunes
24	$PM_{2.5}$	Particle matter less than 2.5 micrometers
25	PM_{10}	Particle matter less than 10 micrometers
26	DEM	Digital elevation model
27	IMO	Iran meteorological organization

Abstract

Wind erosion and shifting sand dunes as a land degradation process is a serious problem in Iran. There are significant gaps in our knowledge of Iran sand dunes in national scale for the English speaking international scientific community as well as wind erosion and sand transport in Sistan plain. Identifying active dunes and monitoring areas with migrating sand are important prerequisites for mitigating these damages. In addition, wind erosion is one of the most serious problems in the Sistan region, located in the East of Iran and near the border of Afghanistan.

This thesis has two major purposes: (1) to assess sand dune activity in national scale of Iran (2) to investigate wind regime and investigated spatial and temporal patterns of wind erosion process in Sistan region. With regard to first objective, the spatial variation of the wind energy environment based on the sand drift potential (DP), with using Fryberger and Dean's (1979) method, was calculated from 204 meteorological stations in and around Iran's deserts. Three commonly dune activity models – the Lancaster mobility index (1988), the Tsoar mobility index (2005), and the index developed by Yizhaq et al. (2009) – were used for the evaluation of Iran's sand dune activity.

The analysis of the indices showed that the dunes activity was characterized by great spatial variations across Iran's deserts. All three models identified fully active dunes in the Sistan plain, the whole of the Lut desert, as well as in the Zirkuh Qaien and Deyhook regions, while the dunes in the northern part of Rig Boland, Booshroyeh and in the Neyshabor dunefields were categorized as stabilized dunes. For other dunes, the models show a less unified activity classification, with the Lancaster and Yizhaq models having more similar results while the Tsoar model stands more apart. Overall the three models delivered comparable results in some instances and diverging results in others. The reasons for this are the use of different parameters and their impact on the model construction. The main contradictions of the three models results are revealed when the wind blows for only short times but with a high energy, like in the north of the Dasht-e Kavir desert (Damagan, Foromad) and at some stations in the wind of the 120 days' domain (Sedeh Birjand). Field observation demonstrated that dunes in these areas are completely active, but the Lancaster mobility index (LMI) classified them as inactive or semi-active because of a low to moderate percentage of wind events above the transport threshold. At the same time the DP in this region showed high values and thus the Tsoar mobility index (TMI) classified the dunes as active, while the Yizhaq model (YMI) classified them as active or semi-active. In fact, in spite of high wind energy, the percentage of winds above threshold (W%), that is upper 12 knot or 6.2 m s-1 in this study, was rather low, as high speed winds only occur during the warm season, while the rest of the year is characterized by calm weather. The nature of the wind power parameter varies from the LMI, that is the percentage of winds above threshold (W%) to the TMI and YMI that is DP. DP reflects the quantity (frequency) and quality (intensity) of the wind power, but W% only shows its quantity (frequency of winds above the transport threshold). It seems that if DP was used in the LMI instead of W%, it would provide more favourable results. In addition, the statistical analysis (correlation coefficient) between DP values and the percentage of wind events above the transport threshold (%W) at the meteorological stations in the study area shows a moderate correlation.

Based on this argumentation, W% has been replaced by the DP (vu) as the wind energy parameter in Lancaster mobility index (1988) and a Modified Lancaster Index (MLI) was developed. Based on these model results and fields observations, a modified Lancaster mobility index has been applied to show a more realistic spatial variation of sand dunes activity in Iran's desert areas.
With regard to second objective, the wind regime, formation of aeolian dunes and the rate of sand transport in Sistan and Registan were investigated. The Sistan region in eastern Iran and the Registan region in South-western Afghanistan are strongly influenced by the Sadobist Roozeh wind (the wind of the 120 days), which is blowing along the Iran-Afghanistan border from North to South, then shifts it's direction toward the Southeast into the Sistan region and, finally, continues eastward into south-western Afghanistan, forming the Registan sand seas. It blows during the hot season due to the pressure gradient between the Turkmenistan High and the Pakistan Low. In order to determine the wind regime and the sand transport, wind roses based on long-term datasets from 16 meteorological stations, DP, the Resultant Drift Direction (RDD), the Resultant Drift Potential (RDP) and the RDP/DP ratio have been calculated using Fryberger and Dean's (1979) method. The distribution of the Registan sand dunes was surveyed by using Landsat ETM data, Google Earth scenes and field operations (the latter only in the Iranian part). The spatial differences of the drift potential were simulated using GIS and geostatistical methods overlaying the sand dune map. The results show that DP increases from north to south along the border between Iran and Afghanistan and reaches to highest values in the Sistan region, then decreases gradually in the Registan sand seas. The highest wind energy, based on DP matches, was determined exactly where the ephemeral lakes in the northern part of the Sistan plain are located, which function as a source area of intense dust and sand storms during the dry season. The annual DP calculated in Sistan is one of the highest values (2516 vector units) in inland desert and categorized it into the windiest desert in the world. The temporal trend of the DP showed an increase between 1999 and 2007, followed by a decrease until 2015 in Sistan. The results show that the wind regime in the Sistan and Registan regions is unimodal during the wind of 120 days (the Sadobist Roozeh) period, which is also supported by the dominance of transverse, barchanoid and barchans dunes in both regions.

In continue second objective, we measured the rate of sediment transport in Hamoun-e Baringak, as one of the six ephemeral lakes, producing more aeolian sediment into the atmosphere in Sistan region. In order to investigate the land surface sensitivity to aeolian transport, 74 graduated pins were embedded randomly in the ephemeral Baringak Lake bed and the aeolian transport rates were measured for three events in 2013 individually as well as for the total study period. The spatial and temporal variation of the aeolian transport was also mapped using GIS and geostatistics methods for these events and for the total duration of 103 days. The resulting variogram revealed a high spatial dependence of the different events and showed that geostatistical techniques are a valid tool for the mapping of aeolian sediment transport. The average transport rate in terms of the detected drift height on the dry lake bed was 1.93 cm or 31 kg/m2 between the 5th of August and the 17th of November in 2013.

Zusammenfassung

Winderosion sowie aktive Sanddünen sind charakteristische Phänomene und Begleiterscheinungen der Landdegradation. Sie sind im Iran weit verbreitet. Die Kenntnisstanddefizite über Sanddünenbewegungen im Iran und über Winderosion sowie äolischen Transport im Gebiet der Sistan Plains (Ost-Iran) sind insbesondere in der englischsprachigen Literatur beträchtlich. Kenntnisse über aktive Dünenbewegung und das Monitoring von äolischen Transportprozessen sind aber eine Voraussetzung für Strategien zur Schadensvermeidung. Winderosion ist eines der bedeutendsten Probleme der Sistan Region im Osten vom Iran an der Grenze zu Afghanistan.

Die Dissertation verfolgt zwei Hauptziele: 1) Bewertung der Sanddünenaktivität auf der nationalen Ebene des Iran; 2) Analyse des Windregimes sowie der raum-zeitlichen Muster der Winderosion in der Sistan Region.

Bezüglich des ersten Ziels wurde die räumliche Variabilität des Windenergieumfeldes mittels der Methode von Fryberger & Dean (1979) ermittelt, basierend auf dem Sanddrift-Potential (DP), sowie Daten von 204 meteorologischen Stationen in den Wüsten des Irans und in deren Umfeld. Zur Bewertung der Sanddünenaktivität im Iran wurden drei weit verbreitete Dünen-Modelle genutzt: der Lancaster Mobilitäts-Index (1988), der Tsoar Mobilitäts-Index (2005) sowie ein von Yizhaq et al. (2009) vorgestellter Index.

Die Anwendung und Auswertung der Index-Ermittlungen hat gezeigt, dass die Dünengebiete des Iran große Unterschiede bezüglich der Mobilität aufweisen. Durch alle drei Modelle konnte nachgewiesen werden, dass das Gebiet Sistan Plain, die gesamte Wüste Lut sowie die Zirkuh Qaien und Deyhook Regionen vollständig aktive Dünen aufweisen, während die Rig Boland, Booshroyeh dnd die Neyshabor Dünenfelder im nördlichen Iran als stabilisierte Dünen gekennzeichnet werden konnten. Für andere Dünenfelder konnte eine wenig einheitliche Zuordnung zu den Dünenaktivitätsklassen ermittelt werden. Während die Einstufung mit dem Lancaster Mobilitäts-Index und mit dem Yizhag Mobilitäts-Index eher ähnliche Ergebnisse ergab, wichen die Ergebnisse, die mit dem Tsoar Mobilitäts-Index ermittelt worden, davon ab.

Insgesamt konnten mit diesen Modellen vergleichbare Ergebnisse erzielt werden; in einigen Fällen wurden aber auch voneinander abweichende Resultate ermittelt. Die Ursachen dafür liegen in den verwendeten Parametern und deren Einfluss auf die Modellberechnungen zu Grunde. Heterogene Modell-Ergebnisse wurden berechnet, wenn der Wind nur geringe Zeit andauerte, aber mit hoher Energie blies, wie z.B. im Norden der Dasht-e Kavir Wüste (Damagan, Foromad) und an einigen Stationen (Sedeh Birjand) im Einflussbereich des sog. 120-Tage-Winds. Im Rahmen zahlreicher Geländeaufenthalte konnten Dünen in diesen Gebieten als aktiv gekennzeichnet werden, während sie mittels des Lancaster-Indices (LMI) als nicht aktiv bzw. semi-aktiv hätten eingestuft werden müssen, aufgrund von einem geringen oder nur moderaten Anteil von Windereignissen über dem Transportgrenzwert. Zugleich wurden für diese Gebiete hohe Driftpotentiale ermittelt, und mit dem Tsoar Mobilitäts-Index (TMI) wurden diese Dünengebiete als aktiv eingestuft, während die

Einstufung mit dem Yizhag-Modell (YMI) aktive und semi-aktive Dünen ergab. Trotz hoher Windenergie war der Anteil der Winde, die den Grenzwert (W%) von 12 Knoten oder 6,2 m/sec überschreiten, relativ gering, da Hochgeschwindigkeitswinde nur in der warmen Jahreszeit vorkommen; denn das übrige Jahr herrscht dort Kalmwetter vor. Die Windenergieparameter sind von Modell zu Modell (LMI) (W%), TMI und YMI (DP) unterschiedlich. Das Driftpotential (DP) reflektiert die Quantität (Häufigkeit) und Qualität (Intensität) der Windenergie, während W% nur die Quantität (Windhäufigkeit über den Transportgrenzwert) beschreibt. Wenn DP im LMI anstelle von W% benutzt wird, lassen sich damit wahrscheinlich noch bessere Ergebnisse erzielen. Durch Statistische Analysen (Korrelationskoeffizienten) zwischen den DP-Werten und dem Prozentanteil von Windereignissen über dem Transportgrenzwert konnte für die meteorologischen Stationen des Untersuchungsgebietes eine moderate Beziehung nachgewiesen werden.

Basierend auf diesen Erkenntnissen wurde zunächst W% durch das DP (vu) ersetzt und als Windenergieparameter im Lancaster Mobilitäts-Index (1988) genutzt sowie anschließend ein **M**odifizierter **L**ancaster **I**ndex (MLI) entwickelt. Basierend auf diesen Modellergebnissen und Feldbeobachtungen konnte ein Modifizierter Lancaster Mobilitäts-Index zur Anwendung kommen. Dadurch war es möglich, ein eher realistisches Ergebnis der räumlichen Differenzierung der Sanddünenaktivität für die Wüsten des Irans aufzuzeigen.

Mit Bezug auf das zweite Ziel wurden die Windregime, die Dünenbildung und die Transportraten für die Gebiete Sistan und Registan ermittelt. Sowohl das Sistan Gebiet im Ost-Iran als auch das Registan Gebiet in SW Afghanistan werden sehr stark durch den Sadobist Roozeh Wind (120-Tage-Wind) beeinflusst. Dieser bläst zunächst entlang der Iranisch-Afghanischen Grenze von Nord nach Süd, dann wechselt er die Windrichtung nach SW in das Sistan Gebiet, um schließlich nach Osten, nach SW-Afghanistan, umzubiegen, wo er die Registan Dünenfelder speist. Dieser Wind weht während der warmen Jahreszeit aufgrund eines Druckgradienten zwischen dem Turkmenistan-Hoch und dem Pakistan-Tief.

Um die Windregime und den Sandtransport bestimmen zu können, wurden basierend auf langjährigen Datenreihen von 16 meteorologischen Stationen Windrosen erstellt, DP, die Resultant Drift Direction (RDD), das Resultant Drift Potential (RDP) und das RDP/DP Verhältnis unter Nutzung der Fryberger & Dean's (1979) Methode errechnet. Die Verbreitung des Registan Sanddünenfeldes wurde mittels Landsat ETM Daten, Google Earth Szenen und Geländeaufnahmen (Letztere nur im Iranischen Teil) erkundet. Angaben über die räumliche Differenzierung des Driftpotentials konnten unter Nutzung von GIS und geostatistischen Methoden durch Datenüberlagerung auf der Sanddünenkarte erarbeitet werden. Die Resultate zeigen, dass DP sich von Nord nach Süd entlang der Grenze zwischen dem Iran und Afghanistan vergrößert und seine höchsten Werte in der Sistan Region erreicht; danach nimmt es bis zum Registan Sanddünenfeld sukzessive ab. Die höchsten Windenergiewerte wurden, basierend auf Driftpotentialen, exakt dort bestimmt, wo die ephemeren Seen im nördlichen Teil der Sistan Plain vorkommen, welche dort als Quellgebiete intensiver Staub und Sandstürme während der trockenen Jahreszeit fungieren. Die jährlich ermittelten Driftpotentiale im Sistan Gebiet erreichen die höchsten Werte (2516 vector units) in Binnenland-Wüstengebieten, weshalb es gerechtfertigt ist, dieses Gebiet als die

windigste Wüste der Erde zu bezeichnen. Die zeitliche Entwicklung des Driftpotentials zeigt einen Anstieg zwischen 1999 und 2007, gefolgt durch eine Reduzierung bis 2015 im Sistan Gebiet. Die Ergebnisse zeigen auch, dass das Windregime im Sistan- und im Registan Gebiet eine unimodale Verteilung während der Periode des 120-Tage-Winds (Sadobist Roozeh) aufweist, was auch durch die Dominanz von Transversal-, Barchanoiden- und Barchan Dünen in beiden Gebieten erklärt werden kann.

Im Zusammenhang mit dem zweiten Ziel erfolgte auch die Messung der Sediment- transportraten im Bereich des Hamoun-e Baringak Sees, einem der sechs ephemeren Seen, die enorme Mengen an äolischen Sedimenten für den atmogenen Transport in der Sistan Region bereit stellen. Die Erdoberflächensensitivität gegenüber Abwehungen wurde mittels 74 Erosionsmessstäben ermittelt, die stichprobenartig in den Seebodensedimenten des Baringak Lake eingebettet wurden. Die äolischen Transportraten wurden einzeln während drei Sturmereignissen 2013, sowie auch für die gesamte Untersuchungsperiode bestimmt. Die räumlichen und zeitlichen Unterschiede des äolischen Transports wurden mittels GIS und geostatistischen Methoden sowohl für jedes einzelne Event als auch für die gesamte Untersuchungsdauer von 103 Tagen fixiert. Die daraus resultierenden Variogramme zeigen eine hohe räumliche Abhängigkeit der unterschiedlichen Ereignisse. Zugleich konnte damit nachgewiesen werden, dass die genutzten geostatistischen Techniken ein geeignetes Werkzeug für die kartographische Fixierung des äolischen Sedimenttransports sind. Die durchschnittliche Transportrate als Ausdruck der ermittelten Drifthöhe über dem trockenen Seeboden betrug 1,93 cm oder 31 kg/m2 zwischen dem 5. August und dem 17. November 2013.

6

1

General Introduction

1.1 Introduction and justification

The United Nations Conference on Environment and Development (UNCED) in 1992, defines desertification as land degradation in arid, semi-arid and dry subhumid areas due to factors, including climatic variations and human activities (Middleton and Thomas, 1992). Desertification affects approximately 47% of global land area (Le Houérou, 1996). The main processes causing desertification are water and wind erosion, salinization, vegetation decline, water logging and organic material reduction in hyperarid, arid, semi-arid and dry sub-humid bioclimatic zones (Middleton and Thomas, 1992).

Wind erosion as one of the desertification processes affects approximately 28% of the global land area (Oldeman, 1992). It occurs as a form of land degradation under in all sort of climates (for instance, dune formation in humid climates under particular conditions) but it is especially common in dry-lands which desertification has been accelerated by human activities. Sand and dust storms (SDS) occur when strong or turbulent winds combine with exposed loose soil dry surfaces (UNEP, WMO, UNCCD, 2016). There is certainly no clear trend in the frequency of SDS in this decade for example, the have strongly increased in Inner Mongolia (China) (Shinoda et al. 2011), Xinjiang (china) (Wei et al. 2005), Sistan (Iran) (Miri et al. 2010), Khuzestan (Iran) (Zarasvandi et al. 2011), and north-western Iraq (Yahya and Seker, 2019); while there has been a significant decrease in Central Asia (Indoitu et al., 2012).

The physical process of wind erosion involves three stages: detachment, transport and deposition. The result of this process is the emission and/or mobilization of dust and the formation of areas

of sand dunes. When wind exceeds the threshold shear velocity of a surface, aerodynamic forces detach fine particles (clay, silt and sand) from dust and sand sources and carry them downwind (Bagnold, 1974). Displacement of sediment particles by the wind occurs through a combination of direct wind shear stress and atmospheric turbulence (Nickling, 2006). The sediment particles are transported in three modes by the wind: creep or reptation; saltation; and suspension (Fig. 1.1). The threshold wind speed is forcefully dependent on particle size therefore, very small particles (<60–70 µm) transport in suspension relatively in long distances; larger particles (70–500 µm) move in saltation for distances of tens to hundreds of meters and coarser material (>500 µm) transports on the surface in reptation and creep for shorter distances (Lancaster, 2009). The particles being transported in saltation and creep modes play very important role in the formation of sand dunes.

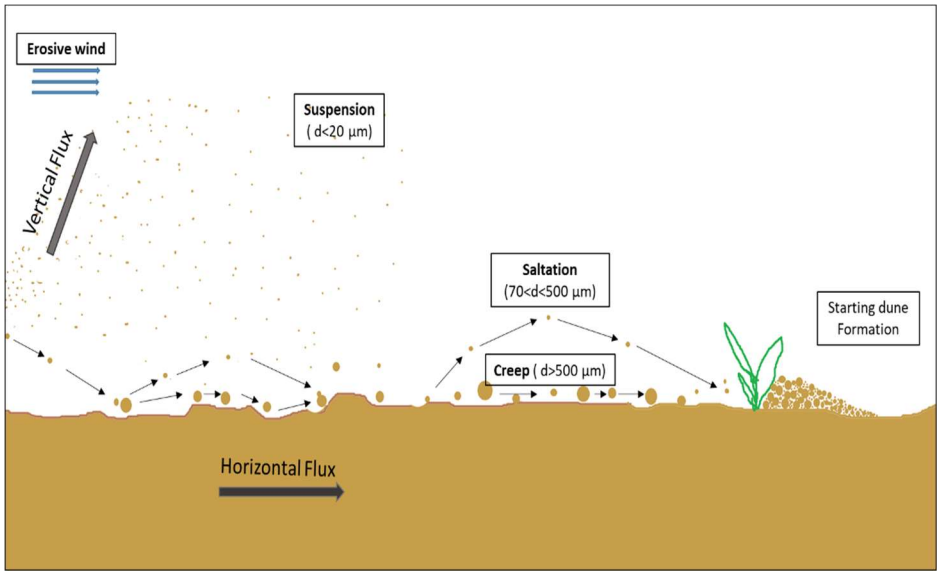

Fig. 1.1 A schematic of the modes of wind sediment transport (Source: own draft)

Wind erosion is costly for the economy, human health and the environment. SDS have numerous positive and negative impacts at regional and global scales.

Positive impacts:

1. It affects cloud nucleation and rainfall.
2. Particles from wind erosion act as a source of nutrients in oceans and tropical forest ecosystems.
3. It provides Fe for metabolized by cyanobacteria and may consequently moderate the nitrogen chemistry of the ocean.

4. It acts as a source of Fe that may be a limiting nutrient for phytoplankton.

Negative Impacts:

1. SDS emissions airborne into the atmosphere can cause asthma and other health problems.
2. Wind erosion decreases agricultural and pastoral productivity by stripping away the fertile top layers of the soil and organic matter.
3. Wind-blown soil can bury or sandblast pastures, crops and fences, contaminate wool and deposit salt on farmlands.
4. Dust deposits unwanted nutrients and salt, threatening plant and animal wellbeing and causing red or blue-green algal blooms.
5. Property and infrastructural damage can be caused by wind erosion, and structures can be buried in blown sand.
6. SDS disrupt commercial activities and transport.
7. SDS can be fill in irrigation canals, reservoirs and create the need for extra cleaning.
8. Wind erosion can cause loss of nutrient-rich topsoil in lands with generally nutrient-poor soils, through selective removal of fine fraction particulates and organic matter.

1.2 Wind erosion in Iran

In Iran, frequent dust emission has occurred in the two vast internal deserts, Dasht-e-Kavir and Dasht-e-Lut (Abdi Vishkaee et al. 2011) and ephemeral lakes within the Sistan (Kaskaoutis et al. 2015), Jazmorian Basin, Khuzestan and Kerman provinces. Hennen (2017) showed that the numbers of days with SDS has increased significantly, with totally 27,680 events and in average of 3,460 events per year in the Middle East between January 2006 and December 2013. Khuzestan and Sistan and Baluchistan provinces as two major regions, suffered significantly from SDS in this decade as is mentioned by Middleton in 1986 too (Fig. 1.2).

However, Sistan and Baluchistan province has suffered from droughts for nearly 20 years. The annual average of number days per year with dust reached 174 in Zabol City, the capital of Sistan county, and 84 days in Ahwaz City, the capital of Khuzestan province in southwest Iran. In Zahak, on the Sistan plain, and Abadan, a city in Khuzestan, trend of day with dust events illustrated a significant increase from 2001 to 2016 (Fig. 1.3). The WHO (2016) classified Zabol City as one of the 20 most polluted cities in the world, on the basis of average $PM_{2.5}$ (217 $\mu g/m^3$) and PM_{10} (527 $\mu g/m^3$) concentration in 2010 (Fig. 1.4).

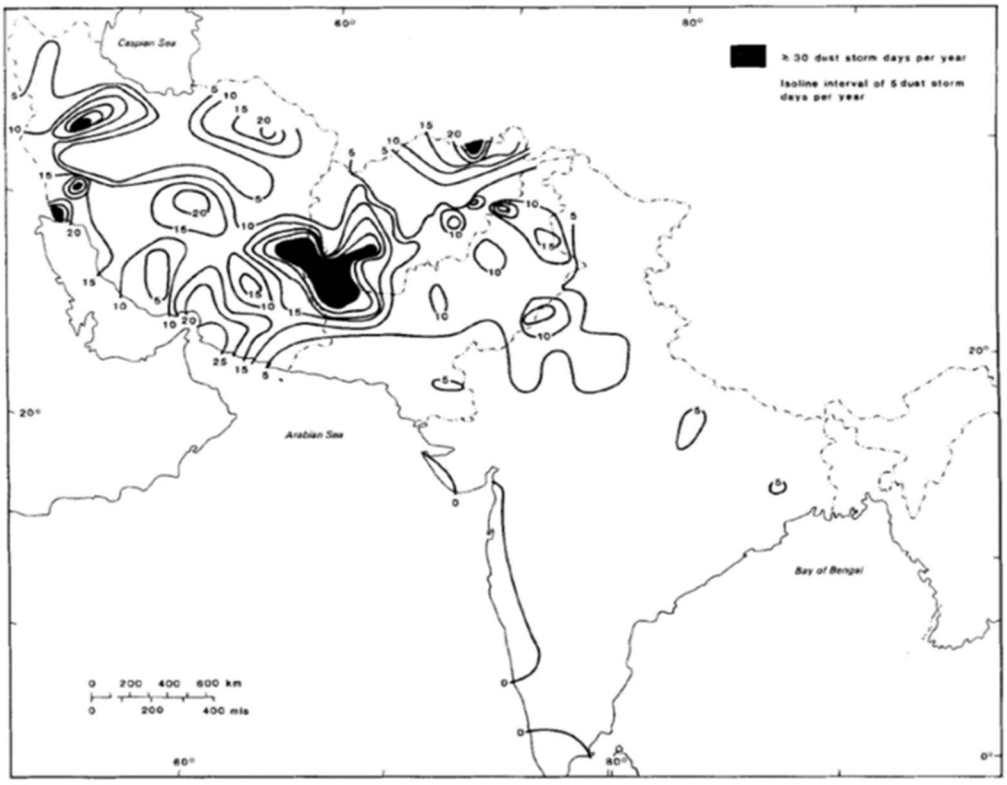

Fig. 1.2 The distribution of dust storms (visibility <1000 m) in south-west Asia (Middleton 1986)

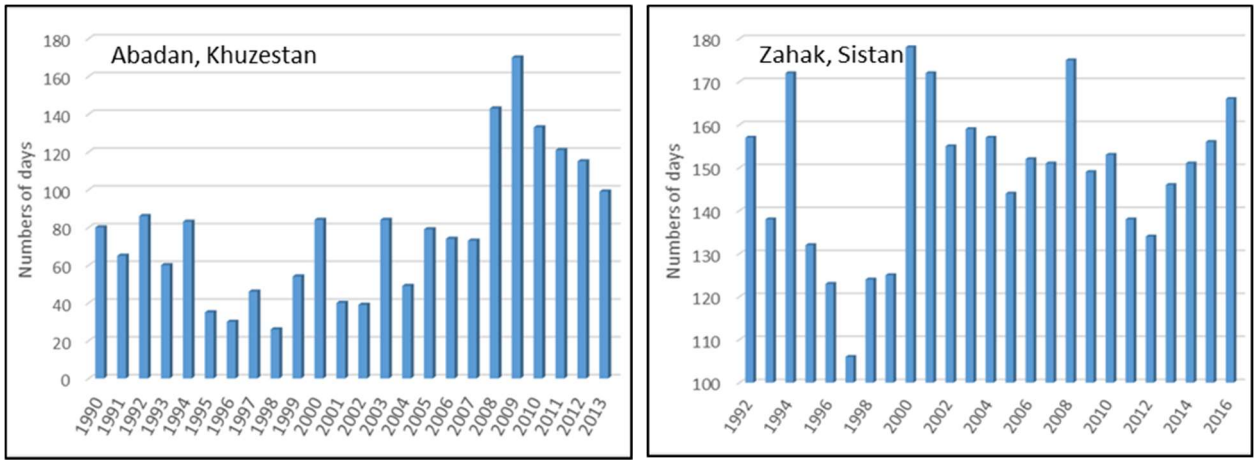

Fig. 1.3 Numbers of days with SDS in Abadan Khuzestan (left) and Zahak Sistan (right) (Source: own draft)

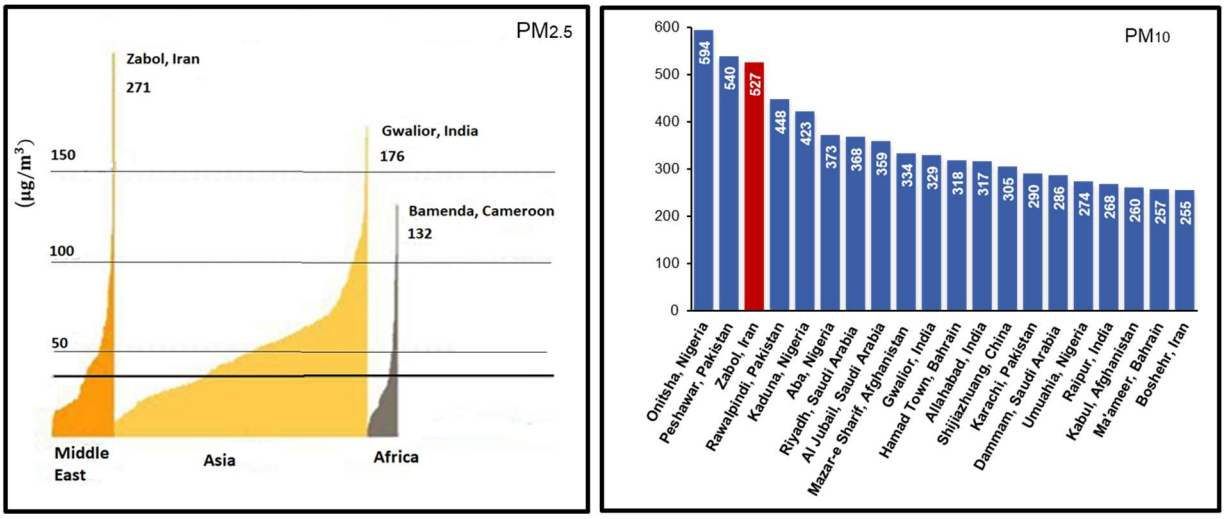

Fig. 1.4 The PM_{10} and $PM_{2.5}$ concentrations in the most polluted cities in the world, (WHO, 2016 cites Department of Environment Islamic republic of Iran 2013).

Another region that suffers from wind erosion in Iran is Kerman Province in south east. Dust storms and shifting sand are serious problems in Rigan, Fahraj and Narmashir Bam regions in Kerman province, having caused damage to rural communities, properties and infrastructure. They occur in July and August with the south or south-westerly winds (Middleton, 1986).

Fig. 1.5 A dusty day in Zabol city, Sistan, Iran

The Jazmorian Basin, in the south-east of the country is another region in Iran that is an active dust and sand source. The trend of SDS in this region showed an increasing frequency during intense drought conditions (2001-2004), with an average of dust storm events being recorded per year (Rashki et al.2017). Washington et al. (2003) reported that two major source areas are in the Makran Coastal Zone (between Jask and Chabahar) and Hamoun-e Jazmorian in south-eastern Iran.

The Yazd-Ardekan Basin, in the center of Iran, is another area exposed to wind erosion and dust storms. Ekhtesasi et al. (2006) showed that the sand dunes and bare lands northwest of Yazd City had a higher vulnerability to wind erosion than other land units which transported dust by NW, SW and W winds.

1.3 Problem statement

• Limited studies have been conducted on the dynamic features of sand dune systems in Iran and wind erosion process in Sistan region, Iran. This thesis is mainly focused on the distribution and activity of sand dunes in Iran, as well as spatial and temporal patterns of wind regime and wind erosion in Sistan, Iran. The present thesis has been conducted due to the following reasons:

• There has been no knowledge about distribution and activity of sand dunes on a national scale available to the English speaking international scientific community, which is a significant problem since Iran contains the most dominant dust and sand source areas in the world.

• There is a growing demand for more information on wind erosion, sand and dust sources, and deposition area in Iran due to the increasing damages inflicted to people and ecosystems as well as uncertain future climate change.

• There is a lack of research into spatial and temporal patterns in wind regime and sand transport in Sistan, Iran, and Registan, Afghanistan. Furthermore, there is no knowledge on the Sadobist Roozeh wind domain causing dust and sand storms in west Asia.

• Poor knowledge is available on sand transport and deflations sediment from ephemeral Hamouns lakes in Sistan and forming sand dunes in Registan induced by wind regime as one of the active dust source in the world.

• There is a lack of quantitative wind erosion and aeolian transport rate in Sistan.

• Due to the vast sources of dust and sand production, it is crucial to find areas prone to wind erosion so as to prioritize stabilization, which has been set as an essential component of this research.

1.4 Thesis Aims and Objectives

This thesis aims at addressing the research problems listed in Section 1.3. The objectives are as follows:

1. To apply and compare current sand dune activity models, develop a new model, and map the spatial activity of sand dunes in Iran.
2. To identify wind regime and sand transport in Sistan (Iran), and Registan (Afghanistan).
3. To map spatial and temporal wind erosion variations in dust and sand source areas using the erosion pin measurement and geostatistical model.

Each of the research aims is met by the followings:

- Review methods for modelling sand dunes activity and select three widely used to simulated in Iran sand dunes system. These models are Lancaster mobility index (1997), Tsoar mobility index (2005) and Yizhaq model (2009). This objective will utilise climatic parameters (hourly wind speed and direction, average monthly temperature, annual precipitation and potential evapotranspiration).

- Modify Lancaster mobility index for assessing Iran's sand dunes activity. This objective will facilitate an assessment of approaches for developing a new model of sand dunes activity in regard to Iran's sand dunes condition.

- Investigate wind regime and sand transport characteristics of Sistan and Registan deserts, and show temporal and spatial variations wind regime to understand wind erosion processes in these regions.

- Describes the relationship between erosive winds and the morphology of sand dunes in Sistan and Registan sand sea.

- Apply the erosion pin method together with geostatistical models to assess spatial and temporal patterns in aeolian sediment transport.

- Apply the model developed in Objective 3 to assess spatial and temporal patterns in land erodibility in Sistan. Spatial patterns in model output showing land areas susceptible to wind erosion will then be related to for prioritizing areas to erosion mitigation measures.

1.5 Thesis structure

The thesis contains 7 chapters which address the research objectives. These include introduction, physical setting and methodology chapters followed by three chapters 4, 5 and 6 constitute three stand-alone publications. This is followed by a synthesis of the research outcomes. The figure 1.6 is a flow chart outlining the structure of the thesis and links the thesis research objectives.

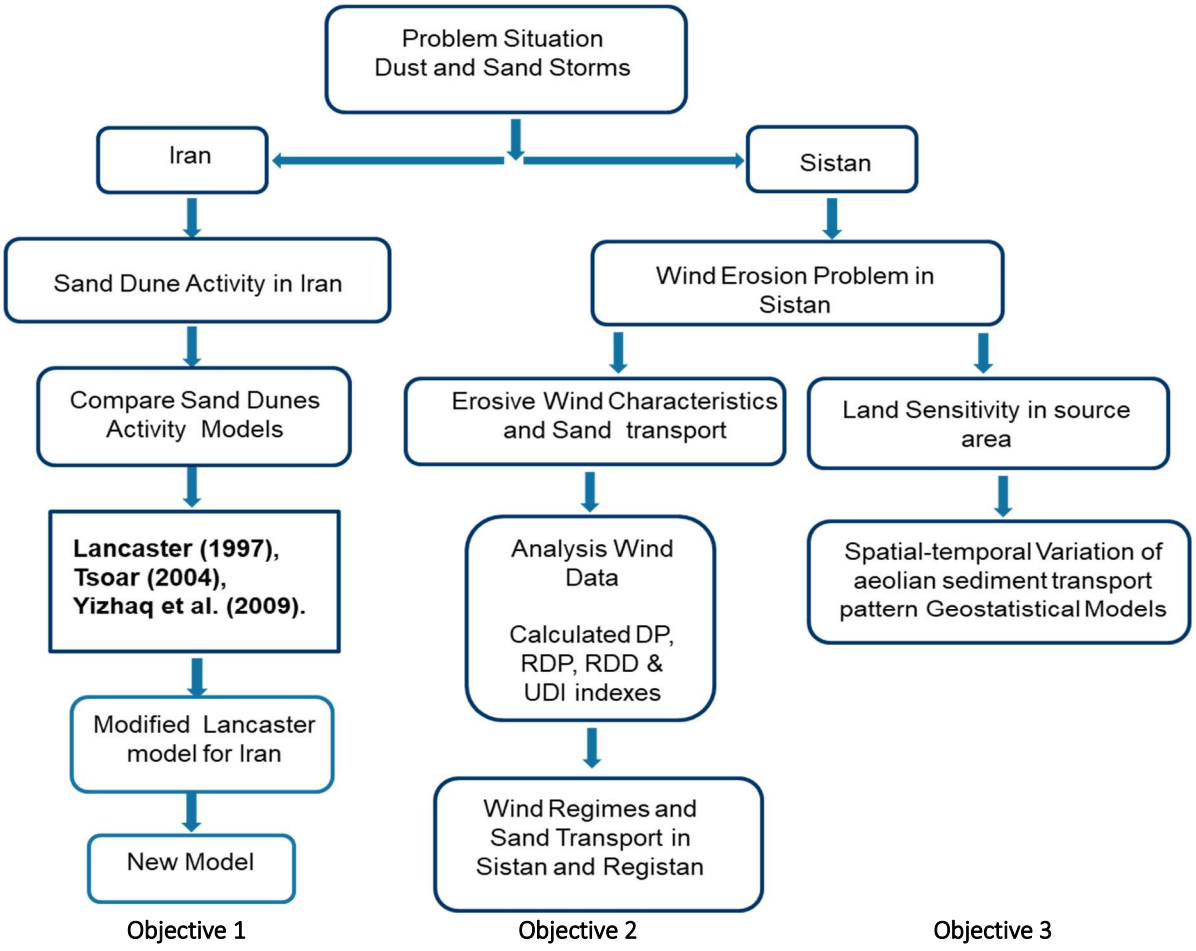

Fig. 1.6 Flow chart of the thesis structure, linking the thesis research objectives

A summary of each chapter included in this thesis:

Chapter 1- General introduction: Provide information on relevant literature and relevance of the research topic. Firstly, the geographical distribution of wind erosion discussed at a global scale. Then wind erosion problems stated in Iran and Sistan.

Chapter 2- Physical settings: Give a general overview of desert condition and the distribution of sand dunes in national scale of Iran and wind erosion challenge at an ephemeral lake as an experimental site in Sistan Plain-.

Chapters 3- Methodology: A review of current data and methods used to describe sand dunes activity and wind erosion process in Sistan. The first section describes the data used to provide spatial distribution wind energy based on DP and the three types models analysis currently used to determine sand dunes activity. Secondly, defining the methodology use to create the erosive wind features and data used to characterize the wind of the 120 days' domain in Sistan and Registan. Finally, a description of the erosion measurement with pin method and mapping spatial and temporal variations of sediment transport using geostatistical method.

Chapter 4- Assessment of the distribution and activity of sand dunes in Iran based on mobility Indices and ground data, consisting of published/accepted paper in peer-reviewed international journals. Provide an integrated analysis of the spatial variations of the wind energy based on DP and sand dune activity across Iran's deserts. In order to assess the dune activity, the Lancaster mobility index (LMI), the Tsoar mobility index (TMI) and the Yizhaq model apply and compare. Based on the results of this comparison and support by field observations data, the Lancaster mobility index modify to better represent the activity of the Iranian dunes.

Chapter 5- Reports on the wind regime, erosive wind characteristics and sand transport in the Sistan and Registan regions (Iran/Afghanistan).

Chapter 6- Presents a field method for monitoring aeolian sediment transport in an ephemeral lake in Sistan and examines application of the data for validating geostatistical model to show spatial and temporal variations wind erosion.

Chapter 7- Final Conclusion: A summary of the findings generated by the research presented in this thesis, discussing limitations and possible applications of sand dunes activity models and wind erosion assessment using pin method and geostatistical technique and future research goals.

1.6 References

Bagnold, R. A. (1974). The physics of blown sand and desert dunes. London: Methuen, 265 pp.

Ekhtesasi M.R., Sepehr, A. (2009). Investigation of wind erosion process for estimation prevention, and control of DSS in Yazd – Ardekan plain, Environmental Monitoring and Assessment, 159: 267–280. https://doi.org/10.1007/s10661-008-0628-4

Hennen, M. (2017). Identifying mineral dust emission sources in the Middle East using remote sensing techniques, (dissertation), Reading, England, Reading university, 217 pp. https://doi.org/file:///D:/refrence/Thesis/Identifying%20mineral%20dust%20emission%20sources%20in%20the%20Middle%20East%20using%20remote%20sensing%20techniques1.pdf

Indoitu, R., Orlovsky, L, Orlovsky, N. (2012). Dust storms in Central Asia: Spatial and temporal variations. Journal of Arid Environments, 85: 62–70. https://doi.org/https://doi.org/10.1016/j.jaridenv.2012.03.018

Kaskaoutis, D. G., Rashki, A., Houssos, E. E., Mofidi, A., Goto, D., Bartzokas, A, Legrand, M. (2015). Meteorological aspects associated with dust storms in the Sistan region, southeastern Iran. Climate Dynamics, 45(1–2): 407–424. https://doi.org/10.1007/s00382-014-2208-3

Lancaster, N. (1997). Response of eolian geomorphic systems to minor climate change: examples from the southern Californian deserts. Geomorphology, 19: 333–347. https://doi.org/10.1016/S0169-555X(97)00018-4

Lancaster, N. (2009). Aeolian features and processes. in Young, R., and Norby, L., Geological Monitoring: Boulder, Colorado, Geological Society of America, p. 1-25. https://doi.org/10.1130/2009.monitoring(01).

Le Houérou, H. N. (1996). Climate change, drought and desertification. Journal of Arid Environments, 34(2): 133–185. https://doi.org/10.1006/jare.1996.0099

Middleton, J. (1986). Dust storms in the Middle East. Journal of Arid Environments, 10(2): 83–96. https://doi.org/10.1016/S0140-1963(18)31249-7

Middleton, N. J. (1986). A geography of dust storms in South-West Asia. Journal of Climatology, 6(2): 183–196. https://doi.org/10.1002/joc.3370060207

Middleton, N. J, Thomas, D. S. (1992). World atlas of desertification, UNEP, 69 pp.

Miri, A., Moghaddamnia, A., Pahlavanravi, A, Panjehkeh, N. (2010). Dust storm frequency after the 1999 drought in the Sistan region, Iran. Climate Research, 41(1), 83–90. https://doi.org/10.3354/cr00840

Nickling, W.G. (1988). The initiation of particle movement by wind. Sedimentology, 35: 499–511. https://doi.org/10.1111/j.1365-3091.1988.tb01000.x

Oldeman, L. R. (1992). Global extent of soil degradation. ISRIC, Bi-Annual Report 1991-1992, pp. 19–36.

Rashki, A., Arjmand, M, Kaskaoutis, D. G. (2017). Assessment of dust activity and dust-plume pathways over Jazmurian Basin, southeast Iran. Aeolian Research Journal, 24: 145–160. https://doi.org/10.1016/j.aeolia.2017.01.002

Shinoda, M., Gillies, J. A., Mikami, M, Shao, Y. (2011). Temperate grasslands as a dust source: Knowledge, uncertainties, and challenges. Aeolian Research Journal, 3(3): 271–293. https://doi.org/10.1016/j.aeolia.2011.07.001

Tsoar, H. (2005). Sand dunes mobility and stability in relation to climate. Physica A: Statistical Mechanics and Its Applications, 357(1): 50–56. https://doi.org/10.1016/j.physa.2005.05.067

UNEP, WMO, UNCCD (2016). Global Assessment of Sand and Dust Storms. United Nations Environment Programme, Nairobi, p.125.

Vishkaee, F. A., Flamant, C., Cuesta, J., Flamant, P, Khalesifard, H. R. (2011). Multiplatform observations of dust vertical distribution during transport over northwest Iran in the summertime. Journal of Geography Research, 116: 1–13. https://doi.org/10.1029/2010JD014573

Washington, R., Todd, M., Middleton, N. J, Goudie, A. S. (2003). Dust-Storm source areas determined by the total ozone monitoring spectrometer and surface observations. Annals of the Association of American Geographers, 93(2); 297-313. DOI:10.1111/1467-8306.9302003 93(2).

Wei, W., Zhou, H., Shi, Y, Abe, O. (2005). Areas of dust storms in Xinjiang, China, During the last 50 years. Water, Air, and Soil Pollution, 5: 207–216.

WHO. (2016). The 20 Most Polluted Cities in the World. https://doi.org/https://www.fabionodariphoto.com/en/most-polluted-cities-in-the-world/

Yahya, B. M, Seker, D. Z. (2019). The Impact of Dust and Sandstorms in Increasing Drought Areas in Nineveh. Journal of Asian and African Studies, 54(3): 346–359. https://doi.org/10.1177/0021909618812913

Yizhaq, H., Ashkenazy, Y, Tsoar, H. (2009). Sand dune dynamics and climate change: A modeling approach. Journal of Geophysical Research: Earth Surface, 114(1): 1–11. https://doi.org/10.1029/2008JF001138

Zarasvandi, A., Carranza, E. J. M., Moore, F, Rastmanesh, F. (2011). Spatio-temporal occurrences and mineralogical – geochemical characteristics of airborne dusts in Khuzestan Province (southwestern Iran). Journal of Geochemical Exploration, 111(3): 138–151. https://doi.org/10.1016/j.gexplo.2011.04.004

2

Physical Setting

2.1 Study area

Regarding objectives and thesis structure, this dissertation was conducted in two different scales. First, the investigation of sand dunes activity was carried out in national scale of Iran, and secondly, temporal and spatial variability of wind erosion is fulfilled in Sistan plain. For the reason that, the characteristics of Iranian deserts and Sistan physical setting are explained in this chapter.

2.2 Iran deserts

2.2.1 Climate

Iran has different types of climate ranged from mild and quite wet on the coast of the Caspian Sea to continental and arid in the plateau and desert and hot on the central and southern area. The mean annual of precipitation is about 240 mm and temperature 17°C that January is the coldest month, with temperatures from 5°C to 10°C, and August is the hottest month at 20°C to 30°C or more. About 70 percent of the average rainfall in the country falls between November and March; June through August are often rainless (Weather Online 2019).

Generally speaking, Iran is located in the dry belt of the world, with 85% of the land mass being classified as arid and semi-arid (Le Houérou, 1992). Desert ecosystem covers 55% of Iran (Khosroshahi et al. 2009). Aeolian landforms dominate the desert interior of the country, and wind erosion processes have long been a natural occurrence in arid and semiarid of Iran (Ahmadi, 1999; Mahmmodi, 2002). This means that large areas of Iran are potentially susceptible to wind erosion. Table 2.1 provides the surface of land covered by hyperarid, arid and semi-arid climates that wind erosion process is active in this area.

Table 2.1 Size and distribution of Iran and the world's arid lands (10^3 km^2) (After Le Houérou, 1992)

Country	Geographical surface area	Bioclimatic zone					
		Eremitic	Hyperarid	Arid	Semi-arid	Total	%
Aridity Index (I) (P/PET × 100)		I<3	3<I<6	6<I<30	30<I<50		
P (Approx. mm)		P<50	50-100	100-400	400-600		
Iran	1636	20	306	685	375	1386	85
World	130737	7500	7059	14330	12651	41540	32

Considering the climatic and environmental conditions, Iran could be divided into four different zones (Fig. 2). Alborz and Zagros mountains in north and west Iran are cold to very cold snow climate with dry summers and wet winters (dry sub-humid and semi-arid); the north of Iran near Caspian Sea with a mild, semi-humid with dry summers and mild winters climate (humid or sub-humid); the southern part near Persian Gulf and Omman Sea with a hot subhumid to dry desert climate and finally, the central and southeastern parts, in Dasht-e Kavir and Lut deserts, with hot and dry desert climate (arid to hyperarid).

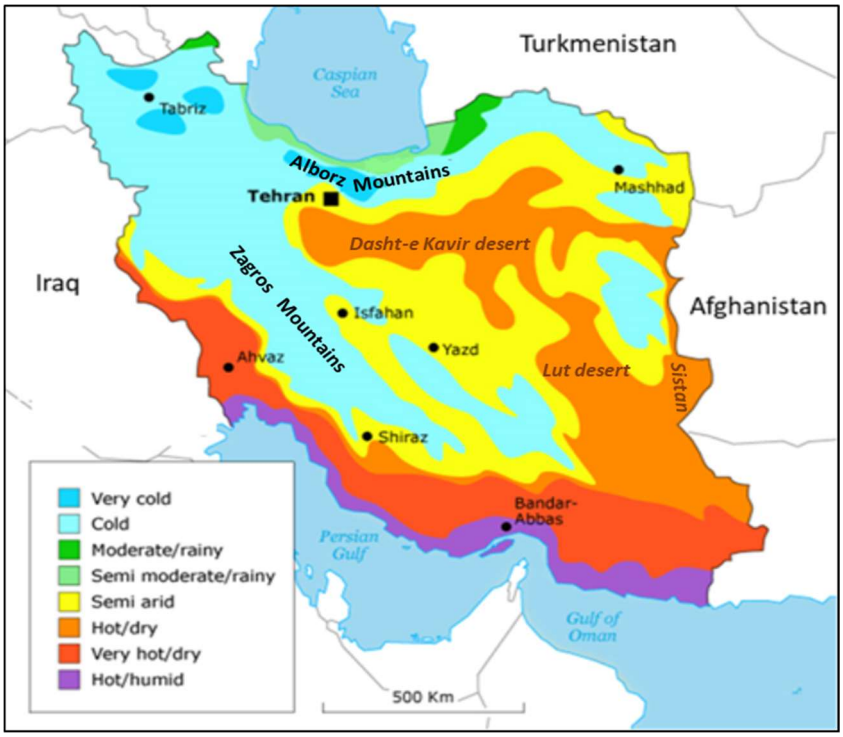

Fig. 2.1 climate zoning in Iran (Sorce picture: Alizade Govarchin Ghale, 2014)

The arid and hyperarid climates in central and south parts of country have high potentially susceptible to wind erosion and major sand seas and dunefields scattered in these regions. Although, wind erosion phenomenon is seen also in some limited parts of semi-arid regions e.g. in West and East Azerbaijan provinces.

2.2.2 Deserts and sand dunes in Iran

Early work on Iran deserts and dunes was contributed by Hedin (1923) and Gabriel (1942). Almost all the dune systems in Iran is scattered in Lut, Dasht-e Kavir, Sistan, Jazmorian, Khuzestan deserts, coastal dunes near Omman Sea and Persian Gulf, and other small parts. The Iran's sand dunes is covered about 4.6 million hectares (2.5 %) of Iran, as seen in Fig. 2.2 and Table 2.2 (Abbasi, 2012). The largest dunes area is located in Kerman and smallest area in Tehran provinces.

Table 2.2 Distribution of sand dunes in Iran's provinces (Abbasi, 2012)

Provinces	Area (ha)	%
Azerbaijan, East	1007	0.02
Azerbaijan, West	1829	0.04
Bushehr	10770	0.23
Fars	2302	0.05
Hormozgan	52545	1.13
Ilam	31301	0.7
Isfahan	613460	13
Kerman	1201066	26
Khorasan, North	2424	0.05
Khorasan, Razavi	485087	10
Khorasan, South	398545	9
Khuzestan	223775	5
Markazi	657	0.01
Qazvin	1040	0.02
Qom	17113	0.4
Semnan	373677	8
Sistan and Baluchistan	813662	18
Tehran	72	0.002
Yazd	405232	9
Iran (Total)	4635563	100

The most important deserts and sand dunes in Iran have been divided into six sub-regions:

Lut desert

The Lut desert or Dasht-e Lut (28 - 37°N; 55 - 60°E) is defined by the hyper-arid depression and the surrounding mountain regions to the northeast, east and south. It is a mostly unhabituated desert with extremely dry and the highest surface temperature on Earth (NASA, 2012). Lut desert produced 4.9% of all dust events in the Middle East, with the largest concentration of sources in the dry flood plains and dried lakes (Hennen 2017). Yalan sand sea as largest sand sea in country (14583 km^2) formed in eastern part of Lut desert due to the multidirectional winds and topography impact. It seems, however, wind erosion plays as an important phenomenon in the formation of the Lut desert

In Rigan, Fahraj, Bam and Narmashir regions in the south of Lut desert, shifting dunes buried rural areas, rail roads, damage to infrastructure and farmlands every year. Near 16 Villages in Rigan abandoned as a result of shifting sand, and 150 villages covered by sand dunes or affected by moving sand dunes (IRNA 2018).

Dasht-e-Kavir desert

The Dasht-e-Kavir as largest desert in country and mostly unhabituated lie in the central of Iran (25 - 40°N; 45 - 63°E and 48 - 52°E). Northerly winds lift surface sediments from surface of Dasht-e Kavir. They deposited in four sand seas, “Rig-e Jinn”, “Rig-e Kaleh”, Rig-e Shotoran in south, and “Rig Boland and Dag Sork” in southwest of this desert. In addition, many dunefields anchored by topography near inselbergs among this desert.

Hamoun Jazmorian

Hamoun-e Jazmorian (24 - 27°N; 57 - 62°E) is located between the provinces of Kerman and Sistan-Baluchistan, which is a major wetland in southeast Iran. As a result of climate change, excessive dam construction and the depletion of groundwater resources, it is leading to complete drying and plays as main source of SDS. The Erosive winds in Jazmorian blow more between May and October and dust activity is to 6.2% of all events in the Middle East (Hennen, 2017). There are two sand dune bodies including a part in the north and one along the Makran mountains in the south of Jazmorian wetland.

Khuzestan Plain

The Khuzestan Plain (31.2°-31.3°N; 48.40°-48.67°E) is the relatively flood plains and low lands region of Iran in southwest of Iran with hot summer where dust storms originated from Lower and upper Mesopotamia includes the Tigris and Euphrates River Basin. Middleton (1986) believed that It is the dustiest area of the Middle East and Hennen (2017) showed that this sub-region produced 20% of all dust emissions in the Middle East. The most SDS that suffered Khuzestan came from Arabian Peninsula, Syria and Iraq (Zoljoodi et al. 2013). The share of internal and external dust

sources was 8.4% and 91.6%, according to Dargahian et al. (2016). Khuzestan sand sea is extended from Iraq into Ilam then Khuzestan provinces in Iran, with 336125 ha area, 78% in Iran and 22% in Iraq.

Coastal desert

The coastal desert is extended as a very long coastline in the margin of Persian Gulf and Oman Sea in the south of country. The coastal dunes are extended along the Omman sea and Persian Gulf coastline in Bushehr, Hormozgan and Sistan and Baluchistan provinces. The dunes between Chabahar and Jask are relatively active and more plant species grow over it than interior dunes because of more humidity from sea.

Other dunefields in country find in Yazd, Khorasan, Semnan, Tehran, Qazvin, east and west Azerbaijan provinces in small parts and different activity as seen in fig.2.2.

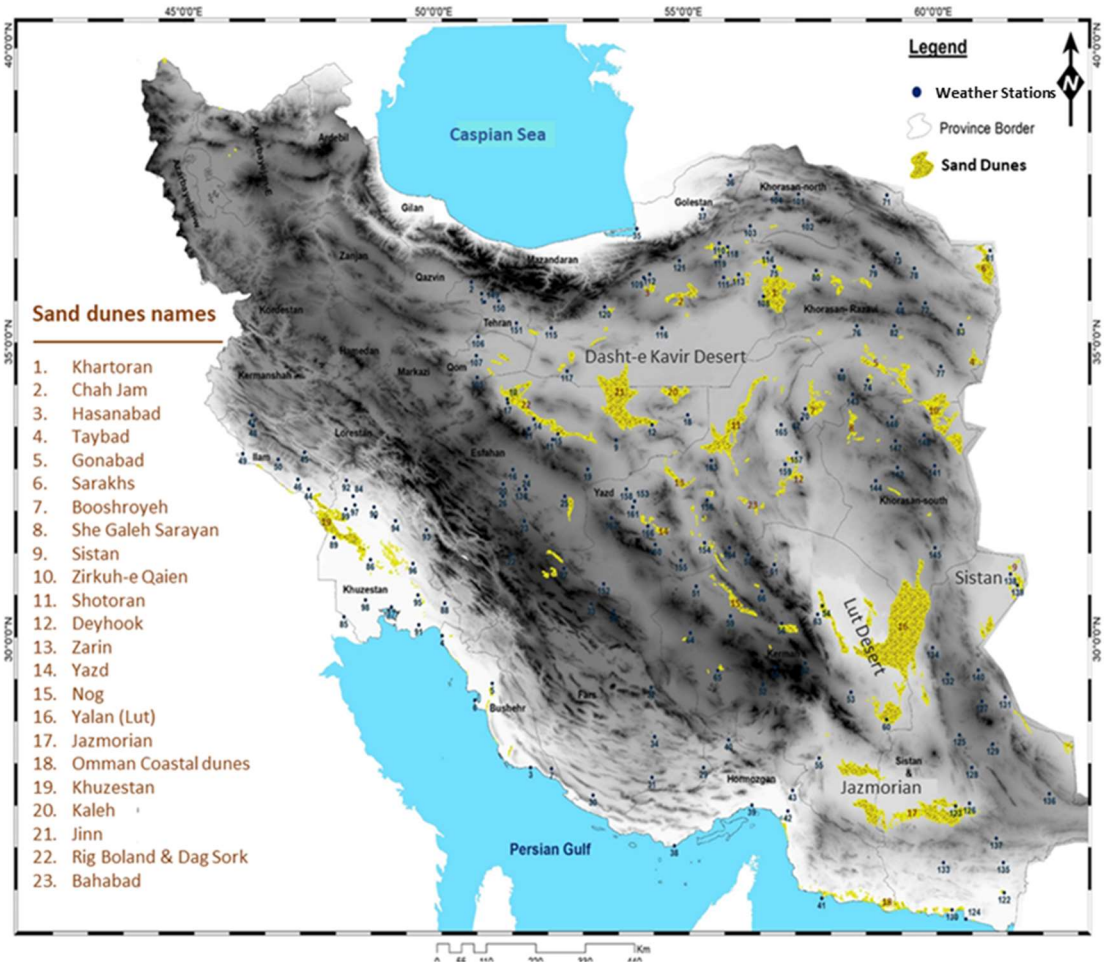

Fig. 2.2 Distribution of sand dunes and weather stations in Iran (Abbasi 2012)

Fig. 2.3 Impressions of the sand dunes in Iran

2.3 Sistan Plain

2.3.1 Location

The Sistan depression is located at the tail end of the Hirmand or Helmand Basin, which is large part of it in the southwest of Afghanistan and minor part in the eastern part of Iran. Hirmand or Helmand river, an important river in its watershed, originates from Baba mountainous in the south of Kabul, after passing through five provinces of Afghanistan and irrigated farmlands, is entered to complex ephemeral lakes in Sistan region. As a result of erosion of highlands, alluvial fine sediments that over millions of years have been accumulated in this depression formed Sistan plain.

The six ephemeral lakes which called Hamouns Lakes, surrounded Sistan plain, those are consist of Hamoun-e Puzzak, Hamoun-e Sabari, Hamoun-e change Sork, Hamoun-e Baringak, Hamoun-e Hirmand and Gowd-e Zareh (Fig. 2.4). Due to prolonged severe droughts in Sistan (Golian et al. 2015) and dams' construction in Afghanistan (Bazrkar et al. 2013) less water reaches to lakes and hydrological drought has dominated the region.

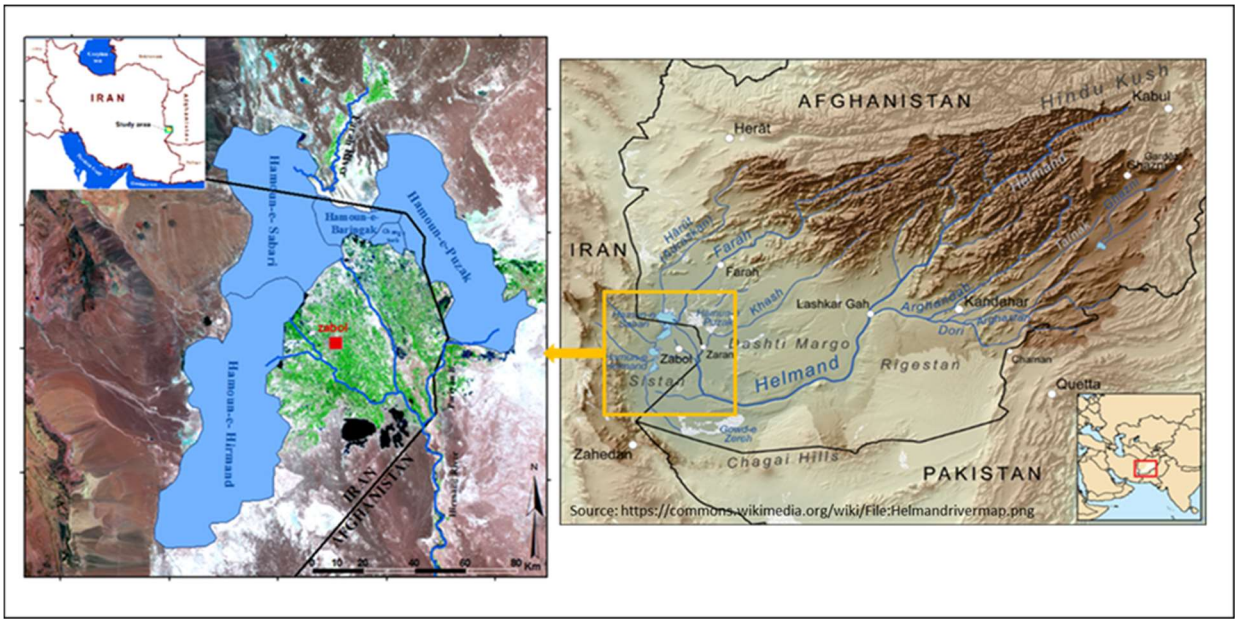

Fig. 2.4 Hirmand Basin and Hamouns complex Lakes in Sistan Plain (Source: own draft)

The economics of more than 220 rural communities in Sistan plain have been dependent on Hamouns Lakes that were disrupted because of droughts and dried lakes. As a consequence of drying up of the lakes, the fishing industry has been brought to a halt and 3500 fishermen have been lost the job (Stöber 1981, Rist 1981, Zia-Tavana 1981).

2.3.2 Climate

The Sistan plain classifies as hyperarid climate, characterized by cold and dry winters and warm and hot summers. The average of mean daily temperature is relatively high with 22.6°C in Zabol, as the capital county of Sistan, with average temperatures of up to 35°C in summer and 8°C in winters. The annual mean air temperature changes a few over Registan and reaches to 18.6°C in Ghandehar. Rainfall is rarely (57 mm), ranged between 129 mm in 2005 to 6.8 mm in 2010 (http://www.chaharmahalmet.ir/iranarchive.asp). The annual precipitation increase over the Registan sand sea from 105 mm just near the Iran-Afghanistan border to 185 mm in Ghandehar in Afghanistan.

From mid-May to September strong winds come regularly from the north to northwest direction caused by a high gradient in air pressure between Turkmenistan linked to Siberian high pressure and Pakistan low pressure called “Sadobist Roozeh” or “the wind of the 120 days”. The mean average wind velocity is 5.2 m s^{-1} in duration 1963-2010. The annual mean air temperature is relatively high range from 21.6°C in Zabol station. Some of the highest evaporation rates in the world have been recorded in Sistan with 1608 mm/year (Afghan Institute de Meteorologie, 1978; Dittmann, 2014; Whitney, 2006).

The Sadobist Roozeh wind blows for four months but Mofidi et al. (2014) showed that this duration is apparently longer with high temporal variations, average 165 days in the recent four decades. This northerly or north-westerly very high energy wind lifts sediment from dried Hamouns Lakes surface in dry season, then transports aeolian and deposits in Registan sand sea which extended from Sistan to Ghandehar in south of Afghanistan. The dust and sand storms suffered to 11 million people who are living in Sistan and south of Afghanistan and the north of Pakistan.

2.3.3 Geological setting

Sistan plain is an Eurasian Plate from tectonic view, formed as Hirmand delta at the last period of geology and by accumulation of sediments and alluvium derived from water, particularly Hirmand is filled and changed to current form. The Helmand Basin has had a long history of sedimentation derived from the uplift of the Hindu Kush-mountains. A period of erosion of these sediments and related volcanic occurred in late Miocene and Pliocene, creating erosional remnant and scraps up to 200m high of the Dasht-e Margo plateau and Sistan (Evenstar et al. 2018). The sediments include clay, silt and sand that in the range, its silt are more.

2.3.4 Sand transport and dunes

The Sadobist Roozeh lifts easily sediments from surface of Hamouns Lakes beds into the four erosive corridors entitled “Gorgori-Puzzak, Niyatak, Jazinak, and Tasoki- Rig Chah” in Sistan plain (Fig. 2.5) (Abbasi 2018). The corridors formed due to topography of Sistan plain. Shifting dunes in Barchans, domes and sand sheet forms transports into the corridors, pass across Hirmand river, and enter Dasht-e Margo and Registan in Afghanistan. They repeatedly blocked the country roads between some major cities and villages, irrigation canals, main stream, farmlands and damages to infrastructures in Sistan (Fig. 2.6 and 2.7). The sand blown fill in canals and local rivers, block water and make problem for farmers every year. The cost of cleaning irrigation canals in Sistan plain was estimated $3 million in 2012.

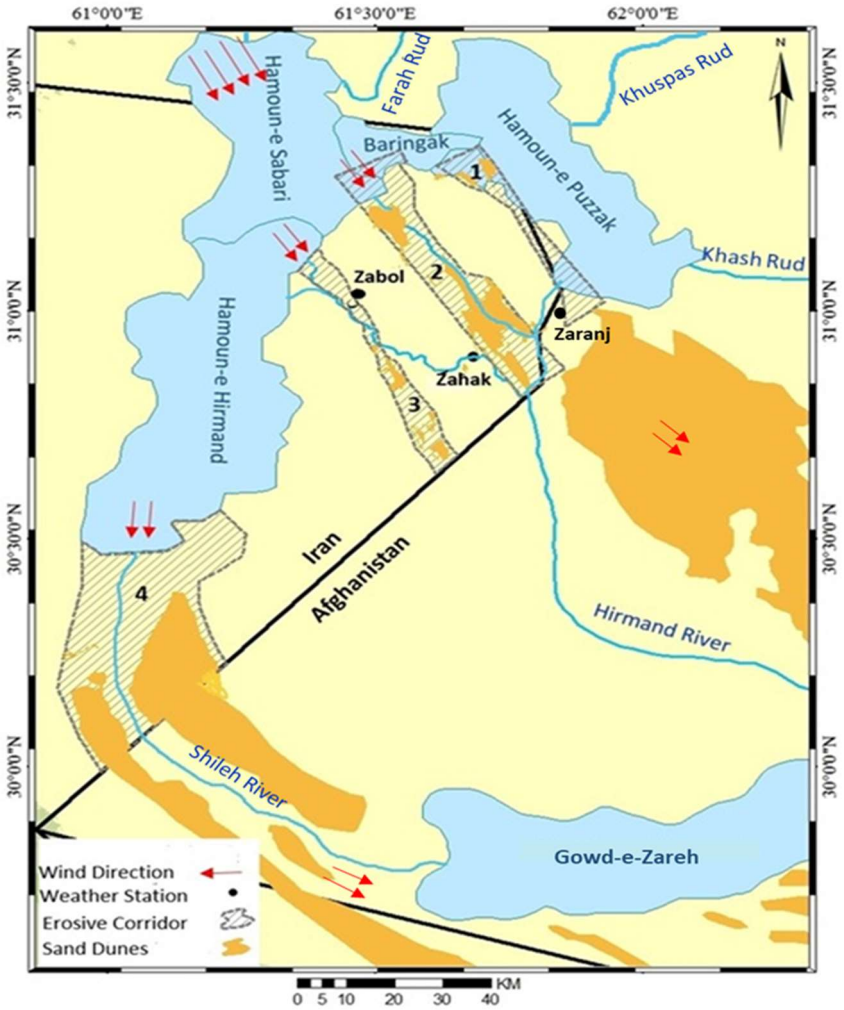

Fig. 2.5 The location of six ephemeral Lakes; Hydrology systems; Sand transport corridors: 1. Gorgori-Puzzak, 2. Niyatak, 3. Jazinak, and 4. Tasoki- Rig Chah, and sand dunes in Sistan region (Source: own draft).

Sistan plain is a sand transportation region and the area of dunes varies in space and time. In one survey, the sand dunes cover about 690 km^2 in Sistan region although it is links to Registan sand sea (Abbasi 2012). It is one of the active sand dunes in Iran and artificial stabilization plans have a history for more than half of the century in Sistan (NIOPDC 1967). Table 2.3 provide the distribution and artificial stabilization sand dunes statue in Sistan in relation four corridors.

Table 2.3 Distribution and artificial fixation sand dunes in Sistan (Abbasi 2012)

Sand dunes	Artificial Stabilized (ha)	Active (ha)	Total Area (ha)
Gorgori-Puzzak	-	1717	1717
Niyatak	12839	6579	19466
Jazinak	-	3412	3412
Tasoki- Rig Chah	1663	42881	44544
Total	14502	54589	69091

The Registan sand sea which originates from ephemeral Hamouns Lakes extended from Sistan to Ghandehar. Sand particles move into corridors in sand sheets form then Barchan and transverse dunes form in Dasht-e Margo (death plain) and finally, deposit in transverse form in Registan.

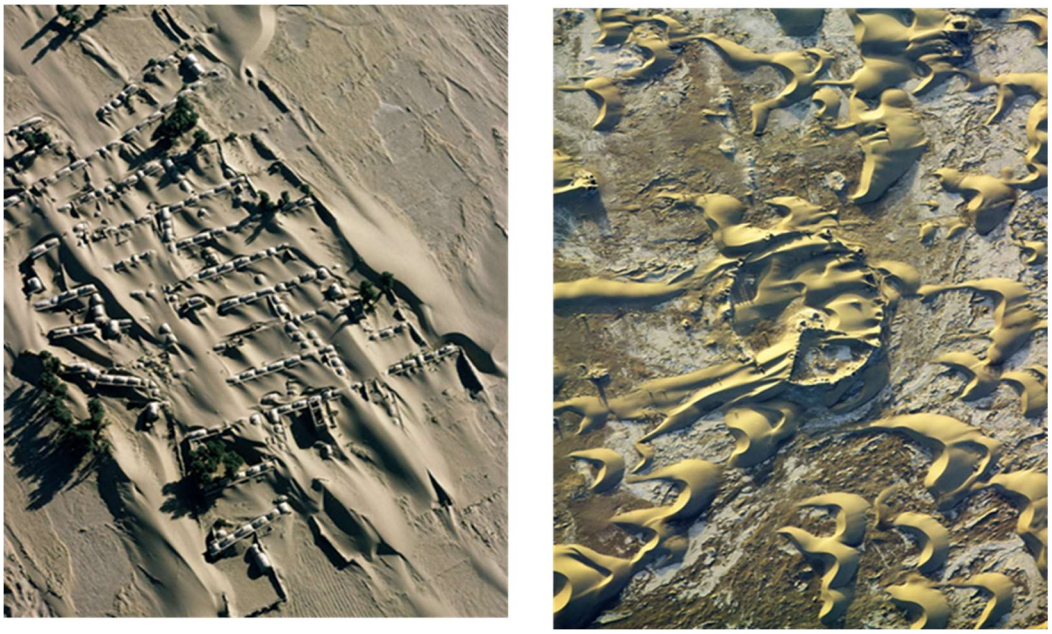

Fig. 2.6 Active sand dunes in Sistan region and Lut desert

Fig. 2.7 Shifting dunes impacts in Sistan

2.4 References

Abbasi, H.R., Gohardoust, A., Khaksarian, F, Ganjali, M. (2018). Morphologic characteristics of aeolian deposits and erosive winds in Sistan plain. Desert Management, 10: 28–42 (in Persian).

Abbasi H.R. (2012). Classification of Iran's Sand Dune Systems: morphology and Physio-chemical properties. Research Institute Forests and Ranglands Iran, technical final report, Tehran, p.465 (in Persian).

Bazrkar, M. H., Nabavi, E., and Eslamian, S. (2013). System dynamic approach to hydro-politics in Hirmand transboundary river basin from sustainability perspective, International Journal of Hydrology Science and Technology, 3(4): 378–398. https://doi.org/10.1504/IJHST.2013.060338

Afghan Institute de Meteorologie. (1978). Meteorological Records of Afghanistan for 1970: Kabul, Open-File Data, 37 pp.

Ahmadi, H. (1999). Applied geomorphology, Desert, wind erosion. Tehran university, 706 pp. (in Persian).

Alizade Govarchin Ghale, Y. (2014). Multitemporal change detection on Urmia Lake and its catchment area using remote sensing and geographical information system. Istanbul Technical University, 228 pp.

Dargahian, F., Lotfinasab, S., Khosroshahi, M., Gohardoost, A. (2016). Determining the share of internal and external resources of dust in Khuzestan province, Journal of Iran Nature, 5(2), 36-41. https://10.22092/irn.2017.113621

Dittmann, A. (2014). National Atlas of Afghanistan. Bonn, 114 pp.

Evenstar, L. A., Sparks, R. S. J., Cooper, F. J., Lawton, M. N. (2018). Quaternary landscape evolution of the Helmand Basin, Afghanistan: Insights from staircase terraces, deltas, and paleoshorelines using high-resolution remote sensing analysis. Geomorphology, 311: 37–50. https://doi.org/https://doi.org/10.1016/j.geomorph.2018.03.018

Gabriel, A. (1953). Durch Persiens Wüsten, Stuttgart,272 pp.

Golian, S., Mazdiyasni, O., and Aghakouchak, A. (2015). Trends in meteorological and agricultural droughts in Iran, Theoretical and Applied Climatology, 119:679–688. https://doi.org/10.1007/s00704-014-1139-6

Hedin, S. (1910). Zu Land nach Indien durch Persien, seistan, Belutschistan. 1. Bd., Leipzig

Hennen, M. (2017). Identifying mineral dust emission sources in the Middle East using remote sensing techniques (Reading university).

https://doi.org/file:///D:/refrence/Thesis/Identifying%20mineral%20dust%20emission%20sources%20in%20the%20Middle%20East%20using%20remote%20sensing%20techniques1.pdf

IRNA (2018) 150 Rigan villages are surrounded by sand dunes, August 6 (in Persian). https://www.irna.ir/news/82992808/150

Khosroshahi, M., Khashki, M., and Ensafi Moghaddam, T. (2009). Determination of climatological deserts in Iran. Iranian Journal of Range and Desert Research, 16(1): 96–113 (in Persian).

Le-Houérou, H.N. (1992) An Overview of Vegetation and Land Degradation in World Arid Lands. In: Dregne, H.E., Ed., Degradation and Restoration of Arid Lands, International Center for Semi Arid Land Studies, Lubbock, 127-163.

Mahmoodi, F. (2002). Sand Seas Distribution of Iran. Research Institute Forests and Ranglands Iran, p. 165 (in Persian).

Middleton, J. (1986). Dust storms in the Middle East. Journal of Arid Environments, 10(2): 83–96. https://doi.org/10.1016/S0140-1963(18)31249-7

Mofidi, A., HamidianPour, M., Saligheh, M., Alijani, B. (2014). Determination of the Onset, Withdrawal and Duration of Sistan wind using a Change Point Approach. Geography and Environmental Hazards, 2: 87–112. https://doi.org/10.22067/geo.v0i0.25026

NASA (2012). What Does It Mean to be Hot? https://earthobservatory.nasa.gov/features/HottestSpot/page2.php

NIOPDC (1967). Summary of information and preliminary studies on the use of petroleum products in agricultural affairs and sand dunes stabilization. The National Iranian oil products Distribution Company, 246 pp. (in Persian).

Peel, M.C., Finlayson, B.L. and McMahon, T.A. (2007). Updated world map of the Köppen-Geiger climate classification, Hydrology and earth system sciences discussions, 4(2): 439-473.

Rist, B. (1981). Die Stadt Zabol. Zur wirtschaftlichen und sozialen Entwicklung einer Kleinstadt im Ost-Iran (Sistan-Projekt I), Selbstverlag des Geographischen Instituts der Universität Marburg, 245 pp.

Stöber, G. (1981) Die Sayad. Fischer in Sistan (Sistan-Projekt III), Selbstverlag des Geographischen Instituts der Universität Marburg, 132 pp.

Weather online (2019). Online service. https://www.weatheronline.co.uk/reports/climate/Iran.htm

Whitney, J. W. (2006). Geology, water, and wind in the lower Helmand Basin, southern Afghanistan: U.S. Geological Survey Scientific Investigations Report 2006–5182, 40 p.

Zia-Tavana, M.H. (1983) Die agrarlandschaft Iranisch-Sistans, aspekte des strukturwandels im 20. Jahrhundert (Sistan-Projekt II), Selbstverlag des Geographischen Instituts der Universität Marburg, 212 pp.

Zoljoodi, M., Didevarasl, A., Saadatabadi, A. R. (2013). Dust events in the western parts of Iran and the relationship with drought expansion over the dust-source areas in Iraq and Syria. Atmospheric and Climate Sciences, 3: 321–336. https://file.scirp.org/pdf/ACS_2013070316185157.pdf

3
Methodology

3.1 Data and methods

This chapter addresses methodology based on triple objectives which are defined in chapter 1. It is divided into three sub-sections, the first subsection is to collection and analyzes meteorological data to simulate three models of sand dunes activity and an approach to develop a new model in Iran's dunes. In the second subsection, the estimation methods of wind regime and sand transport describe in Sistan. The final sub-chapter defines the methodology of field data acquisition of eolian sediment transport and geostatistical models to show spatial and temporal variations in the Hamoun Baringak Lake in Sistan.

3.2 Sand dunes activity

3.2.1 Climatic data

For this study, the climatological records of 204 meteorological stations (see Fig. 4.1) were provided in digital form for the 19-year period 1994-2013 from Iran Meteorological Organization (IMO), including the speed and direction of hourly wind data, monthly average temperature and annual rainfall. There are two types of professional weather or meteorological stations in Iran, Synoptic and Climatology Stations which measured hourly wind data. The wind data records in intervals for 1 or 3 hourly for 24 h in Synoptic Stations but it only measures in three times intervals 3 hourly per day (9:00, 12:00 and 15:00) in Climatology Stations, both at height of 10 m above the ground. It means that in Climatology Stations, wind data were not recorded in the late evening or early morning hours. Almost Synoptic Stations changed to smart weather station and collected data automatically in recent years. The period data in the most Synoptic Stations covered from 1994 to 2013, but some stations, specially Climatology, are shorter due to data limitations (See Appendix A, p. 133-136). Totally, more than 39 million climate data were investigated in this study.

The meteorological stations in Iran are not homogeneously distributed across deserts, and in some case, are far away from the dune fields e.g. in the central part of the Lut and Dasht-e Kavir. Therefore, it couldn't provide a relatively uniform geographic distribution and effects on the assessment of climate maps which simulate by these data. In some cases, the stations are located in relatively large metropolitan areas or mountains may have influenced wind characteristics over time. In total, we tried to collect all data which is available in the deserts of Iran.
For providing data, first of all, the data were arranged in Excel software then convert to notepad which change to acceptable format (Lake format) in WRPLOT software, version 8.0.1 (Lake Environment, 2012). In this way, it would be possible to get report of the percentage occurrence of wind by this software. The reports were arranged into 8 wind speed classes in 16 directions for all weather stations (e.g. for Zabol in Tale 3.1). Wind speeds> 40 knots are very rare and not computed in this study.

Table 3.1 Frequency of wind in different directions and wind speed classes in Zabol Station

Degree			Direction	Speed Classes (knot)								Total
min	mean	max		1_7	7_11	11_17	17_22	22_28	28_34	34_40	>40	
349	360 or 0	11	N	2.4	1.7	1.3	0.5	0.2	0.1	0.0	0.0	6.2
11	23	34	NNE	1.1	0.5	0.1	0.0	0.0	0.0	0.0	0.0	1.7
34	45	56	NE	0.6	0.1	0.0	0.0	0.0	0.0	0.0	0.0	0.7
56	68	79	ENE	1.0	0.4	0.1	0.0	0.0	0.0	0.0	0.0	1.5
79	90	101	E	1.7	0.5	0.1	0.0	0.0	0.0	0.0	0.0	2.3
101	113	124	ESE	1.1	0.5	0.1	0.0	0.0	0.0	0.0	0.0	1.7
124	135	146	SE	0.5	0.2	0.1	0.0	0.0	0.0	0.0	0.0	0.8
146	158	169	SSE	0.7	0.4	0.1	0.0	0.0	0.0	0.0	0.0	1.2
169	180	191	S	0.6	0.2	0.1	0.0	0.0	0.0	0.0	0.0	0.9
191	203	214	SSW	0.2	0.1	0.0	0.0	0.0	0.0	0.0	0.0	0.3
214	225	236	SW	0.3	0.0	0.0	0.0	0.0	0.0	0.0	0.0	0.3
236	248	259	WSW	0.7	0.2	0.0	0.0	0.0	0.0	0.0	0.0	0.9
259	270	281	W	1.3	0.8	0.1	0.0	0.0	0.0	0.0	0.0	2.2
281	293	304	WNW	1.3	1.2	0.6	0.2	0.1	0.0	0.0	0.0	3.4
304	315	326	NW	3.2	4.7	6.0	5.6	4.0	1.5	0.4	0.1	25.5
326	338	349	NNW	2.7	4.4	7.7	7.3	5.8	2.6	0.9	0.3	31.7
Total%				19.5	15.8	16.3	13.8	10.2	4.3	1.3	0.3	81.5

Calm:18.5%

(Source: own draft)

3.2.2 Sand transport calculations

For calculating sand drift potential (DP) and Resultant Drift Direction (RDD), Resultant Drift Potential (RDP) and the ratio of RDP/DP have been used Fryberger and Dean (1979) method. This method has been the most widely used in desert areas (Al-Awadhi et al. 2005; Jewell and Nicoll,

2011; Wang et al. 2005; Yang et al. 2014; Zhang et al. 2015; Zu et al. 2008). DP represents wind power and describes the potential maximum amount of sand transport for each wind direction that includes values above the threshold velocity (Fryberger and Dean, 1979). For comparing results of DP in study area with Fryberger's classes and other researches results, the speed data were changed to knot although Bullard (1997) estimates also in m s^{-1} and provides calibration relations to correct different units.

The rate of sand transport comes from Lettau and Lettau (1978) equation:

$$q = (C'' \rho/g)V^{*2}(V^* - V^*t) \qquad (3.1)$$

where q is the rate of sand drift; C″ is the dimensionless constant based on grain diameter; ρ is the density of air; g is the gravitational acceleration; V* is the shear velocity of wind; and V^*_t is the impact threshold shear velocity of wind. Fryberger and Dean (1979) simplified this equation as following as:

$$Q \alpha V^2 (V\text{-}V_t)\, t \qquad (3.2)$$

Q or DP is a proportion of sand drift, V is average of wind velocity at 10 meter of height, V_t is impact threshold wind velocity, and t is time wind blew. The threshold velocity was considered 12 knots (about 6.2 m s^{-1}) under dry conditions.

Fryberger and Dean (1979) described that the combination of $V^2(V\text{-}V_t)$ in the DP equation is a "weighting factor" so that strong winds are given higher weightings and weaker winds lower weightings. In order to calculate the weighting factor, we need the threshold velocity which was taken as 12 knots at 10-meter height as suggested by Fryberger and Dean, (1979). For calculation of weighting factor, the mean wind speed of a velocity category used into generalized Lettau and Lettau equation (equation 3.2) as it seen in table 3.2. The value of $V^2(V\text{-}V_t)$ is divided by 100 to reduce the magnitude of the weighting factor to allow sand roses plotting simple (Fryberger and Dean, 1979).

Table 3.2 Derivation of weighting factors for relative rate of sand transport (Fryberger and Dean 1979).

Wind speed (knot)	Mean velocity of winds	V^2	$(V\text{-}V_t)$	$V^2(V\text{-}V_t)/100$
11-16	13.5	182.3	1.5	2.7
17-21	19	361.0	7.0	25.3
22-27	24.5	600.3	12.5	75.0
28-33	30.5	930.3	18.5	172.1
34-40	37	1,369.0	25.0	342.

Additional DP, there are three indexes contain of resultant drift potential (RDP), resultant drift direction (RDD) and Unidirectional index (RDP/DP) that use in wind regime study.
The RDP describes the net sand transport potential when winds from various directions interact. After DP calculation for all wind category in different directions (N, NNE, NE, ENE, E, ESE, SE, SSE, S, SSW, SW, WSW, W, WNW, NW and NNW), RDP were calculated based on equation (3.3).

$RDP = (C2 - D2)^{0.5}$ (3.3)

$C = \sum(VU)\ Sin(\theta)$

$D = \sum(VU)\ Cos(\theta)$

(VU) vector units represents the DP in each wind direction (in this study, we grouped winds into 16 sand transport directions, θ is the angle of midpoint of each wind direction class measured clockwise from 0° 0r 360° ,north) .
RDD is the angular direction at clockwise from the geographical north and used to show the direction. In other word, it expresses the angle between RDP and the north in degree.

$RDD = \text{Arctan}(C/D)$ (3.4)

Unidirectional index (UDI) is the ratio of RDP/DP that shows directional variability. If the ratio of UDI values closes to 1 the wind regime will indicate a narrowly unidirectional with a single dominant drift direction, whereas if the values close to 0 there is a multidirectional wind regime with multiple significant drift directions environment. Fryberger and Dean, (1979) classified the wind regime of various desert areas using DP and the ratio of RDP/DP (table 3.3).

Table 3.3 The classification of wind energy environments using sand drift potential (DP) and directional variability (Fryberger and Dean, 1979)

DP (vu)	Wind energy environment	RDP/DP	Directional variability	Directional category
<200	Low	<0.3	High	Complex or obtuse bimodal
200-400	Intermediate	0.3-0.8	Intermediate	Obtuse to acute bimodal
>400	High	>0.8	Low	Wide to narrow unimodal

The results of sand drift potential plots known as sand rose. Sand rose plot is a circle vector histogram represents sand drift potential in the 16 direction of the compass. The arms of sand rose are proportional in length to DP from a given direction as computed in vector unit (vu). If this value is more than 50 mm, the length is scaled by a reduction factor, a number shows into the circle. The sand roses were plotted using power point software (e.g. Fig. 3.1 for Zahedan station).

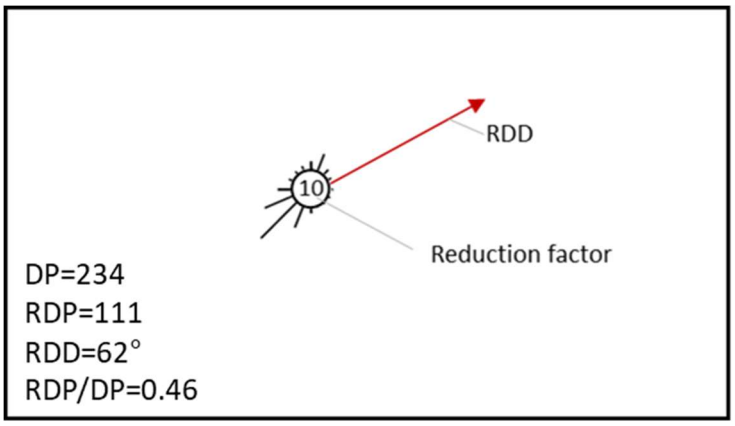

Fig. 3.1 Sand rose of Zahedan climatological station in period (1997-2013) (Source: own draft)

The spatial variations of DP were interpolated using ordinary kriging in geostatistical method with ArcGIS software version 10.3 (ESRI Inc.) over Iran sand dunes.

3.3 Sand dunes activity

3.3.1 Sand dunes distribution

In order to determine the distribution of sand dunes in Iran, we used sand dune maps in scale 1:25,000 that is provided by Research Institute Forests and Ranglands Iran (Abbasi et al. 2012). The extraction and mapping of the dominant sand dunes has been plotted from 2004 to 2009 using image processing, Landsat 7, 8 ETM data, aerial photographs, Google Earth scenes and integrated with field techniques (GPS) to check border (Fig. 2.2, page 23).

3.3.2 Sand dunes activity

Three sand dune models, the Lancaster mobility index, Tsoar mobility index and Yizhaq model were used to assessment dunefield activity in Iran's deserts. Regarding to this goal, Lancaster mobility index (1987) which developed based on the percent time wind above transport threshold (W%) and the ratio of precipitation to annual potential evapotranspiration (P/PET) were simulated in sand dunes of Iran. The ratio of P/PET is the aridity index which affected directly plants growing. This equation is as follow:

$$M = \frac{W\%}{P/PET} \qquad (3.5)$$

The percent time wind above transport threshold (W%) were calculated from hourly wind data frequency in Iran weather stations (see section 3.2.1). The annual potential evapotranspiration (PET) values were estimated by Thornthwaite equation (1948) by average monthly temperature in weather stations. To calculation of PET, the calculator online was used: (http://ponce.sdsu.edu/onlinethornthwaite.php). Thornthwaite equation (1948) works based on temperature which gives estimates of potential evapotranspiration on a monthly basis.

$$PET = 16\,(\frac{L}{12})(\frac{N}{30})(\frac{10T_d}{I})^{\alpha} \qquad (3.6)$$

Where PET is potential evapotranspiration in mm/month; Td is the average monthly temperature °C; N is the number of days in the month being calculated; L is the average day length (hours) of the month being calculated:

$\alpha = (6.75 \times 10^{-7})I^3 - (7.71 \times 10^{-5})I^2 - (7.71 \times 10^{-2})I + 0.49239$ (3.7)

$I = \sum_{i=1}^{12}(\frac{T_{m_i}}{5})^{1.514}$:is a heat index which depends on the 12 monthly mean temperatures.

Lancaster mobility index classified dunes as fully active (M>200), active dune with inactive interdune areas (200>M>100), active only on the dune crests (100>M>50), and inactive dunes (M<50). A key graph of sand dune mobility classification based on Lancaster's (1988) index with critical values is shown in Fig. 3.2 which was developed for 204 meteorological stations that used in this study.

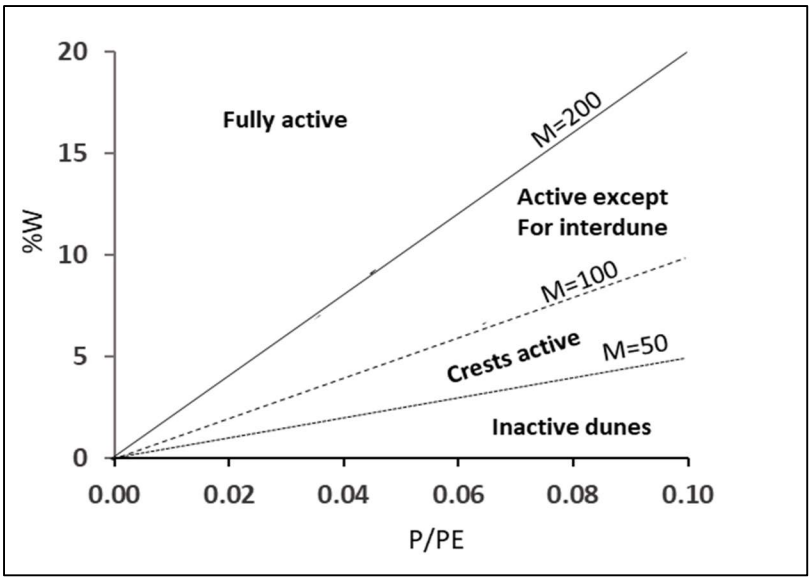

Fig. 3.2 Sand dune mobility classification graph based on Lancaster's (1988) index

Tsoar mobility index (2005) developed an experimental model based on wind power as the most significant factor in sand dunes activity and the effective winds characteristics. It is the mathematical expression of this line:

$$M = \frac{DP}{1000-(750\frac{RDP}{DP})} \qquad (3.8)$$

According to this index, where M>1 sand dune in areas are unvegetated and mobile and when M< 1 dunes are covered by vegetation or stabilized. This equation works where if the annual average rainfall is more than 50 mm. Tsoar (2005) believed That if DP increases above 400 (vu) dunes are active and above 1000 (vu) wind power over vegetated dunes will not cause the total extinction of vegetation. Regarding to this assumption, the graph of DP versus RDP/DP were used to classify the sand dunes of Iran (Fig. 3.3). As it is clear, the line between 400 and 1000 (vu) classifies active and vegetated dunes.

Another parameter in Tsoar mobility index is the ration of DP/RDP. when RDP/DP is low, wind energy is distributed on more than one slope of the dune and the energy exerted on each slope is lower than the same DP with high RDP/DP (Tsoar 2005).

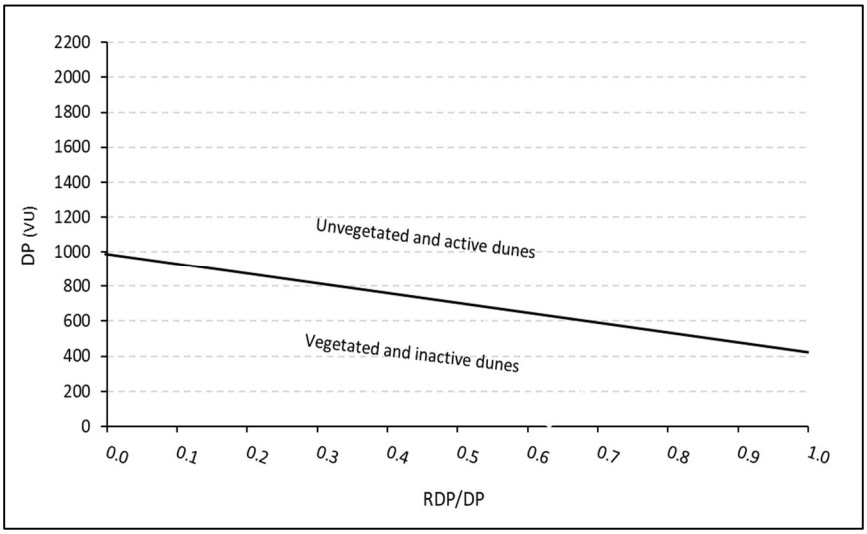

Fig. 3.3 A key of sand dune mobility classification graph based on Tsoar (2005) index

The model of Yizhaq et al. (2009) was simulated in sand dunes of Iran which is developed based on wind power, precipitation rate, and anthropogenic effects, such as grazing and wood gathering. It is a mathematical model as follows:

$$\frac{dv}{dt}=\alpha(p)(v+\eta)\left(1-\frac{v}{v_{max}}\right)-\varepsilon DPg\,(v_c,v)v\;-\;\gamma\,DP^{2/3}\,v-\mu v \qquad (3.9)$$

Where:

v: is the dynamical variable representing areal vegetation cover density, which takes values between 0 (bare dune) and V_{max}>1.

η: is a spontaneous growth cover parameter that describes an average cover due to spontaneous growth for even bare dunes because of soil seed banks, underground roots, seeds carried by wind, animals, etc.

v_{max}: denotes the maximum vegetation cover that the area can support, which depends on the type of vegetation and dune type. v_{max} may also be associated with the vegetation carrying capacity of the system.

α: a simple model that describes the growth of vegetation cover on sand dunes as a function of wind power. α (p) may be expressed between two limits as follow as:

$$\alpha = \begin{cases} \alpha_{max}(1 - \exp\left(-\frac{P - P_{\min}}{c}\right)) & P \geq P_{\min} \\ 0 & P \leq P_{\min} \end{cases} \qquad (3.10)$$

The estimated value of P_{min} is between 50 and 80 mm a^{-1} in the Nizzana (in the western Negev of Israel) area (Tsoar, 2005); Danin (1996) similarly defined 50 mm a^{-1} as the threshold precipitation needed for perennial growth. Yizhaq et al. (2009) also used P_{min} =50 mm a^{-1} to develop this model.

c: quantifies the precipitation-dependent transition range between α = 0 and α_{max}. c is related to the vegetative response to precipitation: larger values of c characterize shrubs, whereas smaller values are typical of herbaceous vegetation.

v_c: It is a critical vegetation cover (ground cover) which provides sufficient blocking for skimming flow, varies for different geographical locations for example, $v_c \approx$ 0.14–0.16 for the Kalahari desert (Wiggs et al. 1995; Wiggs, 2008) to observed $v_c \approx$ 0.35 for the Australian deserts (Ash and Wasson, 1983). Yizhaq et al. (2009) use a hyperbolic function for estimate of $\mathrm{g}(v_c, v)$ as follows;

$$\mathrm{g}(v_c, v) = 0.5(\tan\big(b(v_c - v)\big) + 1) \qquad (3.11)$$

where parameter b quantifies the steepness of the curve, the larger the value of b, the steeper is $\mathrm{g}(v_c, v)$. b can be estimated from field and wind tunnel experiments.

DP: Sand drift potential (see section 3.2).

ε : It stands for the vegetation tolerance to sand erosion and deposition. As ε decreases, tolerance increases.

γ: is a proportional constant that depends on vegetation types.

μ: It is a value that shows the extinction rate due to continuous human activity, such as grazing, clear cutting or burning so that negative values of μ represent stabilization activities and positive value represent effect human activity on vegetation.

For the assessment of the Yizhaq model in Iran, the logarithmic value of precipitation and DP have been used in graphs. Thus, the classification of Iran's sand dunes in three categories active, stabilized-active or semi active and stabilized became possible. As you see in Fig. 3.4, as a key graph of Yizhaq model, the function of v_c is defined for three statues, v_c= 0.2, 0.25 and 0.3. We prefer to use v_c= 0.3 because of shortage vegetation cover over dunes in Iran. This is due to less than 50 mm of rainfall in Yazd and Lut deserts and high aridity, high wind energy (Abbasi et al. 2019) as well as over grazing (Abolghasemi 2010; Filehkesh 2012) in the other deserts.

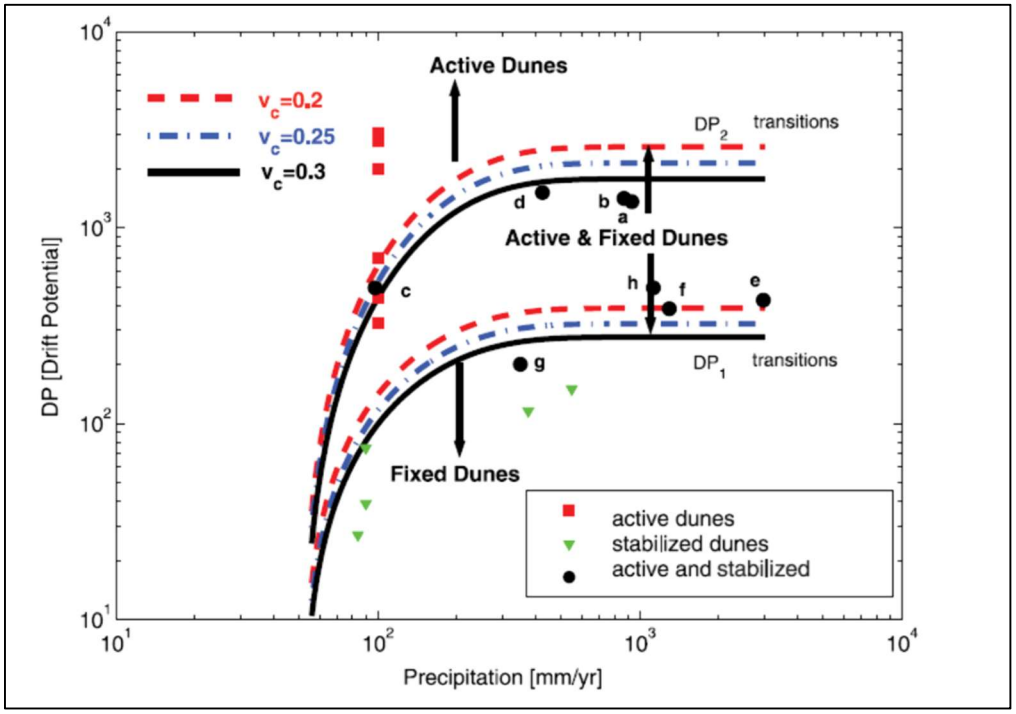

Fig. 3.4 A key of sand dune mobility classification graph based on Yizhaq et al. (2009) model

3.4 Wind regime and sand transport in Sistan and Registan

For the investigations of wind regime and sand transport in Sistan (Iran) and Registan (Afghanistan), 16 meteorological stations were selected in Sadobist Roozeh wind domain. The data of seven Afghanistan's stations derived from the Iowa State University Data Centre online site (www. http://mesonet.agron.iastate.edu/request/download.phtml?network=IR__ASOS) in duration 2011 to 2014 or 2016 and the data of nine Iranian weather stations provided from Iran meteorological organization (IMO) from 1995 to 2015. The speed and direction of hourly wind data were collected and DP, RDP, RDD and the ratio RDP/DP were calculated as well as wind roses and sand roses were plotted.

The characteristics of effective winds were assessed and the spatial variations of DP was interpolated using ordinary kriging in geostatistical method by ArcGIS software version 10.4

(www.esri.com). In addition, temporal variations of effective winds characteristics were investigated.

Dunes occur in a variety of morphological types in self-organized patterns as a response to the wind regime (especially its directional variability) and the supply of sand (Lancaster, 2009). In deserts, usually, dunes find compound or complex forms which made base a morphology classification as seen in Fig. 3.5 (Lancaster, 2005). Parabolic dunes and nebkhas dunes are controlled by the presence of vegetation and Crescentic (transverse), linear, star, and parabolic are free shapes of dunes. Sand sheets and Zibars are also dunes without shape.

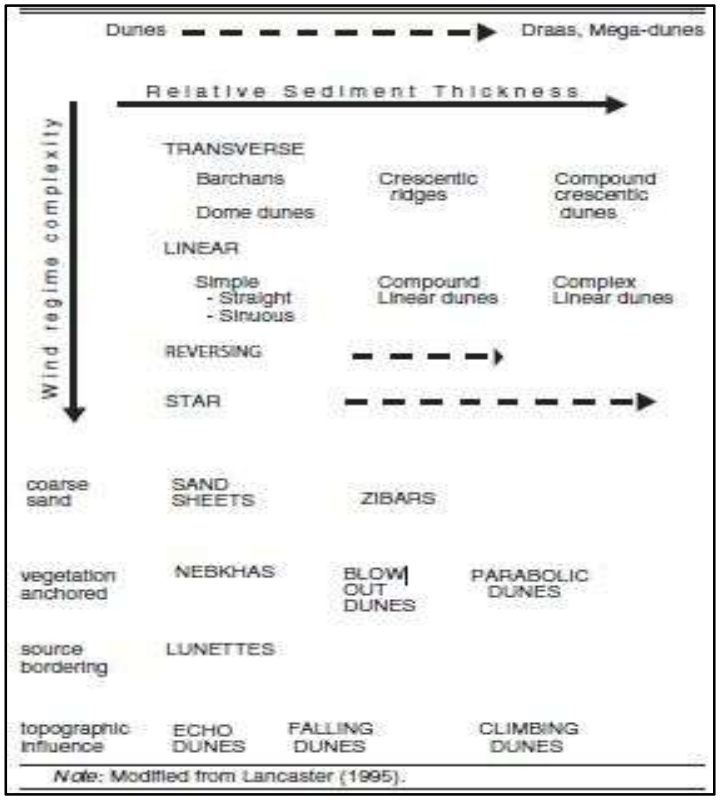

Fig. 3.5 Morphological Classification of Dunes (Lancaster, 2005)

According to this classification, dunes morphology in Sistan and Registan sand sea were mapped and assessment in the relation the directional of effective winds.

3.5 Spatial and temporal variations of the aeolian transport in Sistan

In order to assess aeolian sediment transport in the ephemeral Baringak Lake, we used a combination of meteorological data, field measurements, and geostatistical methods. For the meteorological information, hourly wind data from the Zabol station were adopted. Based on this

high temporal resolution data, seasonal wind roses were created in 36 sectors using the frequency of different wind speeds as a percentage of the total winds. In addition to this long-term analysis, the maximum daily wind speed data for the year 2013 was also plotted against the time.

For measuring the aeolian sediment transport, a network of 74 graduated pins was embedded in the surface soil of Baringak study area. This study area (20 km x 7 km) had been selected based on the interpretation of SDS satellite images (MODIS) and on-site experiences in which showed it produces major sand and dust source in the region. The positions of the pins were determined randomly and then recorded with GPS. All pins were embedded on the 5th of August 2013 and the aeolian transport rates were measured after SDS events on the 28th of August, the 15th of September and the 17th of November in 2013.

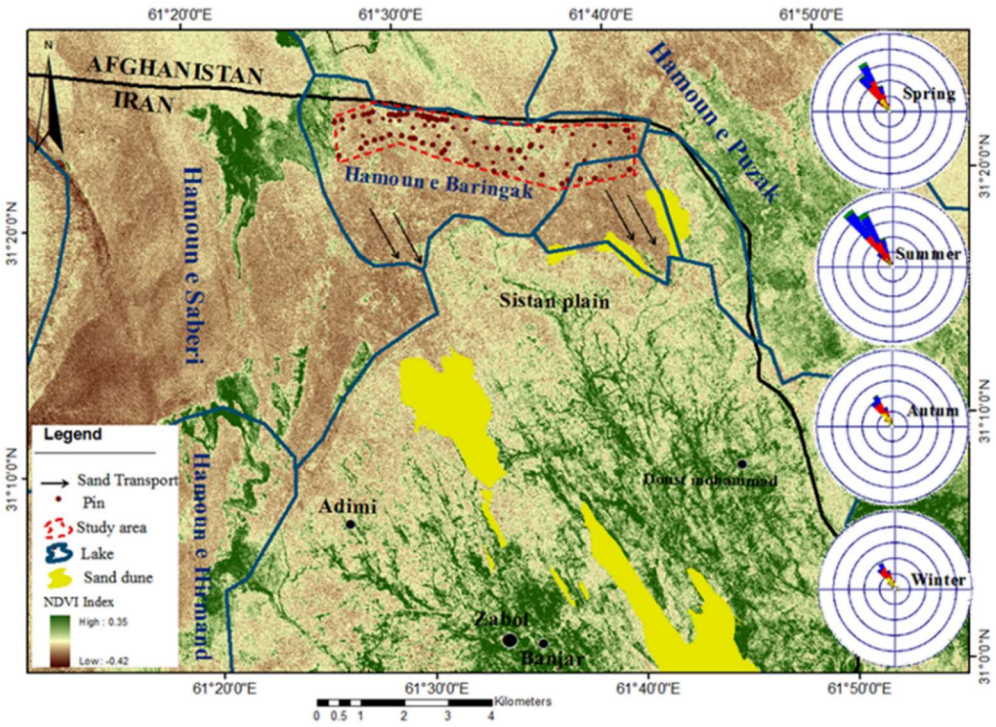

Fig. 3.6 The location of study area, erosion pins and sand transport direction in dried Baringak Lake, and seasonal wind roses in period (1995 - 2015) (Source: Abbasi et al., 2018, p.319)

Fig. 3.7 The general view of the dried bed Hamoun-e Baringak Lake and erosion pin

3.6 Geostatistical analysis

Geostatistics technique is widely applied in environmental research and technology in the three decades. This method is based on the assumption that the spatial and temporal variability includes a random component that has space–time correlation. There are several ways to interpolating data that Kriging is one of the main methods. It is a special way of interpolating and extrapolating control point values based on a multi-varied statistical approach (Veeken 2007). The variogram is the key function in geostatistics as it used to find a fit a model of the spatial correlation and temporal of phenomenon. A variogram is a function describing the degree of spatial dependence of a random spatial random data field or within a stochastic process, and it is a useful tool for the interpretation of the causes of spatial variations (Webster and Oliver, 2001). The shape of the variogram shows something about the rate of change in the data at their *XY* position. The collected field data have been used for the generation of variogram in order to analyze the spatial and temporal dependencies of the aeolian transport rate. A typical variogram has 3 important parameters, Sill, Range and Nugget Effect (Fig. 3.6).

Before analyzing data, the data were tested from point of normal distribution view for three and total period. All data had normal distribution except the second period data which changed to logarithmic data. After that, the data of sediment transport for each of the three periods and for the total duration have been analyzed in fitted models using variogram. In fact, the best fit models of the sediment transport were found for providing the needed spatial continuity. These models were selected based on the high spatial structure of the input data, and the good fit with the sill (C+Co) and nugget (Co) points used for the ordinary kriging. The range and sill parameters explain

the structure of the spatial variations and estimate the unsampled locations with the kriging method (Chappell and Oliver, 1997; Chappell and Agnew, 2001). The spatial interrelation of the sediment transport data was assessed by C/(C+CO), which ranges 0-1. If it stands near “1 “there is suitable spatial interrelation and stand near "0” there is weak spatial interrelation and high nugget effect.

The variogram analysis was carried out in GS+ (version 10) for each event of sediment transport using a fitted model based on an ordinary kriging method. The sediment transport rates were mapped using the geostatistical analysis extension in ArcGIS (version 9.3).

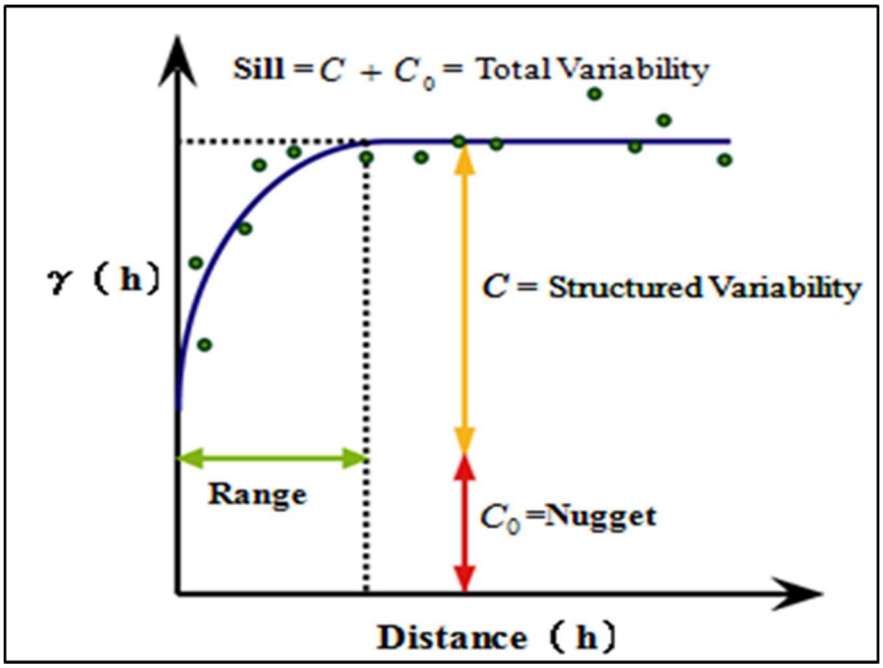

Fig. 3.8 A typical variogram and its important parameters (source: http://www.supergeotek.com)

The results of the kriging interpolation of the sediment transport rate have been cross validated for all three periods and the total duration. This validation focuses on the prediction issue, which evaluates the overall deviation of the predicted values from the observed values. This overall deviation is calculated by the mean absolute error (MAE) and the root-mean-square error (RMSE). The MAE indicates the accuracy of the fitted models and the resulting sediment transport maps.

Finally, the geostatistical analysis using the ordinary kriging mapped the sediment transport rates for each of the three periods as well as for the whole period of this study. The spatial and temporal variations of the transport were interpreted in relation to the frequency and intensity of winds for different periods.

3.7 References

Abbasi H.R., Opp, C., Khosroshahi, M., Rouhipour, H., Kashki, M.T., Dashtakian, K. (2014). Investigation of dune systems in Iran for a digital database and atlas of sand seas. The 3th National Conference Wind Erosion and Dust Storms in Iran,1 5-16 Jan., Yazd University (in Persian). https://www.civilica.com/Paper-ISADMC03-ISADMC03_100.html

Abbasi, H. R., Opp, C., Groll, M. Rohipour H., and Gohardoust, A. (2019), Assessment of the distribution and activity of dunes in Iran based on mobility indices and ground data, Aeolian Research Journal, Volume 41, December 2019, 100539 (in print). https://doi.org/10.1016/j.aeolia.2019.07.005

Abolghasemi, M. (2010). Study of seasonal changes of production and utilization of range plants in 5 Bioclimatic Zones of Iran, Tabas Site in Yazd Province, Research institute of Forest and Rangelands, Final research report no. 4-100-170000-02-8501-85003, 144 pp.

Al-Awadhi, J. M., Al-Helal, A., Al-Enezi, A. (2005). Sand drift potential in the desert of Kuwait. Journal of Arid Environments, 63(2): 425–438. https://doi.org/10.1016/j.jaridenv.2005.03.011

Chappell, A, Oliver, M. A. (1997). Geostatistical analysis of soil redistribution in SW Niger, West Africa. Quantitative Geology and Geostatistics, 8(2): 961–972.

Chappell, Adrian, Agnew, C. T. (2001). Geostatistical Analysis and Numerical Simulation of West African Sahel Rainfall. In A. J. Conacher (Ed.), Land Degradation: Papers selected from Contributions to the Sixth Meeting of the International Geographical Union's Commission on Land Degradation and Desertification, Perth, Western Australia, 20--28 September 1999 (pp. 19–35). https://doi.org/10.1007/978-94-017-2033-5_2

Filehkesh, S. (2012). Study of seasonal changes of production and utilization of range plants in 5 Bioclimatic Zones of Iran, Sabzevar Site in Khorasan Razavi, Research institute of Forest and Rangelands, Final research report no. 4-100-170000-02-8501-85003, 97 pp.

Fryberger, S. G, Dean, G. (1979). Dune forms and wind regime. In: McKee, E.D. (Ed.), A study of global sand seas. Professional Paper 1052, United State Geological Survey, US Government Printing Office, Washington, pp. 137–169.

Jewell, P. W., Nicoll, K. (2011). Wind regimes and aeolian transport in the Great Basin, U.S.A., Geomorphology, 129(1–2): 1–13. https://doi.org/10.1016/j.geomorph.2011.01.005

Lake Environment. (2012). WRPLOT view. https://doi.org/https://www.weblakes.com/products/wrplot/index.html

Lancaster, N. (1987). Formation and reactivation of dunes in the southwestern Kalahari: palaeoclimatic implications. Paleoecology of Africa, 18: 103–110.

Lancaster, N. (1995). Geomorphology of Desert Dunes. London, Routledge, 290 p.

Lancaster, N. (1988). Development of linear dunes in the southwestern Kalahari, southern Africa. Journal of Arid Environments, 14: 233–244.

Lancaster, N. (2009). Aeolian features and processes, in Young, R., and Norby, L., Geological Monitoring: Boulder, Colorado, Geological Society of America, p. 1–25, https://doi.org/10.1130/2009.monitoring(01).

Lettau, K., Lettau, H., 1978. Experimental and micrometeorological field studies of dune migration. In: Lettau, K., Lettau, H. (Eds.), Exploring the World's Driest Climate. University of Wis, Madison, pp. 110–147.

Thornthwaite, C. W. (1948). An approach toward a rational classification of climate. Geographical Review, 38(1): 55–94. https://doi.org/10.2307/210739

Tsoar, H. (2005). Sand dunes mobility and stability in relation to climate. Physica A: Statistical Mechanics and Its Applications, 357(1): 50–56. https://doi.org/10.1016/j.physa.2005.05.067

Veeken, C.H. (2007) Seismic Stratigraphy, Basin Analysis and Reservoir Characterization, Handbook of Geophysical Exploration: Seismic Exploration, 509 pp. https://doi.org/10.1016/S0950-1401(07)80029-2

Wang, X., Dong, Z., Yan, P., Zhang, J., Qian, G. (2005). Wind energy environments and dunefield activity in the Chinese deserts. Geomorphology, 65(1–2): 33–48. https://doi.org/10.1016/j.geomorph.2004.06.009

Webster, R. and Oliver, M. (2001) Geostatistics for Environmental Scientists Statistics in Practice. Wiley, Chichester, 271 p.

Yang, Y. Y., Qu, Z. Q., Shi, P. J., Liu, L. Y., Zhang, G. M., Tang, Y., Sun, S. (2014). Wind regime and sand transport in the corridor between the Badain Jaran and Tengger deserts, central Alxa Plateau, China. Aeolian Research, 12, 143–156. https://doi.org/10.1016/j.aeolia.2013.12.006

Yizhaq, H., Ashkenazy, Y., Tsoar, H. (2009). Sand dune dynamics and climate change: A modeling approach. Journal of Geophysical Research: Earth Surface, 114(1): 1–11. https://doi.org/10.1029/2008JF001138

Zhang, Z., Dong, Z., Li, C. (2015). Wind regime and sand transport in China's Badain Jaran Desert. Aeolian Research, 17: 1–13. https://doi.org/10.1016/j.aeolia.2015.01.004

Zu, R., Xue, X., Qiang, M., Yang, B., Qu, J., Zhang, K. (2008). Characteristics of near-surface wind regimes in the Taklimakan Desert, China. Geomorphology, 96(1–2): 39–47. https://doi.org/10.1016/j.geomorph.2007.07.008

4

Assessment of the Distribution and Activity of Dunes in Iran based on Mobility Indices and Ground Data[1]

Abstract

Sand dune movement causes severe damage to infrastructure and rural settlements in Iran every year. Identifying active dunes and monitoring areas with migrating sand are important prerequisites for mitigating these damages. With regard to this objective, the spatial variation of the wind energy environment based on the sand drift potential (DP) was calculated from 204 meteorological stations. Three commonly used dune activity models – the Lancaster mobility index (1988), the Tsoar mobility index (2005), and the index developed by Yizhaq et al. (2009) – used for the evaluation of Iran's sand dune activity. The analysis of the indices showed that the dune activity was characterized by great spatial variation across Iran's deserts. All three models identified fully active dunes in the Sistan plain, the whole of the Lut desert, as well as in the Zirkuh Qaien and Deyhook regions, while the dunes in the northern part of Rig Boland, Booshroyeh and in the Neyshabor dunefields were categorized as stabilized dunes. For other dunes, the models show a less unified activity classification, with the Lancaster and Yizhaq models having more similar results while the Tsoar model stands more apart. Based on these model results and fields observations, a modified Lancaster mobility index has been applied to show a more realistic spatial variation of sand dunes activity in Iran's desert areas.

Key words: Iran, sand dunes; dune mobility index; wind energy; active dune.

1- Based on Abbasi H.R., Opp C., Groll M., Rohipour H., and Gohardoust A., in Aeolian research 41 (2019).

4.1 Introduction

Deserts cover 907,293 km2 of Iran (Khosroshahi et al. 2009), and sand dune fields are scattered across the arid and rarely the semiarid areas of Iran. Sand seas or Ergs are also known as a "Reg", "Rig" or "Rek" in Iran, Afghanistan, Pakistan, and Tajikistan and the name "Registan" means "sand is accumulated". Very limited studies have been published regarding the sand dunes of Iran (e.g. Ekhtesasi and Dadfar, 2014; Feiznia et al. 2016; Mashhadi and Ahmadi, 2010); and dune morphology in relation to wind regime (Abbasi et al. 2019; Mashhadi et al. 2007; Mesbahzadeh and Ahmadi, 2012; Nazari et al. 2017) but no comprehensive reviews on a national scale are available to the English speaking international scientific community. Ehlers (1980) was the first one to provide a land use map of Iran showing sand dunes covering 182,900 km^2. Mahmmodi (2002) published a book (in Persian) entitled "Sand Seas Distribution of Iran" which covers around 35,385 km^2 (without considering sand sheets and the Nebka dunes). After that, Abbasi (2012) produced sand dune distribution maps using satellite images (Landsat 7 and 8), aerial photographs, Google Earth scenes integrated with field operations. The results of that study showed that the extraction and mapping of the dominance and morphology of sand dunes was carried out in a scale of 1:25,000, which revealed that dunes in Iran extended to 11 sand seas and 97 dune fields, which cover approximately 4.6 million hectares (Table 4.1). Most of the sand dunes in Iran occur in and around the Dasht Kavir and Lut deserts. Dasht Kavir desert is mostly uninhabited and it is the largest desert in north-central of Iran, predominantly characterized by crusty salt ridges and salty marshlands. It is an important source of sand and dust storms during the dry season and therefore Rig Boland, Rig-e Jinn and the Rig-e Khartoran sand seas and several dune fields have formed in and around this desert (Fig. 4.1).

The Lut desert in south-eastern Iran is surrounded by mountains which affect the formation and morphology of the Yalan (Lut) sand sea. It is the largest sand sea in the country, formed by multidirectional winds and the special topography (Lorenz et al. 2015). A survey by the Kerman Agriculture Jihad Organization in 2018 estimated that sand storms lead to annual farmland and garden damages of $4.2 million (640 bln rial) in Rigan (IRNA, 2018) in the southern parts of the Lut desert, a county with a population of just 53,000.

The Jazmorian sand sea, as the second vast sand sea in the country, extends along the north and south of the Jazmorian ephemeral Salt Lake. It features dunes in two parts: one part located south of the ephemeral lake between Iranshahr and Galaeh Ganj in the Sistan and Baluchistan provinces, and a smaller part northwest of the desiccated lake, called the Rudbar dune field in the Kerman province. The Sistan sand dunes originate from the Hamouns ephemeral Lakes in Iran and extend to the Registan sand sea in southern Afghanistan and are strongly influenced by the Sadobist Roozeh (the wind of 120 days) wind (Abbasi et al. 2019). In march 2016, a major sand storm in this region caused extensive socioeconomic disruptions and shifting sand damaged crops and urban infrastructures with a value of more than $71 million in the Sistan plain (Oshida, 2016).

Other dune areas in Iran include the Khuzestan sand sea, also known as the Karkheh sand sea, extending from Iraq into the Ilam and Khuzestan provinces in Iran, as well as coastal dunes formed

near the Persian Gulf and the Omman Sea beaches between the southern Iranian cities of Chabahar and Bushehr.

Table 4.1 Important sand seas and dune fields in Iran (Abbasi, 2012)

The name of Sand dune	Area (km^2)	%
Rig-e Yalan (Lut) sand sea	11529	24
Rig-e Jazmorian sand sea	5588	12
Rig-e Jinn sand sea	4512	9.6
Rig-e Khuzestan sand sea	2614	5.6
Rig-e Shotoran sand sea	2612	5.5
Rig-e Zir kuhe Qaien sand sea	2208	4.7
Rig-e Khartoran sand sea	2081	4.4
Rig Boland and Dag-e Sork sand sea	2013	4.3
Rig-e Sarakhs sand sea	813	1.8
Sistan dune field	641	1.4
Rig-e Booshroyeh sand sea	623	1.3
Coastal dune fields (Persian and Omman Gulf)	1039	2.2
Other dunefields	10082	22
Total	46355	100

Climatic factors, wind and water erosion, population pressure, over-exploitation of water resources, and over-grazing have been identified as the main reasons for desertification in Iran (NAP, 2004). A survey by the Iranian Forest, Rangeland and Watershed Management Organization (FRWO) reported that wind erosion causes annual damages of more than > 18.3 bln USD (IRI-Mal, 2017). Therefore, the stabilization of sand dunes has been a major objective of programs to combat desertification during the past half century. The main method of dune stabilization in Iran is a combination of oil mulch spraying and tree plantation. This method, as a common technique for sand dune stabilization, has been used first on the Khorasan and Khuzestan sand dunes in 1965 (NIOPDC, 1967). Oil mulch, which is a hydrocarbon colloid extracted from petroleum, stabilizes shifting sands, preserves soil moisture and assists to establish vegetation cover (Kowsar et al. 1969). Amiraslani and Dragovich (2011) provided a list of major plant species used in Iran's desertification projects in different provinces of Iran. In order to control wind erosion and carbon sequestration, more than 2 million hectares of dry forests (mostly *Haloxylon sp.*) have been planted around and on top of Iran dunes during the last fifty years.

Sand dune activity is defined as changes in migration rates and/or variations in the amount of sand shifting on the dune itself (Thomas 1992). Bullard et al. (1997) provided a comprehensive literature review on various sand dune mobility models, as seen in Table 4.1. Wilson (1973) developed one of the earliest dune activity models, using annual average rainfall as a factor determining mobility.

On a global scale he separated active from stable dunes by a precipitation threshold of 150 mm. Ash and Wasson (1983) presented two dunes mobility indexes (equations (4.1) and (4.2) in Table 4.2) based on precipitation as well as on actual and potential evapotranspiration in Australia, which was immediately modified by Wasson in (1984) by adding the percentage of time with wind speeds above the transport threshold parameter (W%) (equation 4.4). Lancaster (1987) adapted this model for dunes in the south-western Kalahari (equation 4.5). One year later he simplified his dune mobility index (M) as he based it on W% and the ratio of precipitation to annual potential evapotranspiration (P/PET) in 1988 (equation 4.6). He classified dunes as fully active (M>200), active dune with inactive interdune areas (200>M>100), activity only on the dune crests (100>M>50), and inactive dunes (M<50). The Lancaster mobility index (abbreviated LMI in this paper) is used widely in discussing dune activity under different climate conditions in the global sand seas and dune fields (e.g. Bullard et al. 1997; Gaylord and Stetler 1994; Lancaster 1997; Lancaster and Helm 2000; Muhs and Maat 1993; Muhs and Holliday 1995; Muhs et al. 2003; Tsoar and Blumberg 2002; Wang et al. 2007; Wolfe 1997).

In more recent years, Tsoar (2005) developed an experimental model based on the assumption that the wind power is the most significant factor in sand dunes activity and thus his model uses the effective winds characteristics for different sand dune sites (equation 4.7). The model assumes that dunes are active under high wind power and vegetated under low wind power if rainfall is above 50 mm and there is no human pressure. Wind power, which grows with the cube of the wind velocity, is expressed as the drift potential (DP), which is generally calculated based on Fryberger and Dean's (1979) method according to this equation:

$$DP = V^2(V - V_t)t \qquad (4.10)$$

Where DP is the sand drift potential in vector units (vu), V is wind velocity at 10 m above ground, Vt is the threshold wind velocity (set at 12 knots or about 6.2 m s-1) under dry conditions and t is the time for which the wind speed was above the threshold.
The unidirectional index is the ratio of the resultant drift potential (RDP) to the drift potential (DP) and shows the directional variability of the wind (equation 4.11).

$$RDP = (C2 - D2)^{0.5} \qquad (4.11)$$

$$C = \sum(VU)\, Sin(\theta)$$

$$D = \sum(VU)\, Cos(\theta)$$

The vector units (vu) in above formula represents the DP in each wind direction (in this paper, the wind directions were grouped into 16 direction classes of sand transport), θ is the midpoint angle of each wind direction class measured clockwise from 0° or 360° (north).

Table 4.2 Sand Dune Mobility Models

Reference	Equation	Threshold Value	Region in which developed
Wilson (1973)	–	Dunes active when rainfall < 150	The world map
Ash and Wasson (1983)	$M = [5 \times 10 - 4(P)^2]/(\frac{AP}{PE})$ (4.1) $M = [3.8 \times 10 - 4(U)^4](\frac{AP}{PE})$ (4.2)	Mobility occurs when M≥1.0	Australia
Talbot (1984)	C = $V^3/(P)^2$ (4.3)	C<10, dunes inactive 5<C<10, limited aeolian activity C>10, dunes active	Sahel
Wasson (1984)	$M = 0.21(0.13W + ln\frac{PET}{P})$ (4.4)	Mobility occurs when M≥1.0	Australia
Lancaster (1987)	$M = 0{\cdot}25(0{\cdot}10W + ln\frac{PET}{P})$ (4.5)	Mobility occurs when M≥1.0	Southwest Kalahari
Lancaster (1988)	$M = \frac{W\%}{P/PET}$ (4.6)	>200, dune fully active 100–200, dunes active and interdunes inactive 50–100, crest areas only active <50, dunes inactive	Southwest Kalahari , Namib, Mojave deserts
Tsoar (2005)	$M = \frac{DP}{1000 - \left(750\frac{RDP}{DP}\right)}$ (4.7)	M<1 Covered by vegetation M>1 Uncovered by vegetation	Several deserts
Yizhaq et al. (2007)	$\frac{dv}{dt} = \alpha(v+\eta)\left(1 - \frac{v}{v_{max}}\right) - \varepsilon\, DP\, \theta(v_c - v)v - \gamma\, DP^{2/3}\, v$ (4.8)		Several deserts
Yizhaq et al.(2009)	$\frac{dv}{dt} = \alpha(p)(v+\eta)\left(1 - \frac{v}{v_{max}}\right) - \varepsilon\, DP\mathrm{g}\,(v_c, v)v - \gamma\, DP^{2/3}\, v - \mu v$ (4.9)		Several deserts

Definitions: M = mobility, P = annual precipitation, PE = annual potential evapotranspiration, AP = actual annual evapotranspiration, C = wind erosion factor, U = V–Vt, V = mean annual wind speed, Vt = threshold wind velocity, W =percent of time wind above transport threshold, DP=drift potential, v= the dynamical variable representing areal vegetation cover density, ε= stands for the vegetation tolerance to sand erosion and deposition, γ= proportional constant of vegetation types, η = A spontaneous growth cover parameter,

(Source: Bullard 1997, changed by Abbasi et al. 2019, in print)

Tsoar (2005) indicated that when RDP/DP is high, the winds blows unidirectional and the wind energy is highly effective on the dune mobility, while a low RDP/DP exerts the effective wind on different slopes of dune. If RDP/DP stands close to 1 it indicates a narrow unidirectional drift potential, and if it stands close to 0 it indicates a wide multidirectional drift potential.

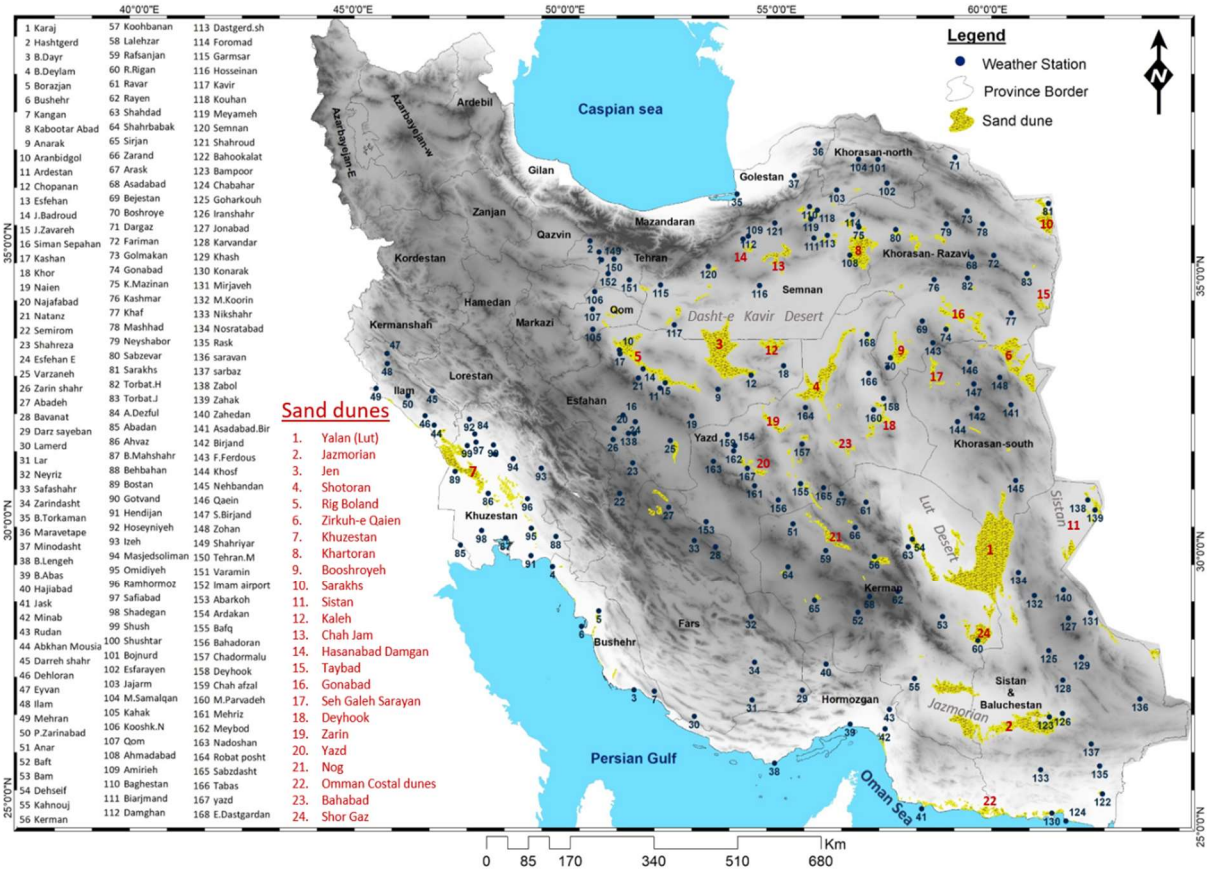

Fig. 4.1 Sand dunes distribution and location of meteorological stations used in this study (Source: Abbasi et al. 2019, in print)

The Tsoar mobility index (TMI) is valid above 50 mm/yr rainfall and classifies dunes into “covered by vegetation or stabilized” (M<1) and “uncovered by vegetation or active (M>1). This model has been developed in 43 dune fields (e.g. in the Negev desert) and was also tested on coastal dunes in Ceará (Brazil). The DP ranged from 692 to 2173 VU and the annual rainfall went up to 1443 mm (Tsoar et al. 2009). Based on these tests the TMI concludes that vegetation will start covering the sand dunes when the wind power falls below 1000 DP (Tsoar, 2005).

Yizhaq et al. (2007) developed one of the most recent mathematical models for simulating dune activity with respect to wind power and vegetation cover (equation 4.8 in Table 4.2) and then further improved it based on wind power and precipitation rates (equation 4.9) under similar climatic conditions (Yizhaq et al. 2009). In these models, wind power determines the sand transport capacity, while the vegetation cover, which, in turn, is controlled by the precipitation, determines the amount of the sand available for transportation. Both models classify dunes as

fixed, active or partially active, but fixed dunes can be reactivated during very strong winds and stabilized again once the wind power decreases (Yizhaq et al. 2009).
Ashkenazy et al. (2012) investigated the future activity of currently fixed dune fields in the Kalahari and in Australian deserts based on Yizhaq's model in two climate change scenarios and demonstrated that both dunes fields remain stable until the end of the 21st century because the DP will stay small and precipitation will remain above the minimal threshold necessary for vegetative growth.
The aim of this study is to provide an integrated analysis of the spatial variations of the wind energy based on DP and sand dune activity in Iran. In order to assess the dune activity, the Lancaster mobility index (LMI), the Tsoar mobility index (TMI) and the Yizhaq model were applied and compared. Based on the results of this comparison and supported by extensive field observations, the Lancaster mobility index has been modified to better represent the activity of the Iranian dunes.

4.2 Material and methods

In order to determine the distribution of sand dunes in Iran, we used sand dune maps in scale 1:25 000 that provided by Research Institute Forests and Ranglands Iran (Abbasi et al. 2012). The speed and direction of hourly wind data were recorded in intervals for 1 or 3 hourly for 24 h per day at height of 10 m above the ground were obtained from 204 meteorological stations (near 39 million records) in and around Iran deserts (Fig. 4.1) from Iran Meteorological Organization (IMO). The data cover the period 1994 to 2013, but some stations are shorter due to data limitations.

The percent time wind above transport threshold (W%), was considered 12 knots or 6.2 m s^{-1}, were also calculated for weather stations. Potential evapotranspiration (PE) values were generated using Thornthwaite's (1948) method using calculator online (http://ponce.sdsu.edu/onlinethornthwaite.php). Sand drift potential (DP), Resultant drift potential (RDP) and the ratio of RDP/DP have been calculated using Fryberger and Dean (1979) method according to equations 4.10 and 4.11. The spatial variation of DP was interpolated using ordinary kriging in geostatistical method with ArcGIS software version 10.3 (ESRI Inc.).
Three sand dune models, the Lancaster mobility index (LMI), Tsoar mobility index (TMI) and Yizhaq model (Equations 4.6, 4.7 and 4.9 in Table 4.2), were calculated and compared to assessment dunefield activity for each station around Iran's deserts.
Finally, according to winds characteristics and dunes activity in some parts of Iran's desert, we modified Lancaster model regarding to wind power and sand transport feature in Iran.
The spatial variation of mobility indexes was interpolated using ordinary kriging in geostatistical method with ArcGIS software version 10.3 (ESRI Inc.).

4.3 Results

4.3.1 Spatial variability of sand drift potential

Climatic conditions in Iran are mainly controlled by the pressure systems of the westerly cyclones, the Siberian high pressure and the southwest Monsoon airstreams (Kehl, 2009). During the dry season, when sand and dust storms are a common phenomenon, four wind regimes are predominant in Iran's deserts: (I) the Shamal wind from north-western direction, which covers most parts of Iran and Iraq, (II) westerly cyclones or the prevailing westerlies, which blow from the west to the east in the middle latitudes, (III) the Sadobist Roozeh wind as a very strong northerly or north-westerly wind covering the east and southeast of the country, and (IV) an intense south-westerly wind or monsoon, which dominates over the eastern parts of the Omman Sea (Abbasi et al. 2019; Alizadeh-Choobari et al. 2014; Chaichitehrani and Allahdadi, 2018; Bou Karam et al. 2017; Garzanti et al. 2013; Rashki et al. 2019; Shao et al. 2011; Yu et al. 2016).

In addition, the irregular topography and large mountain ranges in and around Iran's deserts affect the surface winds, sand transport and dune formation. Alborz and Zagros, the two main mountains ranges surrounding Iran's deserts, and other small mountain ranges, like Karkas, Kuhbanan, Makran, Barez and Bazman mountains, are located into the central deserts of Iran. The Sadobist Roozeh wind accelerates into a corridor between the Hindu-Kush Mountains in Afghanistan and the Bageran and Ahangran Mountains in southern Khorasan (Abbasi et al. 2019; Whitney , 2006). Zir kuhe Qian, Sistan and Registan and a part of Yalan (Lut) sand seas are formed by this Sadobist Roozeh wind. In addition, several dune fields are formed in association with topography obstacles e.g. Rig-e Jinn, Zirkuh Qaien, Rig-e Talhe, Rig-e Kuhe Gogerd and the Booshroyeh sand dunes.

The spatial analyses of the drift potential showed considerable variation from high to low energy environments in the arid and semiarid areas of Iran between 1994 and 2013 (Fig. 4.3). Fryberger and Dean (1979) classified the wind energy environment based on DP (vu) into high (DP>400), moderate (200<DP<400) and low (DP<200). The highest levels of annually DP occurred in the Sistan plain with 2,516 and 1,716 (vu) in Zabol and Zahak (Abbasi et al. 2019). High wind energy environment also occurs in the eastern and southern Lut desert (Nosratabad, Karvandar, R. Rigan, Khusf), the northern and central part of Dasht-e Kavir desert (Hosseinan, Damgan, Torood, Kalateh Mazinan, Dastgerd Shahroud), Zir Kuh Qaien region (Zohan, Khaf, Asadabad), the western of Jazmorian (Kahnoj), Deyhook in Yazd province and the western edge of Khuzestan border (Abkhan Mousian), as seen in Fig. 4.2.

Moderate wind energy environment covers most of Iran's deserts e.g. the central-west part of Dasht-e Kavir desert (Kavir or Caravanserai Shah Abbasi), the western and south-western parts of the Lut desert (Shahdad, Daheseyf, Mohammadabad Koorin, Bam), the south-eastern and western parts of the Khuzestan province (Bostan, Mahshahr, Omidiyeh, Hendijan) and the Omman Sea coast from Jask to Konarak. A low energy wind environment can be found in the southwest of Dasht-e Kavir desert (Kashan, Aran Bidgol, Natanz, Janglbani Badroud, Jangalbani Zavareh), the eastern part of Jazmorian (Bampoor, Iranshahr), Sarakhs, Ferdous, Booshroyeh, Gonabad and the central and northern parts of Khuzestan province (Ahvaz, Shush, Shushtar and Ramhormoz), Sabzevar and Neyshabor region.

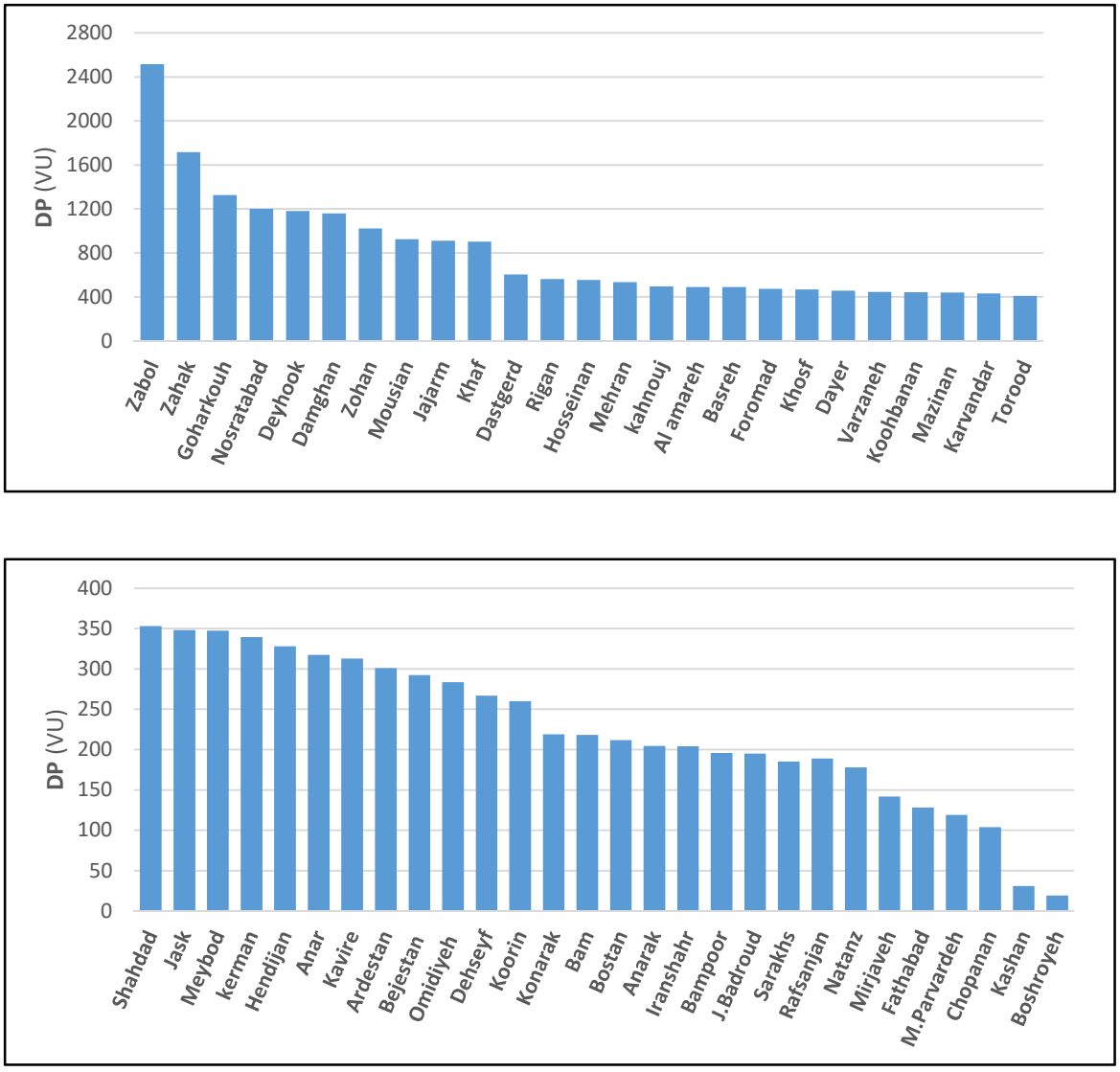

Fig. 4.2 Annual drift potential (DP) at selected meteorological stations near sand dunes in Iran (Source: Abbasi et al. 2019, in print)

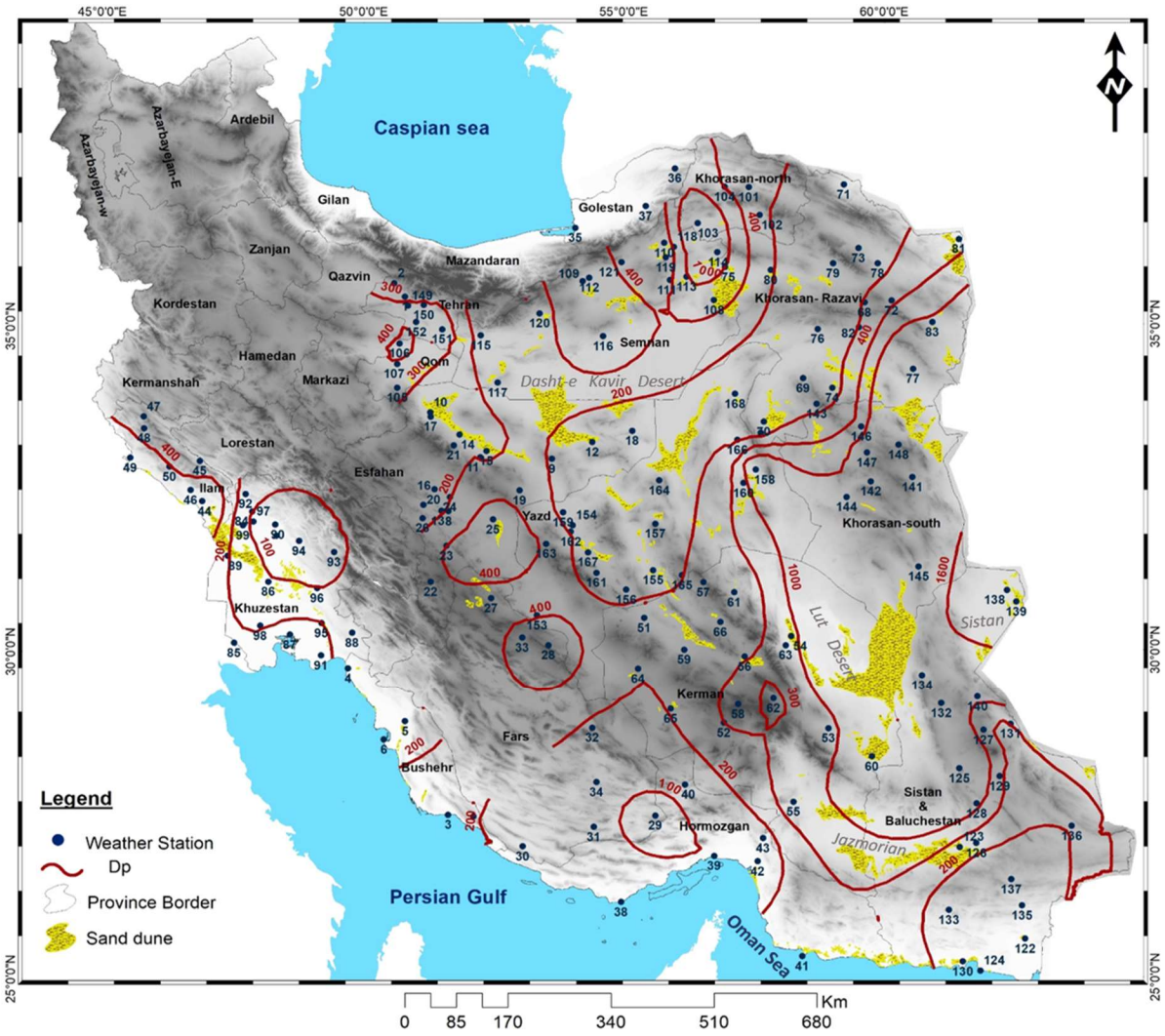

Fig. 4.3 Spatial variation of sand drift potential (DP in vu) in Iran's deserts (Source: Abbasi et al. 2019)

4.3.2 Lancaster mobility index

The long-term mean annual rainfall for the arid and semi-arid regions in Iran is 141 mm (Modarres and da Silva 2007) and at the stations selected for this study the annual precipitation ranged from 31 mm in Shahdad (western Lut desert) to 298 mm in Shushtar in Khuzestan, with an average of 144 mm. The annual potential evapotranspiration was calculated at 1572 mm/yr, with a range between 789 and 3969 (mm/yr) in Foromad and Shush, respectively.

Analysis of the LMI revealed a considerable spatial variation over the Iranian sand dune system from very active to inactive categories (Fig. 4.4 and 4.5), following the distribution of the wind power, precipitation and potential evapotranspiration. Fully active dunes (LMI>200) were detected in the whole Lut desert, due to the low precipitation of 30-40 mm, high

evapotranspiration (in the western and southern parts) and frequent strong winds (in the eastern part). Other regions with fully active dunes were the central and southern parts of Dasht-e Kavir as well as in the whole of Sistan, Baluchistan, and in some parts of the Yazd and Khorasan provinces. In Sistan, for example, the combination of the 120 days wind, which enables sand transport during 40-46% of the time, low precipitation (53-103 mm) and a high potential evapotranspiration (1230-1608 mm/yr) leads to the formation of active dune fields. Especially the values of the potential evapotranspiration in Sistan and western Afghanistan are among the highest rates recorded around the globe (Afghan Institute of Meteorology, 1978; Dittmann, 2014). Regarding to the LMI, the Shotoran, Rig-e Jinn, Deyhook, and Sagand sand dunes in central Iran were fully active dunes as well. These results were confirmed by field observations with the exception of the southern part of Rig-e Jinn (Chopanan).

In addition, the coastal dunes in the Omman Sea region from Konarak to Jask are fully active because of moderate to high percentages of wind speeds above the transport threshold (23-31%), rainfall (97-196 mm) and a high potential evapotranspiration (2002-2491 mm/yr).

There is considerable variation of dune activity in the Jazmorian sand sea so that the Iranshahr and Bampoor meteorological stations, in the eastern part, were classified as fully active due to high evapotranspiration. But field observations rather indicate that these dunes are inactive because of the low frequency of wind speeds above the transport threshold (12-17%) and existing vegetation cover. Due to summer rainfall, which was created by the SW-monsoon system in Baluchistan (Babaeian, 2017; Saligheh and Sayadi, 2017), Capparis decidua trees stabilized the western parts of the Jazmorian sand dunes, as shown by (Keneshloo and Damizadeh, 2015). The activity of dunes generally increased towards the central and western part because the frequency of higher wind speeds increased to 26% at the Kahnouj meteorological station.

The Khuzestan sand sea extends from Iraq into the Ilam and Khuzestan provinces in Iran. The Iraqi part, Ilam and the western border of Khuzestan are active due to a high percentage of times with wind speeds above the transport threshold (26-41%). From there it decreases rather sharply towards the central area near Ahvaz, which only showed a low percentage (5-7%) of threshold excess. In the south-eastern part of the Khuzestan sand sea, the dune activity increases again because the wind speed percentage above the threshold reaches up to 18-20%. Rouhipour (2006) measured the migration rate of dunes in the central Khuzestan sand sea, between Ahvaz and Andimeshk cities, to be an average of 1 m/yr, with more movement towards the crest.

Regions with partly active dunes (100<LMI<200) were registered mainly in the Khartoran, central and south-eastern parts of Rig Boland sand seas, as well as in the Nog, Tabas, Sabzevar, and Hasanabad dune fields. The Khartoran sand sea had almost constantly active dunes except for the interdunes with 20-22 % of all winds above the transport threshold and a P/PET ratio of 0.14-0.18. The Sarakhs sand sea, Kerman, Minab, and Chabahar dune fields showed active dune crests (50<LMI<100) because of the low percentage of winds above the transport threshold. In these regions, the ratio of P/PET ranged from 0.07 to 0.18 and the annual frequency of sand-transporting winds from 5 to 16%.

Inactive dunes (LMI<50) are widespread in the northern part of Rig Boland (around Kashan and Aran Bidgol) and in the Booshroyeh sand sea. In these regions, the ratio of P/PET ranged from 0.10 to 0.12 and W% ranged from 2 to 4%.

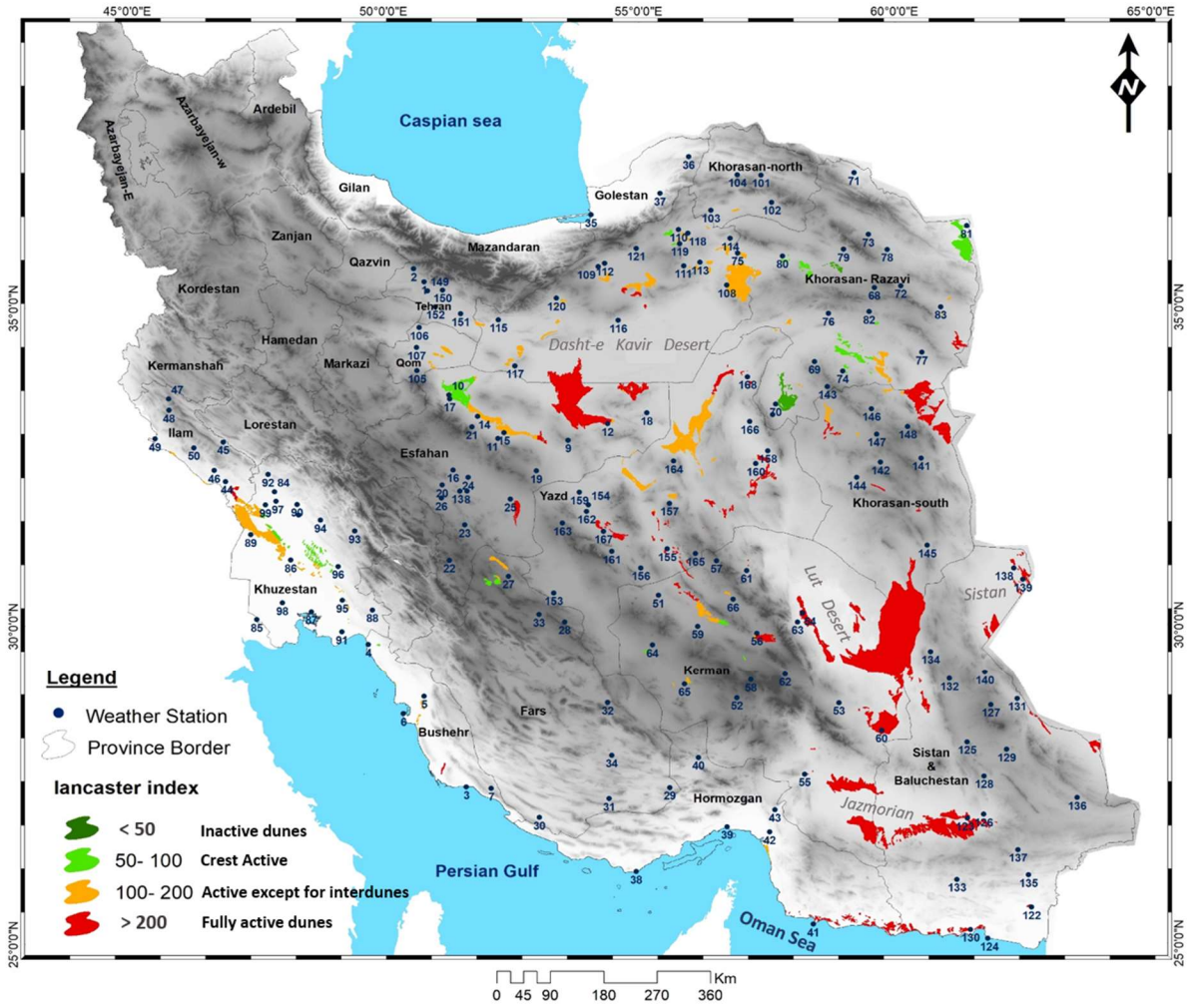

Fig. 4.4 Sand dune activity in Iran's deserts based on Lancaster's (1988) mobility index (Source: Abbasi et al. 2019, in print)

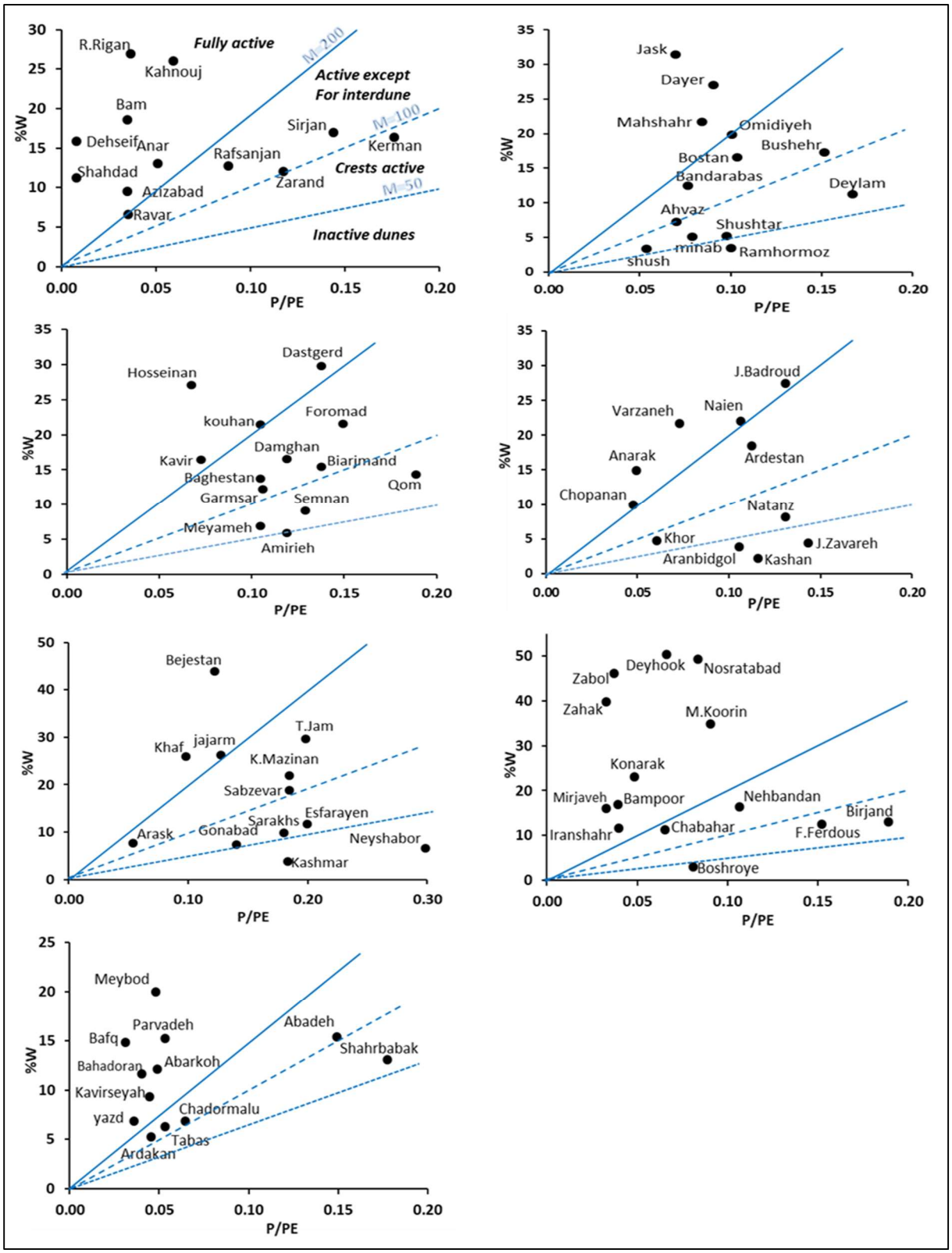

Fig. 4.5 Dune field mobility in Iran's deserts based on Lancaster's (1988) index (Source: Abbasi et al. 2019, in print)

4.3.3 Tsoar mobility index

The analysis of the Tsoar mobility index (TMI) (Tsoar, 2005) indicated that most of Iran's deserts fall into the "inactive and vegetated (M<1)" and partially into the "unvegetated and active (M>1)" categories (Fig. 4.6).

Regarding to the TMI, active dune fields were detected in Sistan, most parts of the Lut desert, the western part of Jazmorian, the northern regions of the Dasht-e Kavir desert, Zirkuh Qaien, and small part of Yazd desert (Fig. 4.7). In these regions, DP ranged from 410 to 2516 (vu) and the RDP/DP ratio was between 0.17 and 0.97.

As the TMI works only where the annual average rainfall is above 50 mm, the sand dunes in the western parts of the Lut desert (Dehsief, Ravar) and in some parts of the Yazd province (Yazd and Bafg) were assumed primarily "unvegetated and mobile".

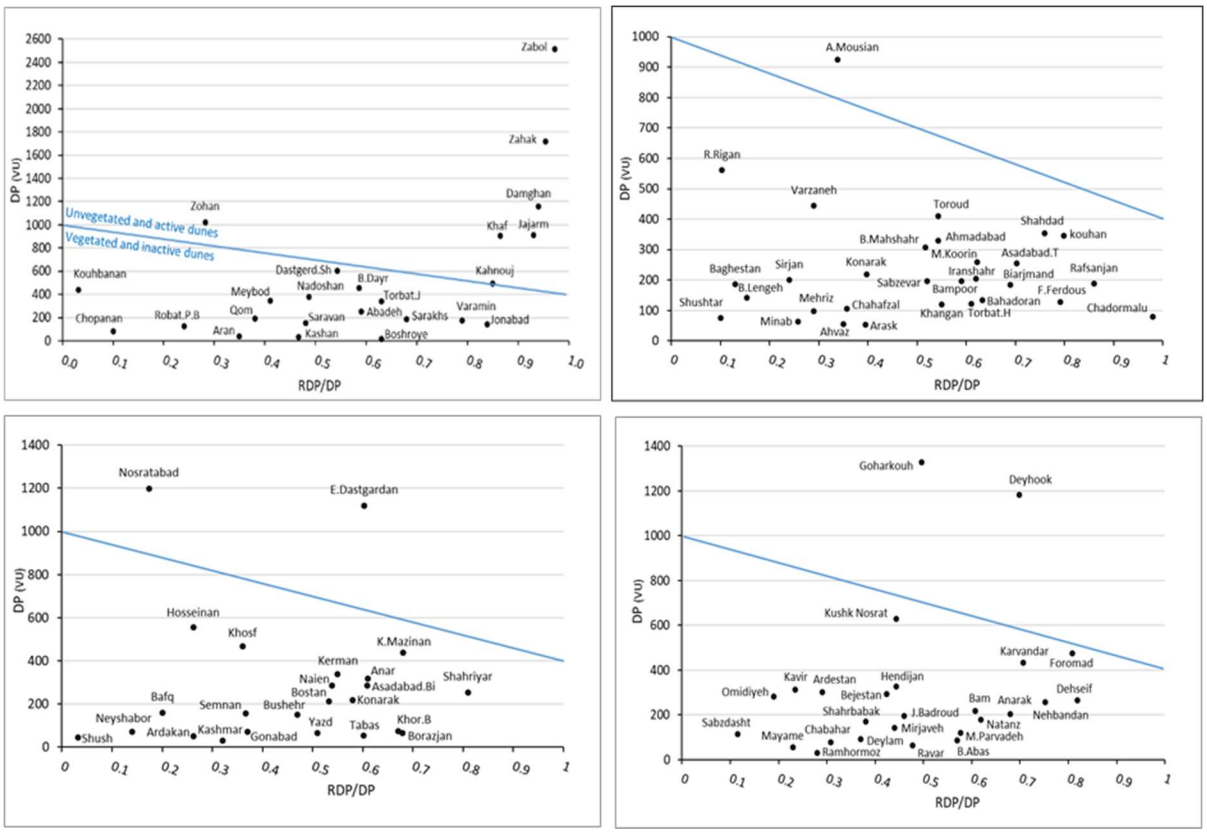

Fig. 4.6 Dune field mobility in Iran's deserts based on Tsoar's (2005) index (Source: Abbasi et al. 2019, in print)

The TMI reveals that the Sistan and Zirkuh Qaien sand dunes are active due to the presence of the strong unimodal the Sadobist Roozeh wind, exactly as mentioned above (see chapter 3.1). The DP value in this region ranged from 2516 to 1717 vu and the RDP/DP ratio from 0.97 to 0.95.

In addition, most parts of the Lut desert were classified as "active and unvegetated" as the eastern part of Lut desert (Nosratabad) was characterized by a high wind energy environment with high

DP (1199 vu). But the RDP/DP ratio of 0.17 revealed multidirectional winds. Dunes in the western part of the Lut desert were also classified as “unvegetated” because of the low precipitation (<50 mm rainfall at Shahdad and Dehsief), while the southern parts (Bam, Rahmatabad Rigan and Mohammadabad Koorin) were categorized as inactive dunes due to a moderate DP and a low to moderate RDP/DP ratio. These TMI results contradict the field observations, which showed that the dunes are active throughout the whole Lut desert because of low precipitation (53- 57 mm) and extremely arid conditions.

Furthermore, the northern part of the Dasht-e Kavir desert, consisting of the Hasanabad (Damgan), Jajarm, Foromad, Yazdo, and Dastgerd Shahroud dune fields, contains active dunes because of the high wind energy, as discussed in chapter 3.1. The other dune fields around this desert were classified as “inactive”, due to their low DP and RDP/DP ratio. Eshgabad Dastgardan, in the north of the Shotoran sand sea, also showed active dunes in the TMI classification, with a high drift potential and intermediate directional variability.

Based on the TMI analysis, the western part of the Khuzestan sand sea, near the border to Iraq (Mousian) was active due to a high DP. Towards the central and south-eastern parts of this region the DP, and with it the activity of the dunes, decreased.

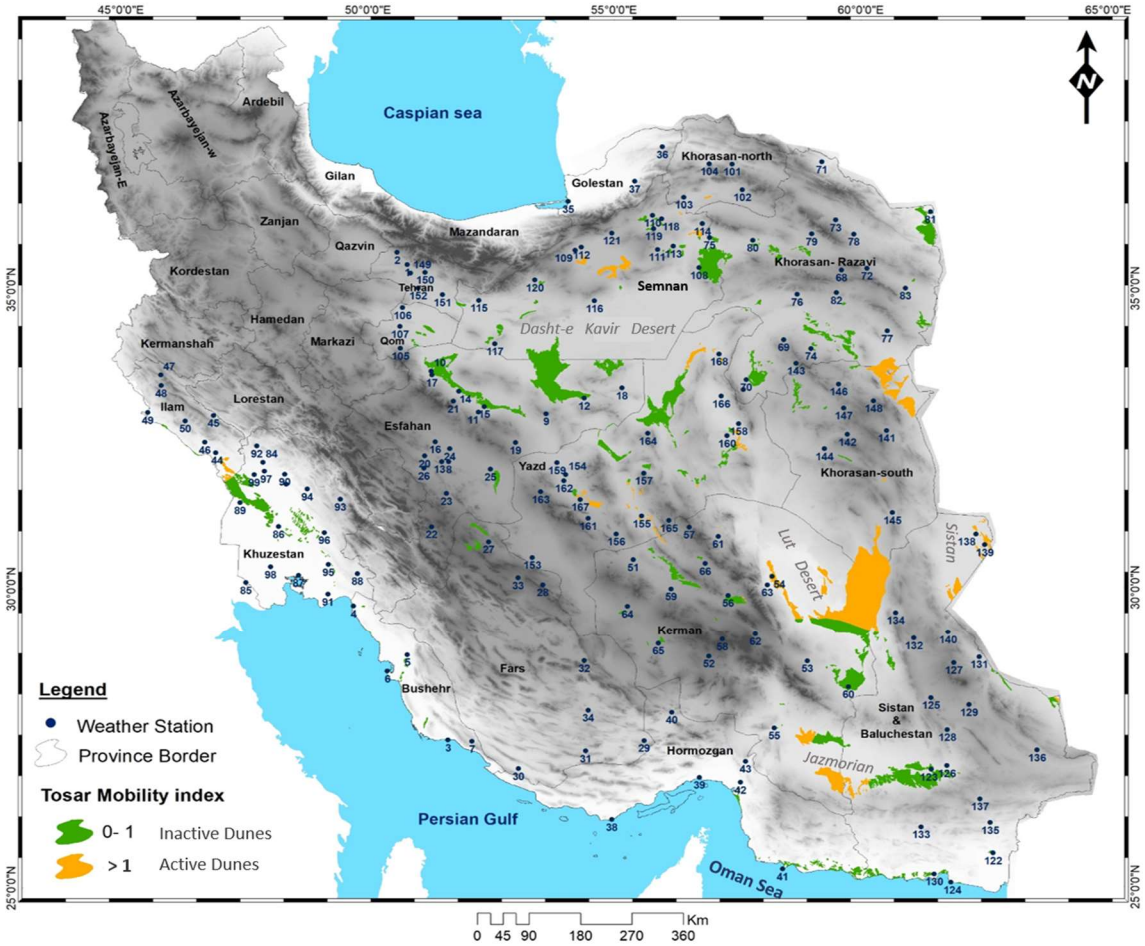

Fig. 4.7 Sand dune activity in Iran’s deserts based on Tsoar's (2005) index (Source: Abbasi et al. 2019, in print)

Another region with active dunes, based on the TMI, was the western part of the Jazmorian sand sea (Kahnouj). The activity of dunes there decreased gradually from west to east as the wind energy and the RDP/DP ratio decreased in the same direction over the sand sea.
The rest of the country's sand dunes were classified as inactive because the average annual wind power (DP) and the RDP/DP ratio were too low to sustain active dunes.

4.3.4 Yizhaq mobility index (YMI)

The main elements of Yizhaq model (Equation 4.8 in Table 4.2) are wind power, precipitation rate, and anthropogenic effects, such as grazing and wood gathering (Yizhaq et al. 2009). According to this model, dunes are classified into active, active and stabilized (semi-active), and stabilized. In this model there are three activity graphs due to different values of the ground vegetation cover ($v_c = 0.2, 0.25\ and\ 0.3$), which is a function of precipitation. For this study $v_c = 0.3$ was used because most sand dunes in Iran are bare or have only a low vegetation cover due to the low precipitation and overgrazing.

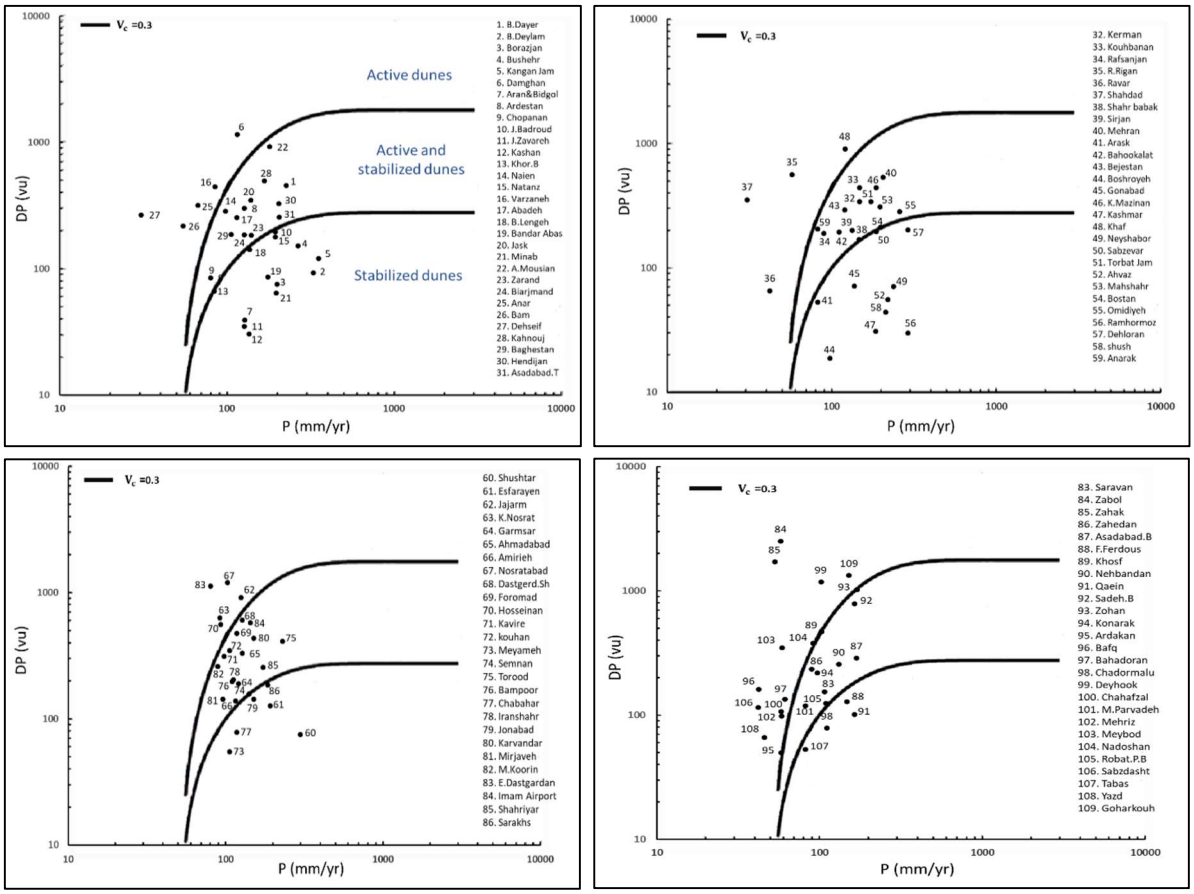

Fig. 4.8 Dune field mobility index values in Iran's deserts based on Yizhaq et al. (2009) model (Source: Abbasi et al. 2019, in print)

The analysis of the YMI illustrates a significant spatial variation in the activity grades of sand dunes in Iran (Fig. 4.8). The active dunes covered the whole of Lut desert, Sistan plain, most parts of the sand dunes in Yazd province, and the northern and central areas of the Dasht Kavir desert (Fig. 4.9). The spatial distribution of the annual precipitation over active dunes ranged from 31 to 170 mm and the DP varied between 49 and 2,516 vu.

The sand dunes in the Lut desert are active because of the high wind energy in the eastern and southern parts (Nosratabad, Rahmatabad Rigan), a low precipitation and moderate wind energy in the western and south-western parts (Shahdad, Dehsief, Bam and Azizabad Bam) and low precipitation in the northwest (Ravar). Sand dunes in the Sistan plain (Zabol and Zahak), Zirkuh Qaien (Khaf, Zohan), Hasanabad (Damgan), and in the Jajarm dunefields in the northern part of Dasht-e Kavir were also active because of the high wind energy.

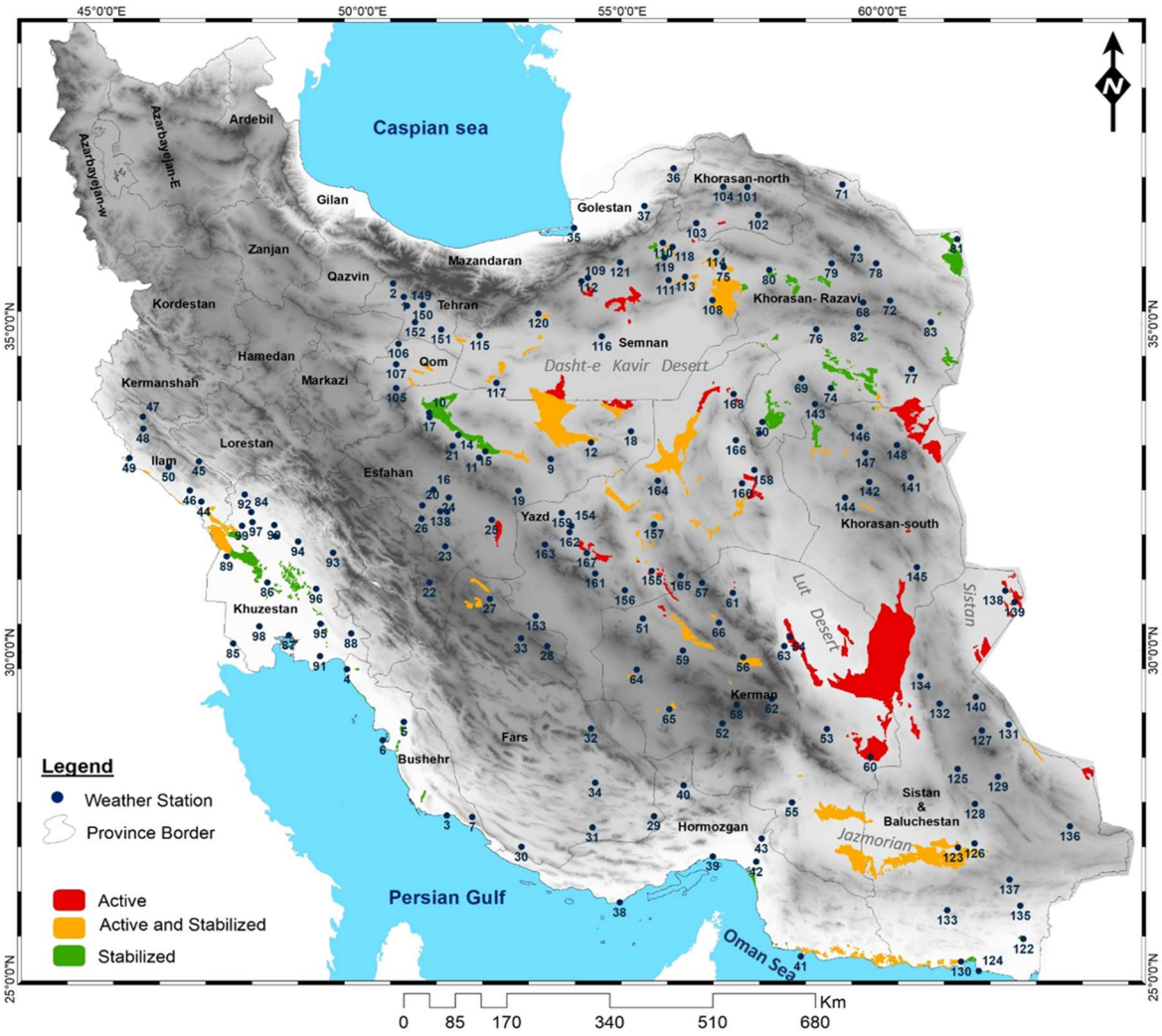

Fig. 4.9 Sand dune activity in Iran based on the Yizhaq et al. (2009) model (Source: Abbasi et al. 2019, in print)

The northern part of the Shotoran sand sea (Eshgabad Dastgardan) and the Deyhook dunefields in the Yazd province were classified as active due to a high wind energy. In addition, the Yazd, Bahabad and Bafg dunefields were classified as active because of the low precipitation rates.
The Khartoran, Jazmorian, Jinn, Khuzestan, and in southern part of the Shotoran sand seas, as well as the Kaleh, Kerman, Nog dune fields, and Omman Sea coastal dunes between Konarak and Jask were categorized as semi-active with an annual average rainfall variability between 80 and 259 mm and a DP between 85 and 924 (vu).
Stabilized dunes were detected in the Sarakhs, Booshroyeh, and Rig Boland sand seas as well as in the Sagand, Esfrayen, Gonabad, Kashmar, Sabzevar, and Minab dune fields. In addition, the YMI analysis of the stabilized dunes revealed that the DP ranged from 19 to 202 (vu) and annual average rainfall from 82 to 329 mm.

4.3.5 Comparison of the three models and development of a new model

For comparing the three sand dune mobility models (LMI, TMI, YMI), 27 meteorological stations, which are located at the edges of dune fields, were selected. Table. 4.3 shows the dune mobility classifications based on the three models as well as the relevant meteorological parameters. As mentioned above, LMI classifies dunes into four groups; fully active (A), active dunes with inter-dune stability (A.I.S), dunes where only the crest is active (C.A), and inactive or stabilized dunes (S). The TMI uses only two classes; stabilized (S) and active (A) dunes. Yizhaq's model categorizes dunes as active (A), stabilized and active (or semi-active) (S.A), and stabilized (S). Due to the unequal number of classes in the three models, a direct comparison of semi-active dunes is difficult. For this comparison study it was assumed that the C.A. and A.I.S. classes (LMI model) are equivalent to the S.A. class in Yizhaq's model (Table 4.3).

When the wind energy environment is high all three models provide highly comparable results; e.g. all models show fully active sand dunes in Sistan (Zabol), the eastern part of the Lut desert (Nosratabad), Deyhook, and Jajarm. These results are also consistent with other studies, which revealed that the Sistan Hamouns Lakes are one of the main dust and sand sources in western Asia (e.g. Cao, et al. 2015; Ekhtesasi and Gohari, 2013; Kaskaoutis et al. 2014; Miri et al. 2010; Rashki et al. 2013; 2012). Rezazadeh et al. (2013) observed that the highest number of days with dust events in the Middle East occurred in Sistan as a result of the strong wind of Sadobist Roozeh. And field measurements place the average movement of big barchans in Sistan at 20 to 40 m/yr (Abbasi et al. 2019), which is one of the highest movement rates in comparison with other deserts e.g. 17 m/yr at the North-eastern Brazilian coast (Maia et al. 2005), 20 m/yr in the northern part of Mauritania in the Sahara Desert (Ould Ahmedou et al., 2007), 18 m/yr in the Salton Sea in California (Haff and Presti, 1995) or 8 m/yr in south of Dasht-e Kavir Iran (Maghsoudi et al. 2017). The sediment deflation rate from the Sistan ephemeral Lakes, the source of material for the formation of sand dunes, has been measured directly in the field at about 2 cm in the Sadobist Roozeh wind duration in 2013 (Abbasi et al. 2018).

The detection of typical aeolian landscapes in the Lut desert shows that wind erosion is an active phenomenon in this area as well. The largest continuous Yardangs on Earth are more than 100 km long and are located in the western part of the Lut desert (Ehsani and Quiel, 2008; Goudie, 2007; Radebaugh et al. 2017), while the tallest star dunes can be found in the southeast of the Yalan sand sea (Lorenz et al. 2015).

Table 4.3 Comparison of the three sand dune activity models and relevant meteorological parameters in Iran for selected meteorological stations in and around Iranian deserts

Sand dunes (meteorological stations)	Rain (mm)	PET (mm/yr)	W %	DP (vu)	Lancaster MI	Tsoar MI	Yizhaq Model	MLI	Field Observation
Sistan (Zabol)	58	1556	46	2516	A	A	A	A	A
Yalan (Nosratabad)	103	1234	49	1200	A	A	A	A	A
Yalan (Dehsief)	31	3805	16	267	A	A	A	A	A
Yalan (Shahdad)	31	3805	11	353	A	A	A	A	A
Yalan (R.Rigan)	58	1574	27	562	A	S	A	A	A
Bafg	42	1357	15	161	A	A	A	A	A
Deyhook	102	1543	50	1182	A	A	A	A	A
Jajarm	125	983	26	912	A	A	A	A	A
Jazmorian (Bampoor)	110	2806	17	196	A	S	S.A	A	C.A
Jazmorian (Kahnouj)	168	2836	26	496	A	A	S.A	A	A
Booshroyeh	97	1204	3	19	S	S	S	S	S
Rig Boland (Aran Bidgol)	128	1212	4	39	S	S	S	S	S
Rig Boland (J.Badroud)	195	1491	27	196	A	S	S.A	C.A	C.A
Rig Boland (Naien)	98	921	0.22	285	A	S	S.A	A.I.S	A.I.S
Khartoran(K.Mazinan)	187	1012	22	439	A.I.S	S	S.A	A.I.S	A.I.S
Khartoran (Ahmadabad)	128	926	20	330	A.I.S	S	S.A	A.I.S	A.I.S
Khartoran (Foromad)	118	789	22	475	A.I.S	A	S.A	A	A
Hasanabad (Damgan)	116	970	23	1159	A.I.S	A	A	A	A
Khuzestan(A.Mousian)	180	2807	19	924	A	A	S.A	A	A
Khuzestan (Bostan)	198	1908	17	212	A.I.S	S	S.A	A.I.S	A.I.S
Khuzestan (Ahvaz)	220	2965	7	55	C.A	S	S	S	S
Ilam (Mehran)	205	2171	25	543	A	S	S.A	A	A
Rig-e Jinn (Chopanan)	80	1685	10	85	A	S	S.A	A.I.S	C.A
Jask	139	2002	31	348	A	S	S.A	A	A
Rafsanjan	90	1016	13	189	A.I.S	S	S.A	A.I.S	A.I.S
Gonabad	137	981	7	71	C.A	S	S	S	S
Sabzevar	187	1012	19	196	A.I.S	S	S	C.A	C.A
Kerman	148	841	16	340	C.A	S	S.A	A.I.S	A.I.S
Seh Galeh Sarayan	164	784	10	786	S	A	S.A	A	A
Yazd	45.6	1284	7	66	A.I.S	A	A	A.I.S	A.I.S
Fully Active%					66	31	42	64	
Semi-active%					34	-	43	33	
Stabilized%					1	69	15	3	

A: Active dunes; S.A: Stabilized and Active; C.A: Crest Active; A.I.S; Active dunes, interdunes Stabilizes; S: Inactive and Stabilized dunes:
(Source: Abbasi et al. 2019, in print)

More differentiated results were obtained when the LMI classified dunes as active due to a high potential evapotranspiration, e.g. in the southern Lut desert (Rahmatabad Rigan) and the eastern part of Jazmorian (Bampoor and Iranshahr). Regarding to LMI and Yizhaq model, the Rigan dune field is active, while the TMI classified it as stabilized in spite of a high wind energy (DP=562 vu) and a low ratio of RDP/DP. KNRWMO (2016) reported that dust storms and shifting sand are among the serious problems in the Rigan, Fahraj and Narmashir Bam regions. They cause damages to 250 rural communities and annually disrupt transport on 160 km of the Kerman-Zahedan railway. This shows that the TMI classification, in this case, did not match the conditions on site.

In the eastern part of the Jazmorian sand sea (Bampoor), characterized by a low wind energy and a high potential evapotranspiration, the three models delivered different results (Table 4.3). The LMI classified these dunes as active, the TMI as stabilized and the Yizhaq model as semi-active. As mentioned in chapter 3.1 and according to own field observation, these dunes are stabilized because of summer rainfall. Therefore, it seems that the temporal distribution of the precipitation, especially summer rainfall, which controls the vegetation growth, has a major effect on the dune activity. These summer rains do not reach the western part of the sand sea (Kahnouj) and the dunes there are, according to LMI and TMI, fully active, while the Yizhaq model categorized them as semi-active.

Overall the three models delivered comparable results in some instances and diverging results in others. The reasons for this are the use of different parameters and their impact on the model construction. The main contradictions of the three models results are revealed when the wind blows for only short times but with a high energy, like in the north of the Dasht-e Kavir desert (Damagan, Foromad) and at some stations in the Sadobist Roozeh' domain (Sedeh Birjand). Field observation demonstrated that dunes in these areas are completely active, but the LMI classified them as inactive or semi-active because of a low to moderate percentage of wind events above the transport threshold (10-23%). At the same time the DP in this region showed high values (475-1159) and thus the TMI classified the dunes as active, while the Yizhaq model classified them as active or semi-active. In fact, in spite of high wind energy, the percentage of winds above threshold was rather low, as high speed winds only occur during the warm season, while the rest of the year is characterized by calm weather (Maghsoudi et al. 2013).

The nature of the wind power parameter varies from the LMI (W%) to the TMI and YMI (DP). DP reflects the quantity (frequency) and quality (intensity) of the wind power, but W% only shows its quantity (frequency of winds above the transport threshold). It seems that if DP was used in the LMI instead of W%, it would provide more favourable results. In addition, the statistical analysis (correlation coefficient) between DP values and the percentage of wind events above the transport threshold (%W) at the meteorological stations in the study area (Fig. 4.10) shows a moderate correlation (r2=0.47).

Based on this argumentation, W% has been replaced by DP (vu) as the wind energy parameter in Lancaster mobility index (1988), as seen in Equation 4.12.

$$M = \frac{\mathrm{DP}}{P/PET} \qquad (4.12)$$

Where M is the mobility index, DP is the annual sand drift potential in vector units based on Fryberger and Dean (1979) (Equation 4.10), P is the annual precipitation in mm, and PET is the annual potential evapotranspiration estimated from Thornthwaite's (1948) method in mm/yr.

The result is a Modified Lancaster Index (MLI). In order to group the index results into four distinct mobility classes, extensive field observations and expert interviews were used to identify the class thresholds which is outlined in the rightmost column in table 4.4. Based on this Iranian ground data, dunes are fully active when M exceeds 3,000; active dunes with stabilized interdunes areas are found when M lies between 1,500 and 3,000; stabilized dunes with activity only at the crests can be related to an M between 750 and 1,500; and completely stabilized dunes occur when M is

less than 750. Lancaster and Hesse (2016) further developed the MLI for their mapping of the global digital dune activity and categorized dunes into the four classes active, partly active, inactive and degraded.
Table 4.3 compares the results of the MLI with the other three indices and shows that dunes in the Sistan plain, Zirkuh Qaien, the whole of the Lut desert, and some parts of the Yazd, Khuzestan and Dasht-e Kavir deserts are fully active (Fig. 4.11). These results are confirmed by the LMI and YMI and in parts by the TMI. But there are also some differences in the northern part of the Dasht-e Kavir desert (Damgan and Foromad), the central part of the Rig Boland (Jangle Badroud and Naien), Seh Galeh Sarayan, Kerman, Bejestan and Gonabad dune fields, and the south-eastern part of Rig-e Jinn (Chopanan) as seen in Fig. 4.12.

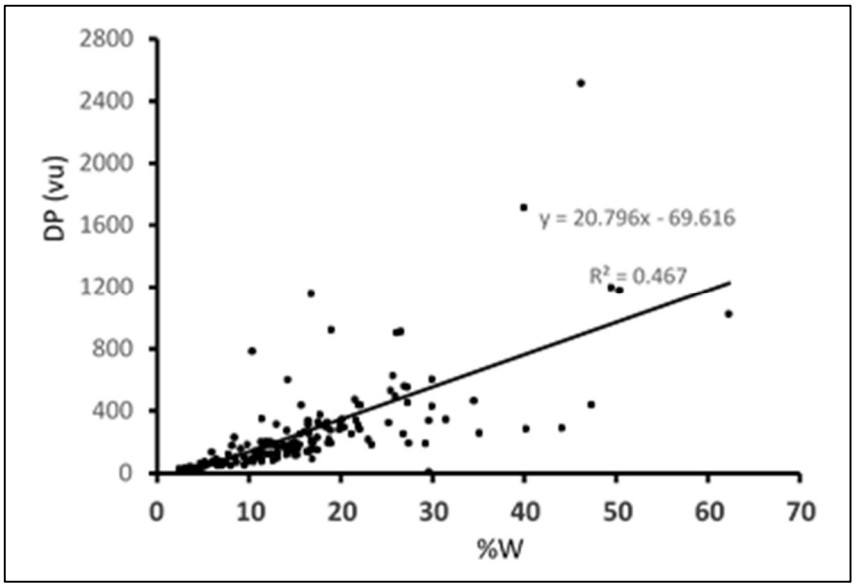

Fig. 4.10 Relation between sand drift potential (DP) and the percent time wind above transport threshold (W) in selected meteorological stations in Iran. (Source: Abbasi et al. 2019, in print)

Regarding MLI results, the dunes in the northern part of the Dasht-e Kavir deserts (Damagan and Foromad) are fully active, with 1159 and 475 v.u DP, as observed in the field as well as in expert's interviews, while LMI and TMI classified these dunes as semi-active. In addition, the dunes in the central Rig Boland sand sea (Jangle Badroud and Naien) are semi-active, with 195 and 285 v.u DP, while the LMI see them as fully active. This result matches with own field observations and with Ahmady Birgani et al. (2017) studies that showed only more than 200 ha/yr were added to the eastern part of Rig Boland sand sea and that there is no encroachment in the north and western parts. The northern part of Rig-e Jinn, near the Hosseinan weather station in the central Dasht-e Kavir desert, has been classified as fully active by the MLI, but it decreases to semi-active in the southern part (Chopanan) due to a low wind energy, while the LMI categorized it as fully active. The results of activity classification in Seh Galeh Sarayan dunefields based on MLI and LMI are also

completely different as the MLI classified it as fully active while the LMI categorized it as stable (Table 4.3) because the percentage of wind events above the transport threshold is low (10%) in spite of high DP (786 v.u).

Totally, the results show a good relationship between the dune activity and these climatic parameters for the Iranian deserts, especially in the north of the Dasht-e Kavir desert and in the Kerman and Seh Galeh Sarayan dune fields, where the model agreement was better than for the other three mobility indices.

Table 4.4 A summary of present conditions of dune activity in Iran

Deserts or Sand dunes names (weather station)	Present conditions of dune activity	MLI*	Reference
Sistan (Zabol)	Fully active crescentic and sand sheets	A	Abbasi et al. (2019)
Lut, Yalan (Nosratabad)	Fully active barchans and liners	A	Field observations
Lut, Yalan (Dehsief)	Fully active sand sheets and Nebkhas	A	Yazdi et al. (2014), Field observation
Lut, Yalan (Shahdad)	Fully active dunes into and margin of Yardangs	A	Ehsani and Quiel (2008), Field observation
Lut (Rigan)	Fully active barchans	A	KNRWMO (2016),(Heidari et al. 2017)
Bafg	Fully active barchanoid and transverses dunes	A	Ahmadi, et al. (2001)
Deyhook	Fully active crescentic and topographic dunes	A	Field observation and expert interviews
Jazmorian (Bampoor)	Inactive and stabilize liner dunes	A	Field observation and Abbasi (2012)
Jazmorian (Kahnouj)	Fully active barchans and liner dunes	A	Field observation and Abbasi (2012)
Booshroyeh	Inactive transverse dunes	S	Expert interviews
Rig Boland (Aran Bidgol)	Inactive barchans	S	Ahmady Birgani et al. (2017) and Field observation
Dasht-e Kavir (K.Mazinan)	Active sand sheets, interdunes stabilizes	A.I.S	Expert interviews
Khartoran (Ahmadabad)	Active barchans and transverse dunes, interdunes stabilizes	A.I.S	Mashhadi et al.(2007) and Field observation
Dasht-e Kavir (Foromad)	Fully active topographic dunes	A	Field observation and expert interviews
Hasanabad (Damgan)	Fully active barchan dunes	A	Field observation and expert interviews
Khuzestan(A.Mousian)	Fully active sand sheets	A	Field observation and Abbasi (2012)
Khuzestan (Bostan)	Active sand sheets and transverse , interdunes stabilizes	A.I.S	Field observation and Rouhipour (2006)
Khuzestan (Ahvaz)	Crest active liner dunes	S	Rouhipour (2006)
Ilam (Mehran)	Active sand sheets	A	Field observation and Abbasi (2012)
Rig-e Jinn (Chopanan)	Active liner dunes, interdunes stabilizes	A.I.S	Field observation
Coastal dunes (Jask)	Fully active sand sheets	A	Ekhtesasi and Dadfar (2014)
Rafsanjan	Active barchans, interdunes stabilizes	A.I.S	Field observation and expert interviews
Gonabad	Inactive and stabilizes by vegetation	S	Field observation and expert interviews
Sabzevar	Crest Active, plinths Inactive	C.A	Field observation and expert interviews
Kerman	Artificial stabilized by vegetation	A.I.S	Field observation
Seh Galeh Sarayan	Active topographic dunes	A	Expert interviews
Yazd	Active dunes. interdunes stabilizes	A.I.S	Ekhtesasi and Sepehr (2009)
Sarakhs	Sand sheet vegetated	C.A	Field observation
Dasht-e Kavir Deseret, north of Rig-e Jinn (Hosseinan)	Fully active dunes	A	Expert interviews
Zirkuh Qaien (Khaf)	Fully active barchans, artificial stabilized	A	Field observation and Tavakoli (2002)
Shotoran (E. Dastgardan)	Active liners, stars and barchans	A	Field observation and expert interviews

* MLI: Modified Lancaster Index, A: Active dunes; C.A: Crest Active, plinths stablize ; A.I.S; Active dunes, interdunes Stabilizes; S: Inactive and Stabilized dunes

(Source: Abbasi et al. 2019, in print)

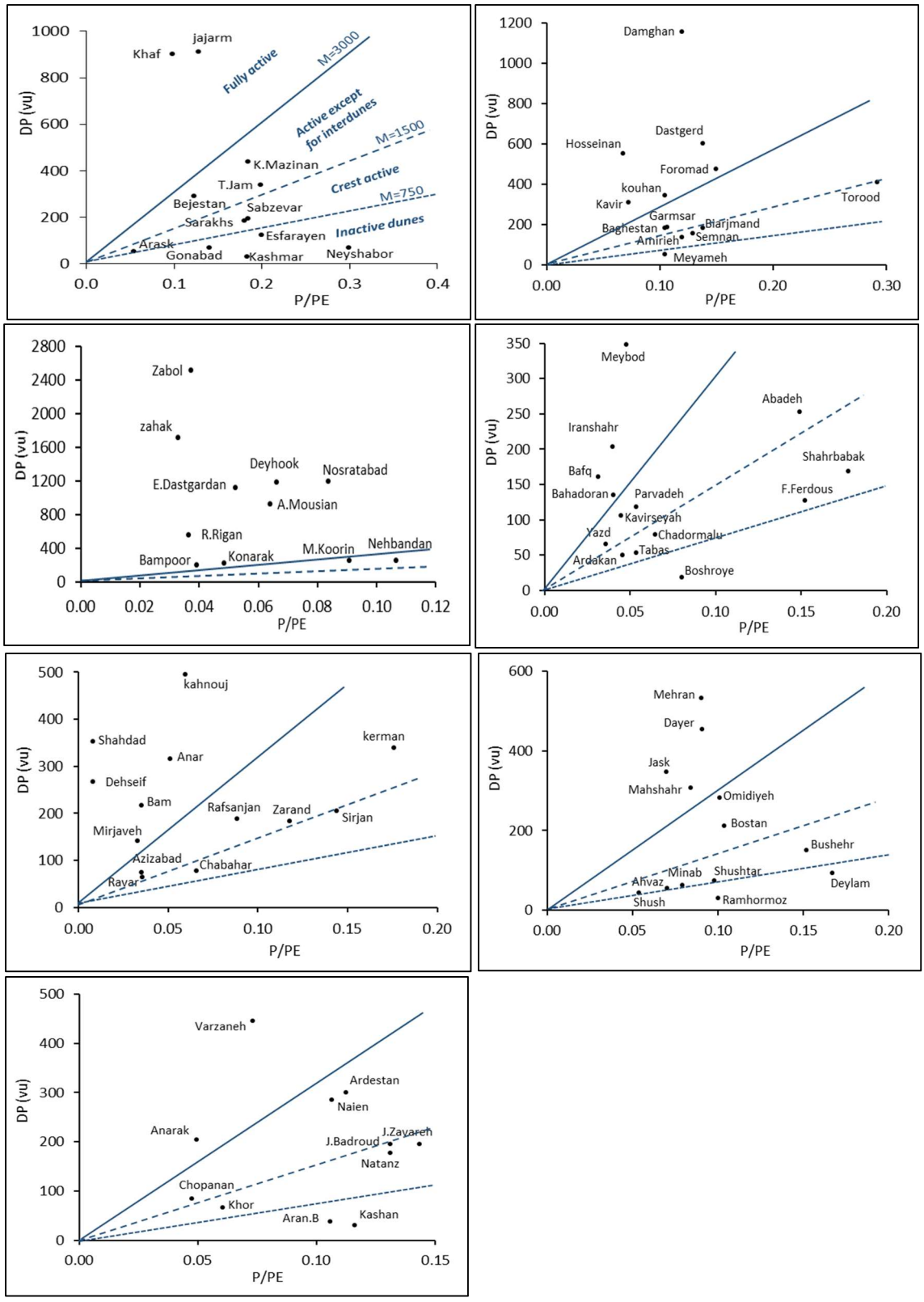

Fig. 4.11 Dune field mobility index values based on the Modified Lancaster Index (MLI) in Iran's deserts (Source: Abbasi et al. 2019, in print)

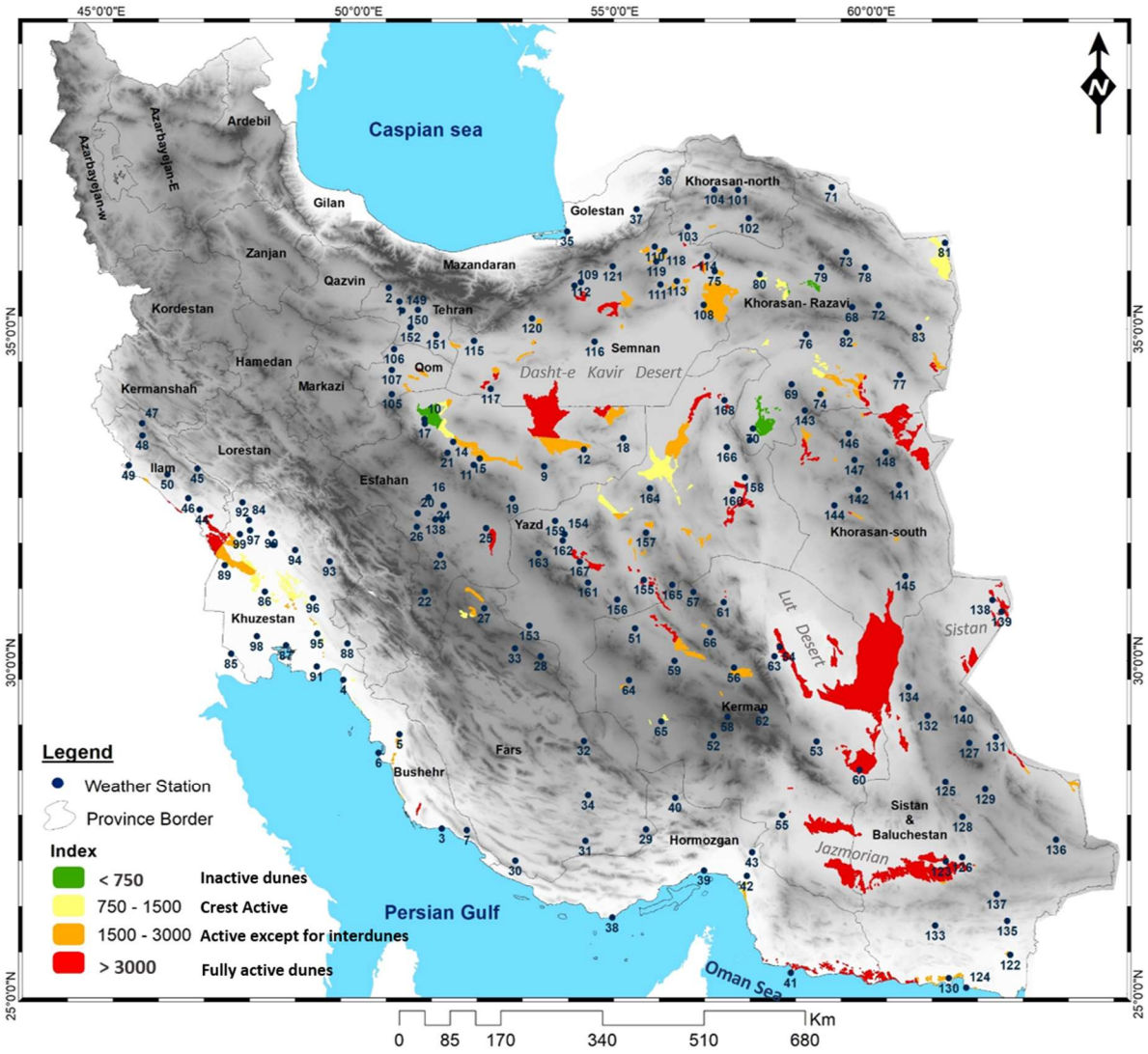

Fig. 4.12 Sand dune activity in Iran based on the Modified Lancaster Index (MLI) (Source: Abbasi et al. 2019, in print)

4.4 Conclusions

The stabilization of dunes has been a major objective of anti-desertification programs over the past half-century in Iran (Amiraslani and Dragovich, 2011). Accordingly, the identification of areas with active dunes is of paramount importance in prioritizing the monitoring and stabilization efforts. Such an approach, however, requires suitable models on a national scale. With regards to

this objective, the wind energy environment based on DP and three more commonly used dune activity models were evaluated in and around Iran's deserts. The comparison of the models showed that the Lancaster and Yizhaq models yield very similar results except for those cases in which percentage of times of winds above the transport threshold (W%) isn't following the DP, e.g. in the north of Dasht-e Kavir and in the Seh Galeh Sarayan dune fields. By combining both approaches, a modified Lancaster mobility index, based on DP, precipitation and potential evapotranspiration was used with good results. The spatial variation of the wind energy, based on the sand drift potential, has changed from high to low in the Iranian sand dunes. According to this variation of DP, precipitation and potential evapotranspiration, the dune activity in Iran shows large spatial variations on a national scale.

From common points of results, four models classified dunes in Sistan plain, whole of Lut desert, Zirkuh Qaien and Deyhook as fully active and in the northern and western parts of Rig Boland, Booshroyeh and Neyshabor dunefields as stabilized dunes. For other dunes, there are obvious differences in activity classification, at least between the TMI and two other models. The highest similarities were found between the LMI and MLI, followed by the Yizhaq model.

As the meteorological stations are not homogeneously distributed across Iran's deserts, and are far away from the dune fields e.g. in the central part of the Lut and Dasht-e Kavir, the assessment of the dune activity requires complementary field observations, as was already pointed out by Bullard et al. (1997).

It seems that further studies are needed to consider different climate change scenarios to prediction sand dunes activity in Iran.

Acknowledgments

This work has benefited from access to the Iran Meteorological Organization database. The authors gratefully acknowledge Dr. Victor Miguel Ponce in San Diego State University, who provided an online calculator for the potential evapotranspiration using the Thornthwaite method on his website: http://ponce.sdsu.edu/onlinethornthwaite.php.

4.5 References

Abbasi, H., Opp, C., Groll, M., Gohardoust, A. (2019). Wind regime and sand transport in the Sistan and Registan regions (Iran/Afghanistan). Zeitschrift Für Geomorphologie, 62(Suppl.1): 41–57. https://doi.org/10.1127/zfg_suppl/2019/0543

Abbasi, H. R., Opp, C., Groll, M., Rohipour, H., Khosroshahi, M., Khaksarian, F., Gohardoust, A. (2018). Spatial and temporal variation of the aeolian sediment transport in the ephemeral Baringak Lake (Sistan Plain, Iran) using field measurements and geostatistical analyses. Zeitschrift Für Geomorphologie, 61: 315–326. https://doi.org/10.1127/zfg/2018/0451

Abbasi H.R. (2012). Classification of Iran's Sand Dune Systems: morphology and Physio-chemical properties. In Research Institute Forests and Ranglands Iran, technical final report, Tehran, 419 p (in Persian).

Afghan Institute de Meteorologie. (1978). Meteorological Records of Afghanistan for 1970: Kabul, Open-File Data, p.37.

Ahmadi, H., Ekhtesasi, M.R., Feiznia, M. R., Ghanei Bafghi, M. J. (2001). Source identification of south Bafgh sand dunes. Biaban, 6(2): 33–48 (in Persian)

Ahmady-Birgani, H., McQueen, K. G., Moeinaddini, M., Naseri, H. (2017). Sand dune encroachment and desertification processes of the Rig Boland Sand Sea, Central Iran. Scientific Reports, 7(1), 1–10. https://doi.org/10.1038/s41598-017-01796-z

Alizadeh-Choobari, O., Zawar-Reza, P., Sturman, A. (2014). The "wind of 120days" and dust storm activity over the Sistan Basin. Atmospheric Research, 143: 328–341. https://doi.org/10.1016/j.atmosres.2014.02.001

Amiraslani, F., Dragovich, D. (2011). Combating desertification in Iran over the last 50 years: An overview of changing approaches. Journal of Environmental Management, 92(1): 1–13. https://doi.org/10.1016/j.jenvman.2010.08.012

Ash, J. E., Wasson, R. J. (1983). Vegetation and sand mobility in the Australian desert dunefield. Zeitschrift Fur Geomorphologie, 45(Suppl.): 7–25.

Ashkenazy, Y., Yizhaq, H., Tsoar, H. (2012). Sand dune mobility under climate change in the Kalahari and Australian deserts. Climatic Change, 112(3–4): 901–923. https://doi.org/10.1007/s10584-011-0264-9

Babaeian, I. (2017). On the Relationship between Indian Monsoon Withdrawal and Iran' s Fall Precipitation Onset. Theoretical and Applied Climatology, 134(1–2): 95–105. https://doi.org/10.1007/s00704-017-2260-0

Bou Karam, D. F., Flamant, C., Chaboureau, J., Banks, J., Cuesta, J., Brindley, H., Oolman, L. (2017). Dust emission and transport over Iraq associated with the summer Shamal winds. Aeolian Research, 24: 15–31.

Bullard, J. E., Thomas, D. S. G., Livingstone, I., Wiggs, G. F. S. (1997). Dunefield activity and interactions with climatic variability in the southwest Kalahari Desert. Earth Surface Proc. Land. 22(2): 165–174. https://doi.org/10.1002/(SICI)1096-9837(199702)22:2<165::AID-ESP687>3.0.CO;2-9

Cao, H., Liu, J., Wang, G., Yang, G., Luo, L. (2015). Identification of sand and dust storm source areas in Iran. J. Arid Land, 7(5), 567–578. https://doi.org/10.1007/s40333-015-0127-8

Chaichitehrani, N., Allahdadi, N. (2018). Overview of Wind Climatology for the Gulf of Oman and the Northern Arabian Sea. Am. J. Fluid Dynamics, 8(1), 1–9. https://doi.org/10.5923/j.ajfd.20180801.01

Dittmann, A. (2014). National Atlas of Afghanistan. Bonn, p.114.

Ehlers, E. (1980). Iran: Grundzüge e. geograph. Landeskunde, Wissenschaftliche Buchgesellschaft. (Abt. Verlag) 18,596.

Ehsani, A. H., Quiel, F. (2008). Application of self-organizing map and SRTM data to characterize yardangs in the Lut desert, Iran. Remote Sens. of Environ. 112(7), 3284–3294.

Ekhtesasi M.R., Sepehr, A. (2009). Investigation of wind erosion process for estimation, prevention, and control of SDS in Yazd – Ardekan plain. Environmental Monitoring and Assessment, 267–280. https://doi.org/10.1007/s10661-008-0628-4

Ekhtesasi, M. R., Gohari, Z. (2013). Determining Area Affected by Dust Storms in Different Wind Speeds, Using Satellite Images (Case Study: Sistan Plain, Iran). Desert, 17, 193–202.

Ekhtesasi, M. R., Dadfar, S. (2014). Investigation on Relationship between Coastal Hurricanes and Sand Dunes Morphology in South of Iran. Physical Geography Research Quarterly, 45(4), 61–72. https://doi.org/10.22059/jphgr.2014.50072

Feiznia, S., Pourtayeb, F., Ahmadi, H., Shirani, K. (2016). Source finding of sediments around Gavkhuni using geochemical method. Iranian Journal of Range and Desert Research, 22(4), 695–710. https://doi.org/10.22092/ijrdr.2016.106042

FRWO. (2004). Combat Desertification and Mitigate the Effects of Drought of Islamic Republic of Iran Compiled by: Retrieved from Forest, Range and Watershed Management Organization website: https://knowledge.unccd.int/sites/default/files/naps/2017-08/iran-eng2004.pdf

Fryberger, S.G., Dean, G. (1979). Dune forms and wind regime. In Mckee, E.D., ed. A study of global sand seas, US Government Printing Office Washington, Professional paper 1052, 137–169.

Grazanti, E., Vermeesch, P., Andò, S., Vezzoli, G., Valagussa, M., Allen, K., Al-Juboury, A. I. A. (2013). Provenance and recycling of Arabian desert sand. Earth-Science Reviews, 120, 1–19.

Gaylord, D., Stetler, L.D. (1994). Aeolian-climatic thresholds and sand dunes at the Hanford Site, south-central Washington, U.S.A. 28, 95–116. https://doi.org/10.1016/S0140-1963(05)80041-2.

Goudie, A.S.(2007). Mega-yardangs: a global analysis. Geography Compass 1 (1), 65–81.

Haff, P.K., Presti, D.E. (1995). Barchan Dunes of the Salton Sea. In: Tchakerian, V.P. (Ed.), Desert Aeolian Processes. Chapman and Hall, London, pp. 9–10.

Heidari, F., Shirani, K., saboohi, R. (2017). Source of Eolian Facies using Geomorphological and Sedimentological Methods (Case Study: Ab-Barik Watershed of Bam in Kerman). J. Water Soil Sci. 21 (3), 39–54 (in persian).

IRNA (2018). Sand storm damage estimate of 640 Billion Rails to Rigan, 4 April (in Persian). http://www.irna.ir/kerman/fa/News/82877364.

Kaskaoutis, D.G., Rashki, A., Houssos, E.E., Goto, D., Nastos, P.T. (2014). Extremely high aerosol loading over Arabian Sea during June 2008: the specific role of the atmospheric dynamics and Sistan dust storms. Atmos. Environ. 94, 374–384. https://doi.org/10.1016/j.atmosenv.2014.05.012.

Kehl, M. (2009). Quaternary Climate Change in Iran-The State of Knowledge. Erdkunde 63 (1), 1–17. https://doi.org/10.3112/erdkunde.2009.01.01.

Keneshloo, H., Damizadeh, G.R. (2015). Relationship Between Moringa peregrina, Salvadora oleiodes and Cappparis decidua Habitats and Soil Characteristics in Sistan and Baluchistan Province by CCA Method. J. Forest Wood Products 68 (2), 429–449 (in Persian).

Khosroshahi, M., Khashki, M., Ensafi Moghaddam, T. (2009). Determination of climatological deserts in Iran. Iranian J. Range Desert Res. 16 (1), 96–113 (in persian).

KNRWMO (2016). Dust and wind erosion control plan in the eastern of Kerman province, Rigan, Fahraj, Narmashir and Bam, technical report. Kerman Natural Resources and Watershed Management Office 31.

Lancaster, N. (1987). Formation and reactivation of dunes in the southwestern Kalahari: palaeoclimatic implications. Palaeoecol. Africa 18, 103–110.

Lancaster, N. (1988). Development of linear dunes in the south western Kalahari, southern Africa. J. Arid Environ. 14, 233–244.

Lancaster, N. (1997). Response of eolian geomorphic systems to minor climate change: examples from the southern Californian deserts. Geomorphology 19, 333–347. https://doi.org/10.1016/S0169-555X(97)00018-4.

Lancaster, N., Helm, P. (2000). A test of a climatic index of dune mobility using measurements from the southwestern United States. Earth Surf. Proc. Land. 25 (2), 197–207. https://doi.org/10.1002/(SICI)1096-9837(200002)25:2<197::AIDESP82>3.0.CO;2-H.

Lancaster, N., Hesse, P. (2016). Geospatial Analysis of Climatic Boundary Conditions Governing Dune Activity. The Geological Society of America, Annual Meeting. https://doi.org/10.1130/abs/2016AM-283707.

Lorenz, R. D., Fenton, L., Lancaster, N. (2015). The Tallest Dunes in the Solar System? Dune Heights on Earth, Mars, Titan and Venus. In: Fourth Annual International Planetary Dunes Workshop, 19-22 May, Boise, Idaho. LPI Contribution No. 1843, p.8031.

Maghsoudi, M., Geography, F., Navidfar, A., Mohammadi, A. (2017). The sand dunes migration patterns in Mesr Erg region using satellite imagery analysis and wind data. Nat. Environ. Change 3 (1), 33–43. https://doi.org/10.22059

Maghsoudi, M., Geography, F., Navidfar, A., Mohammadi, A. (2017). The sand dunes migration patterns in Mesr Erg region using satellite imagery analysis and wind data. Natural Environment Change, 3(1), 33–43. https://doi.org/10.22059/jnec.2017.225011.62

Maghsoudi, M., Yamani, M., Khoshakhlagh, F., Shahriar, A. (2013). Impact of Wind and Atmospheric Patterns in Location and Direction of Dasht-e Kavir Ergs. Physical Geography Research Quarterly, 45(2), 21–38. https://doi.org/10.22059/jphgr.2013.35142

Mahmmodi, F. (2002). Sand Seas Distribution of Iran. Research Institute Forests and Ranglands Iran, p.187 (in Persian).

Maia, L.P., Freire, G.S.S., Lacerda, L.D. (2005). Accelerated dune migration and aeolian transport during El Nino events along the NE Brazilian coast. J. Coastal Res. 21 (6),1121–1126. https://doi.org/10.2112/03-702A.1.

Mashhadi, N., Ahmadi, H., Ekhtesasi, M.R., Feiznia, S., Feghhi, G. (2007). Analysis of sand dunes to determine wind direction and detect sand source sites (case study : Khartooran Erg, Iran). Desert 12, 69–75. https://doi.org/10.22059/JDESERT.2008.31068.

Mashhadi, Naser, Ahmadi, H. (2010). Sand sources determination based on granolometry of surface soils or sediment (sediment generation potential). 17(4), 499–517 (in persian).

Mesbahzadeh, T., Ahmadi, H. (2012). Investigation of sand drift potential (Case study: Yazd - Ardakan plain). J. Agric. Sci. Technol. 14 (4), 919–928.

Miri, A., Moghaddamnia, A., Pahlavanravi, A., Panjehkeh, N. (2010). Dust storm frequency after the 1999 drought in the Sistan region, Iran. Climate Res. 41 (1), 83–90. https://doi.org/10.3354/cr00840.

Muhs, D.R., Maat, P.B. (1993). The potential response of eolian sands to greenhouse warming and precipitation reduction on the Great Plains of the U.S.A. J. Arid Environ. 25 (4), 351–361.

Modarres, R., da Silva, V. de P.R. (2007). Rainfall trends in arid and semi-arid regions of Iran. J. Arid Environ. 70, 344–355. https://doi.org/10.1016/j.jaridenv.2006.12.024.

Muhs, D.R., Holliday, V.T. (1995). Evidence of Active Dune Sand on the Great Plains in the 19th Century from Accounts of Early Explorers. Quat. Res. 43 (2), 198–208. https://doi.org/10.1006/qres.1995.1020.

Muhs, D.R., Reynolds, R.L., Been, J., Skipp, G. (2003). Eolian sand transport pathways in the south western United States : importance of the Colorado River and local sources. Quat. Int. 104, 3–18.

NAP (2005). National Action Programme to Combat Desertification and Mitigate the Effects of Drought of Islamic Republic of Iran. The Forest, Rangeland and Watershed Management Organization, Tehran, pp. 1–48. https://knowledge.unccd.int/sites/default/files/naps/2017-08/iran-eng2004.pdf 2004.

Nazari, A., Abbasi, H.R., Ahmadi, H., Rahdari, M.R. (2017). Quantitative Modeling of Dunefields High and Space Using Geomorphometric Studies in Central Deserts of Iran. Iranian J. Range Desert Res. 24 (1), 210–223. https://doi.org/10.22092/ijrdr.2017.109861.

NIOPDC (1967). Summary of information and preliminary studies on the use of petroleum products in agricultural affairs and sand dunes stabilization. The National Iranian oil products Distribution Company, p. 246 (in persian).

Kowsar, A., Boersma, L., Jarman, C.D., 1969. Effects of petroleum mulch on soil water content and soil temperature. Soil Sci. Soc. Am. J. 33, 783e786.

Oshida (2016). Droughts and storms Damages are not compensable in Sistan. http://www.oshida.ir/.

Ould Ahmedou, D., Ould Mahfoudh, A., Dupont, P., Ould El Moctar, A., Valance, A., Rasmussen, K.R. (2007). Barchan dune mobility in Mauritania related to dune and interdune sand fluxes. J. Geophys. Res. Earth Surf. 112(F2).

Radebaugh J., Kerber, L., Narteau, C., Rodriguez, Gao, X. (2017). Yardangs and Dunes of Iran's Lut Desert Reveal Winds on Planetary Surfaces. Lunar and Planetary Science XLVIII (2017).

Rashki, A., Kaskaoutis, D.G., Rautenbach, C.J.d.W., Eriksson, P.G., Qiang, M., Gupta, P. (2012). Dust storms and their horizontal dust loading in the Sistan region, Iran. Aeolian Res. 5, 51–62. https://doi.org/10.1016/j.aeolia.2011.12.001.

Rashki, A., Kaskaoutis, D.G., Goudie, A.S., Kahn, R.A. (2013). Dryness of ephemeral lakes and consequences for dust activity: the case of the Hamoun drainage basin, Southeastern Iran. Sci. Total Environ. 463–464, 552–564. https://doi.org/10.1016/j.scitotenv.2013.06.045.

Rashki, A., Kaskaoutis, D.G., Mofidi, A., Minvielle, F., Chiapello, I., Legrand, M., Francois, P. (2019). Effects of Monsoon, Shamal and Levar winds on dust accumulation over the Arabian Sea during summer – The July 2016 case. Aeolian Res. 36 (2019), 27–44. https://doi.org/10.1016/j.aeolia.2018.11.002.

Rezazadeh, M., Irannejad, P., Shao, Y. (2013). Climatology of the Middle East dust events. Aeolian Res. 10, 103–109. https://doi.org/10.1016/j.aeolia.2013.04.001.

Rouhipour, H. (2006). Seasonal Fluctuations of Soil Moisture Content and Condensation Process in Khuzestan Sand Dune. 14th International Soil Conservation Organization Conference (ISCO 2006) 1–5.

Saligheh, M., Sayadi, F. (2017). Summer precipitation determinant factors of Iran' s South-East. Nat. Environ. Change 3 (1), 59–70. https://doi.org/10.22059/jnec.2017.233128.66.

Shao, Y., Wyrwoll, K., Chappell, A., Huang, J., Lin, Z., McTainsh, G.H., Yoon, S. (2011). Dust cycle : an emerging core theme in Earth system science. Aeolian Res. 2 (4), 181–204. https://doi.org/10.1016/j.aeolia.2011.02.001.

Talbot, M.R. (1984). Late Pleistocene rainfall and dune building in the Sahel. Palaeoecol. Africa 16, 203–214.

Tavakoli, H. (2002). Investigation on botanical and habitat characteristics of Ammodendron persicum. Pajouheh & Sazandegi 61 (4), 73–79.

Thomas, D.S.G. (1992). Desert dune activity: concepts and significance. J. Arid Environ. 22 (1), 31–38.

Thomas, D.S.G., Knight, M., Wiggs, G.F.S. (2005). Remobilization of southern African desert dune systems by twenty-first century global warming. Nature 435 (7046), 1218–1221. https://doi.org/10.1038/nature03717.

Thornthwaite, C.W. (1948). An approach toward a rational classification of climate. Geogr. Rev. 38 (1), 55–94. https://doi.org/10.2307/210739.

Tsoar, H. (2005). Sand dunes mobility and stability in relation to climate. Physica A 357(1), 50–56. https://doi.org/10.1016/j.physa.2005.05.067.

Tsoar, H., Levin, N., Porat, N., Maia, L.P., Herrmann, H.J., Tatumi, S.H., Claudino-Sales, V. (2009). The effect of climate change on the mobility and stability of coastal sand dunes in Ceará State (NE Brazil). Quat. Res. 71 (2), 217–226. https://doi.org/10.1016/j.yqres.2008.12.001.

Wang, X., Dong, Z., Yan, P., Zhang, J., Qian, G. (2005). Wind energy environments and dunefield activity in the Chinese deserts. Geomorphology 65 (1–2), 33–48. https://doi.org/10.1016/j.geomorph.2004.06.009.

Wasson, R.J. (1984). Late Quaternary palaeoenvironments in the desert dunefields of Australia. Late Cainozoic Paleoclimates of the Southern Hemisphere 419–432.

Whitney, J.W. (2006). Geology, water, and wind in the lower Helmand Basin, southern Afghanistan, p. 40. https://pubs.usgs.gov/sir/2006/5182/.

Wilson, I. G. (1973). Ergs. Sedimentary Geology, 10(2), 77–106. https://doi.org/https://doi.org/10.1016/0037-0738(73)90001-8

Wolfe, S.A. (1997). Impact of increased aridity on sand dune activity in the Canadian Prairies. J. Arid Environ. 36 (3), 421–432. https://doi.org/10.1006/jare.1996.0236.

Yazdi, A., Emami, M.H., Shafiee, S.M. (2014). Dasht-e Lut in Iran, the Most Complete Collection of Beautiful Geomorphological Phenomena of Desert. Open J. Geol. 04(06), 249–261. https://doi.org/10.4236/ojg.2014.46019.

Yizhaq, H., Ashkenazy, Y., Tsoar, H., 2009. Sand dune dynamics and climate change: a modelling approach. J. Geophys. Res. Earth Surf. 114 (1), 1–11. https://doi.org/10.1029/2008JF001138.

Yizhaq, H., Ashkenazy, Y., Tsoar, H. (2007). Why do active and stabilized dunes coexist under the same climatic conditions? Phys. Rev. Lett. 98 (18), 98–101. https://doi.org/10.1103/PhysRevLett.98.188001.

Yu, Y., Notaro, M., Kalashnikova, O.V., Garay, M.J. (2016). Climatology of summer Shamal wind in the Middle East. J. Geophys. Res. Atmos. 121 (1), 289–305.

5

Wind regime and sand transport in the Sistan and Registan regions (Iran/Afghanistan) [2]

Abstract:

Both, the formation of aeolian dunes and the rate of sand transport in arid environments are controlled by the wind regime. The Sistan region in eastern Iran and the Registan region in South-western Afghanistan are strongly influenced by the wind of 120 days (Sadobist Roozeh wind), which is blowing along the Iran-Afghanistan border from North to South, then shifts it's direction toward the Southeast into the Sistan region and, finally, continues eastward into south-western Afghanistan, forming the Registan sand seas. It blows during the hot season due to the pressure gradient between the Turkmenistan High and the Pakistan Low. In order to determine the wind regime and the sand transport, wind roses based on long-term datasets from 16 meteorological stations, the Drift Potential (DP), the Resultant Drift Direction (RDD), the Resultant Drift Potential (RDP) and the RDP/DP ratio have been calculated using the Fryberger (1979) method. The distribution of the Registan sand dunes was surveyed by using Landsat ETM data, Google Earth scenes and field operations (the latter only in the Iranian part). The spatial differences of the drift potential was also mapped using GIS and geostatistical methods overlaying the sand dune map. The results show that the drift potential (DP) increases from north to south along the border between Iran and Afghanistan and reaches to highest values in the Sistan region, then decreases gradually in the Registan sand seas. The highest wind energy, based on DP matches, was determined exactly where the ephemeral lakes in the northern part of the Sistan plain are located, which function as a source area of intense dust and sand storms during the dry season. The temporal trend of the DP showed an increase between 1999 and 2007, followed by a decrease

2 - Based on: Abbasi H.R., Opp C., Groll M., and Gohardoust A., in Zeitschrift für Geomorphologie - Volume 62 (2019), Suppl.1, 041-057.

until 2015 in Sistan. The results show that the wind regime in the Sistan and Registan regions is unimodal during the wind of 120 days (the Sadobist Roozeh) period, which is also supported by the dominance of transverse, barchanoid and barchans dunes in both regions.

Key words: Sistan; sand transport; drift potential; wind energy; Sadobist Roozeh.

5.1 Introduction

Effective winds play as key factor to abrade soil particles from aeolian sources, create dust and sand storm, and form dunes in desert area. Wind regime and aeolian sand transport used widely to identification dunes morphology (Cooke, et al. 1993; Thomas, 1986; Lancaster, 2005; Livingstone and Warren, 1996; McKee, 1979) and dune formation (Breed and Grow, 1979; Fryberger and Dean, 1979; Lancaster, 2005; Livingstone and Warren, 1996; Wasson, 1984). A thorough understanding of the characteristics of the wind regime in which a sand transport is expected to work is a pre-requisite for the successful planning of any sand dune fixation projects. It also shows the spatial and temporal variability of wind speed and direction over Ergs which help to spatial prioritization of sand dunes stabilization.

To study wind regime and sand transport usually calculated sand drift potential (DP) and related key variables i.e. resultant drift direction (RDD), resultant drift potential (RDP) and unidirectional index (UDI=RDP/DP) with using wind speed and direction data. DP and key parameters related to DP represents wind power and describes the potential maximum amount of sand transport for each wind direction that includes values above the threshold velocity (Fryberger and Dean, 1979). There are different methods to analysis sand transport potential (e.g. Fryberger and Dean, 1979; Nickling and Wolfe, 1994) but Fryberger and Dean method (1979) has been the most widely used in most papers and its theoretical curve agree very well with wind tunnel measurement in compared other methods which tested by Belly (1964). The Fryberger method, which is a modification of the Lettau and Lettau (1978) equation, is designed to give a relative rather than absolute description of the effect of wind energy on sand drift. Sand drift potential (DP) is defined as the wind potential power to transport sediments in a given direction (Fryberger, 1979) which also described wind energy environment.

Different annual trends of drift potential highlighted by some authors from different desert. Livingstone et al. (2010) in Namib Sand Sea digital database of aeolian dunes shows a time series data for annual DP, RDP and RDP/DP for the Gobabeb ground station covering the period 1980–2002, so this region has a low energy wind regime. Al-Awadhi et al. (2005) presented Changes in the amount of DP in Kuwait's meteorological stations, and showed that 77% of the annual resultant DP occurs during the summer period. Wang et al. (2007) showed changes in the wind energy environment and dune activity in China’s deserts from 1990 to 1999, and classified most of China’s deserts into moderate to low-energy wind environments on base of DP that decreased in most dune fields from 1980 to 2003. Jewell and Nicoll (2011) found that DP varied considerably

over a 50 years in the Great Basin desert in the united State of America and found no relationship between DP and climate change. Yang et al. (2014) concluded climate change did not obviously effect on calculated potential sand transport parameters (DP, RDP, RDD) and on the annual mean wind velocity in China Badain Jaran desert. In addition, some Iranian authors reported DP parameters for some meteorological stations. For example, Mesbahzadeh and Ahmadi (2012) calculated the annual DP amount in Yazd – Ardekan in central of Iran (118 V.U), greatest DP occurs in spring then winter, and the lowest DP occurs in autumn. Ekhtesasi and Dadfar (2014) Investigated relationship between coastal storms and sand dunes morphology at Bandar-e-Jask and show the maximum of DP (336 V.U) occurred that lead to the formation of longitudinal dunes in South of Iran.

Sistan depression located on the east of Iran near Afghanistan border surrounded by six ephemeral lakes called Hamoun-e Puzzak, Hamoun-e Chonge Sork, Hamoun-e Baringak, Hamoun-e Sabari, Hamoun-e Hirmand and Gowd-e-Zareh. They played as major dust and sand sources in dry season in southwest Asia. A very strong wind entitles Sadobist Roozeh wind (the wind of 120 days) which forms in warm season due to the pressure gradient between the Turkmenistan (Hamidianpour, et al. 2017; Kaskaoutis,et al.2016; Kaviani and Alijani, 2009) or Hindukush high pressure (Choobari, et al. 2014) and low pressure system common over Registan desert. In other hand, Siberian air stream which comes from north to south and different gradient between high lands and Low lands in Sistan and Registan desert form a low level jet stream (Alizadeh Choobari et al. 2014) which called Sadobist Roozeh wind in Sistan region. During the hot and dry season, it can easily drift the sediments of the dry lake beds, produce intense sand and dust storms that effected on the Sistan, southwest Afghanistan and north of the Pakistan (Alam, et al. 2011; Goudie and Middleton, 2006; Rashki, et al. 2013; Rashki, 2012). Annual mean of dusty days in Zabol city reached to 174 days in duration 1995-2015 and peaked to 213 in 2000. WHO (2016) introduced Zabol as most polluted city in the world form $PM_{2.5}$ particles concentration and third as PM_{10} in 2010. Drifting sand and migrating sand dunes damage to crops and farmlands, blocking of irrigation canals and roads, filling of water reservoirs, and burial of villages in Sistan and Registan every year. A Sistani quotation said, “Whatever brought with water is carried by wind”.

In this paper, we investigated wind regime and erosive winds characteristics of Sistan and Registan desert, and show temporal and spatial variation wind regime.

5.2 Study area

The study area is extended between Sistan plain in east of Iran to Registan desert in south-western Afghanistan (Fig. 5.1). It lies between 31.4˚N-29.3˚N to 61.1˚E-66.1˚E and the elevation change between 480 m in Hamoun Lakes to 1200 m on the Registan sand sea near Ghandehar surrounded with mountains in east part. It is located between Zabol County of the Sistan and Baluchistan province in Iran and Nimruz, Helmand and Ghandehar provinces in Afghanistan. The Sistan region

surrounded by six ephemeral lakes called Hamoun-e Puzzak, Hamoun-e Chonge Sork, Hamoun-e Baringak, Hamoun-e Sabari, Hamoun-e Hirmand and Gowd-e-Zareh. Dasht-e Margo (death desert) is adjacent to the study area. The annual precipitation in this region is 56 mm in the Sistan plain, 105 mm just near the Afghan border, and reach to 185 mm in Ghandehar. The annual mean air temperature is relatively high range from 21.6° in Zabol station to 18.6° in Ghandehar. The summers are hot and dry with average temperatures of up to 35°C and the winters are mild (8°C) with an average monthly precipitation of 20 mm. This classifies the region to extremely arid as a hot desert climate (BWh) after Köppen-Geiger(Peel, et al. 2007).

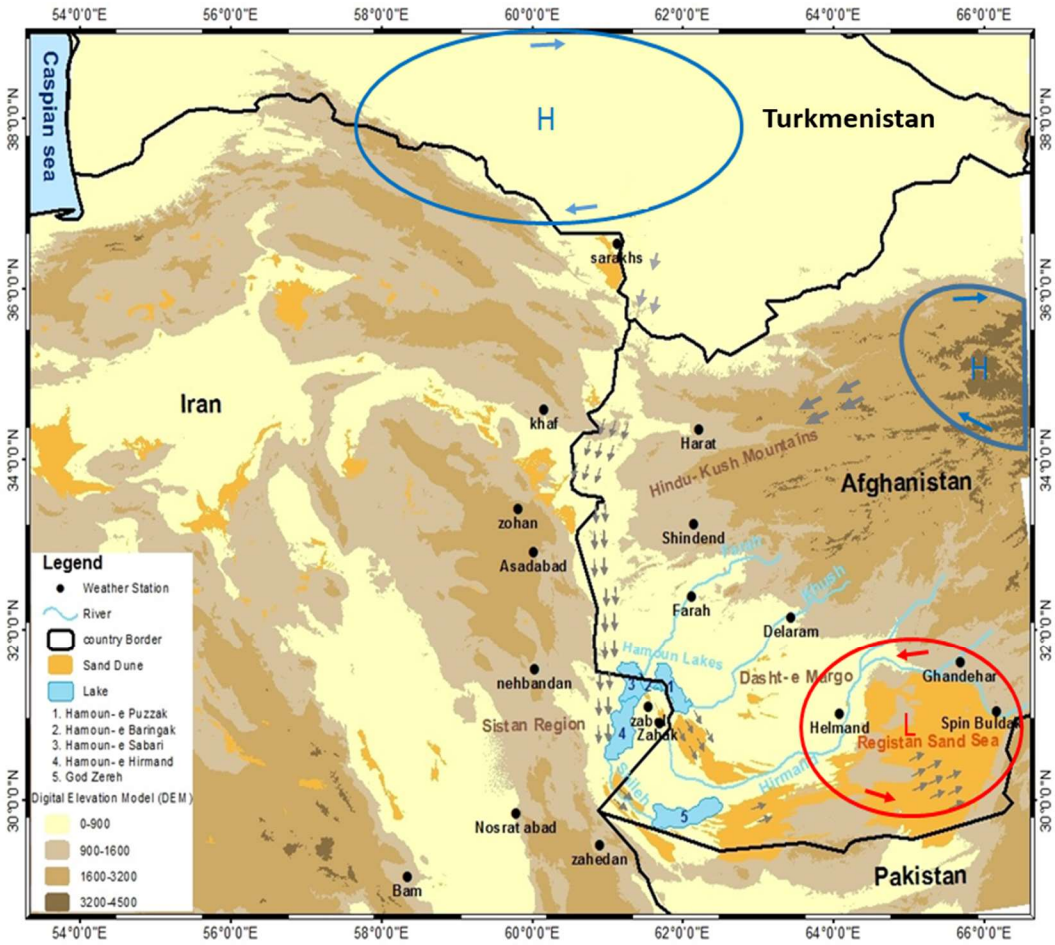

Fig. 5.1 the location of Sistan and Registan desert, the pressure gradient and direction of Sadobist Roozeh wind (Source: Abbasi et al. 2018, p. 44)

5.3 Materials and methods

The speed and direction of hourly wind data were collected from 16 meteorological stations located in Sadobist Roozeh wind domain (Fig. 5.1) in Iran and Afghanistan. The data were recorded in intervals for 1 or 3 hourly for 24h per day at height of 10 m above the ground. The data of Afghanistan's stations derived from the Iowa State University Data Centre online site (www. http://mesonet.agron.iastate.edu/request/download.phtml?network=IR__ASOS) in duration 2011 to 2014 or 2016 and the data of Iranian stations provided from Iran meteorological organization (IMO) from 1995 to 2015.

The wind rose, Sand rose, drift potential (DP), Resultant Drift Direction (RDD), Resultant Drift Potential (RDP) and the ratio of RDP/DP have been calculated using Fryberger and Dean's method (1979) according as follows as;

$DP = V2\ (V-V_t)\ t$ (5.1)

DP is a proportion of sand drift, V is average of wind velocity at 10 meter of height, V_t is impact threshold wind velocity, and t is time wind blew. The threshold velocity was considered 12 knots (about 6.2 m. s^{-1}) under dry conditions.

For comparing results of DP with Fryberger's class and other researches, the speed data were changed to knot although Bullard (1997) estimates also in m s^{-1} and provides calibration relations to correct different units.

$RDP = (C2 - D2)^{0.5}$ (5.2)

$C = \sum(VU)\ Sin(\theta)$

$D = \sum(VU)\ Cos(\theta)$

(vu) vector units represents the DP in each wind direction (in this paper, we grouped winds into 16 sand transport directions, θ is the angle of midpoint of each wind direction class measured clockwise from 0° 0r 360° (north) .

$RDD = Arctan\ (C/D)$ (5.3)

RDD is the angular direction at clockwise from the geographical north.

$UDI = RDP/DP$ (5.4)

Unidirectional index (RDP/DP) is the ratio of the resultant drift potential (RDP) to the drift potential (DP) and shows directional variability. If the ratio of UDI values closes to 1 the wind regime will

indicate a narrowly unidirectional with a single dominant drift direction, whereas if the values close to 0 there is a multidirectional wind regime with multiple significant drift directions environment. Table 5.1 shown the classification of the wind energy environment and directional variability by Fryberger and Dean's method (1979).

Table 5.1 The classification of wind energy environments using drift potential (DP) and directional variability (modified from Fryberger and Dean,1979)

DP (vector unit)	Wind energy environment	RDP/DP	Directional variability	Directional category (probability distribution)
<200	Low	<0.3	High	Complex or obtuse bimodal
200-400	Intermediate	0.3-0.8	Intermediate	Obtuse to acute bimodal
>400	High	>0.8	Low	Wide to narrow unimodal

The spatial variation of DP was interpolated using ordinary kriging in geostatistical method by ArcGIS software version 10.4 (www.esri.com).

5.4 Results and discussion

5.4.1 Wind velocity

It is obviously that the regional topography effects the airflow acceleration, as highlighted by Wilson (1973) and Fryberger and Ahlbrandt (1979). As seen in Fig. 5.2, there is a narrow corridor between the Hindu-Kush Mountains in Afghanistan and the Bageran and Ahangran Mountains in southern Khorasan (Iran), which acts as an accelerator for the Sadobist Roozeh wind speed in that corridor during the warm season which was also mentioned in context from Whitney (2006). The resulting annual mean wind velocity in the corridor and the Sistan area is with mean 4.5 m s^{-1} much higher than in the Registan desert.

The maximum mean wind velocity was 6.2 m s^{-1} at Zabol at the western of study area and the lowest mean velocity (2.9 m s^{-1}) was detected at Spin Buldak at the eastern edge of the Registan desert. The annual mean wind velocity at Zabol, Zahak are 6.2 and 4.8 m s^{-1}, respectively (table 5.2). From this point of view, in comparison with other climatological station around of deserts for examples, Taklimakan (3.0 m s^{-1}), Tengger desert (3.8 m s^{-1}), Badain Jaran desert (4.7 m s^{-1}), Dasht Kavir desert (4.8 m s^{-1}) and Lut desert (5.9 m s^{-1}), Sistan desert has one of the highest of annual mean wind speed in the world. This zone of very high wind speeds in the Sistan region matches the location and extend of the ephemeral lakes and reduced surface roughness. It is clear that the maximum wind velocity occurred on north of Sistan region in which match exactly over ephemeral lakes and decreased gradually over Registan sand sea. In duration study, the strongest storm

occurred at 2012 that wind speed recorded 20 m s^{-1} an averaged 12.5 m s^{-1} for 23 hour period. In addition, Mcmahan (1906) reported a storm over Sistan Basin reached to 120 miles per hours (53.6 m s -1) an averaged 88 miles per hours (39.3 m s-1) for 16 hour period. The strongest storms in Helmand and Spin Buldak stations occurred 18 and 15 m s-1 in duration study, respectively.

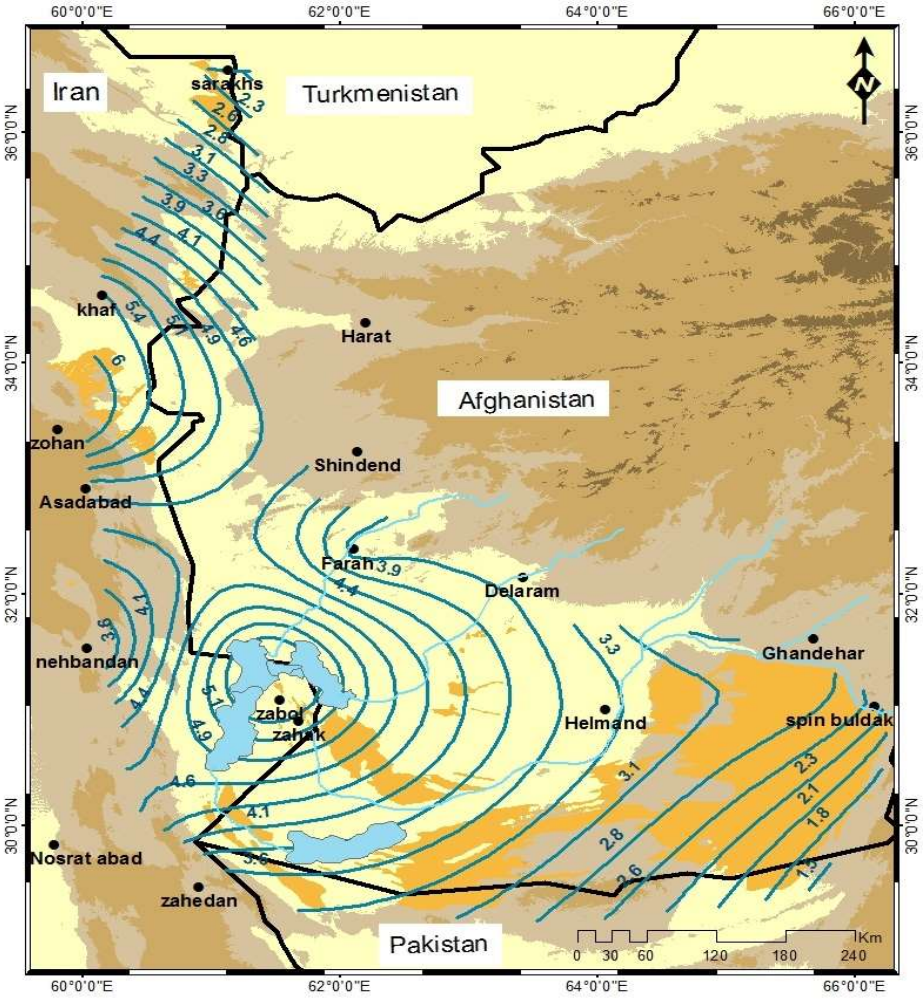

Fig. 5.2 Map of the annual mean wind velocities (in m/s) in the Sistan and Registan deserts. (Source: Abbasi et al. 2018, p. 46)

In terms of time, the monthly average wind speed represented large seasonal variation in Sistan region (Zabol, Zahak stations), with minimum values from December to February and maximum values in June and August coincide with Sadobist Roozeh wind duration. In Sistan region, secondary wind named Levar blows in September also causes a fairly high average wind speed in autumn (Rashki 2012). Other local winds in Sistan region called Haftom (Gav Kush), Goas and Gableh usually have low energy blowing at cold seasons.

In compression, it has mostly low variation in eastern study area e.g. Helmand and Spin Buldak that the maximum wind velocity occurs from March to August and minimum wind velocity occur at Autumn (Fig. 5.3). The maximum wind velocity at Ghandehar occurs in February.

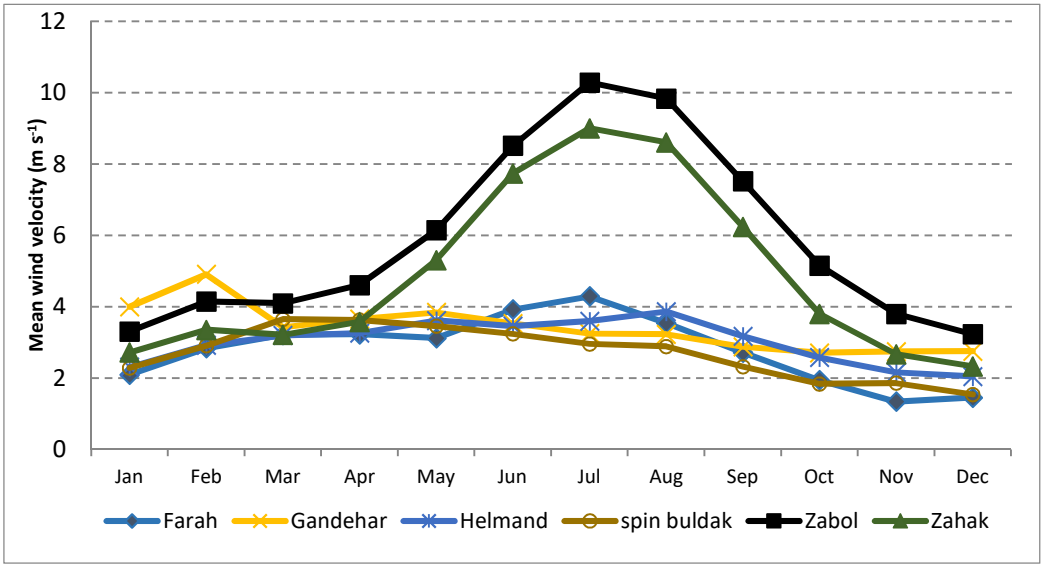

Fig. 5.3 Monthly average of mean wind velocity for seven stations located in Sistan and Registan desert, duration of Iran Stations 1995-2016, Farah and Ghandehar 2010-2016, Delaram and Spin Buldak 2010-2014, Helmand 2012. (Source: Abbasi et al. 2018, p. 47)

Table 5.2 represent the annual mean and annual mean wind velocities upper 6 m s^{-1} that is threshold velocity for sand movement in study area. The maximum mean wind velocity upper threshold velocity was for Zabol (10.7 m s^{-1}), versus a minimum of 7.0 m s^{-1} at Spin Buldak. In addition, the highest proportion of winds greater than the threshold velocity with 62% was at Zabol and Zahak as well. It shows that erosive winds intensify at Sistan region.

Table 5.2 A summary of the wind velocity parameters from Sistan and Registan desert.

Station	Annual mean wind velocity (m s^{-1})			Parameters wind velocity upper 6 (m s^{-1})			
	Mean ± SD	Min	Max	Mean ± SD	Min	Max	proportion
Zabol	6.2 ± 0.7	5.3	7.0	9.5± 0.8	7.9	10.7	46
Zahak	4.8 ± 0.6	3.2	5.6	8.2 ± 0.2	7.9	8.6	39
Delaram	3.4	-	-	7.2	-	-	18
Farah	3.1 ± 0.4	2.8	3.9	7.4 ± 0.3	6.9	7.7	16
Helmand	2.9 ± 0.2	2.6	3.5	7.3 ± 0.4	6.9	8.0	14
Ghandehar	3.1 ± 0.4	2.6	3.3	6.9 ± 0.4	6.5	7.5	16
Spin Buldak	2.4 ± 0.6	1.7	2.9	7.0 ± 0.3	6.6	7.9	13

Duration of Iran Stations 1995-2016, Farah and Ghandehar 2010-2016, Delaram and Spin Buldak 2010-2014, Helmand 2012. (Source: Abbasi et al. 2018, p. 46)

5.4.2 Wind direction

Sistan region and Registan desert is domain of Sadobist Roozeh wind blowing from Northern to south on border of Iran and Afghanistan then it turns to north-western to Southeast direction in Sistan region. Finally, it turns to west-east direction in south-western Afghanistan, as seen in Fig. 5.4. The location of high-pressure system in northeast of Iran and north of Afghanistan and low-pressure system over Registan desert effect on Sadobist Roozeh direction. The dominant wind direction at Zohan, Asadabad, Nehbandan, Shindend and Farah is north. In Zabol and Zahak, the dominant wind direction is northwest. In Helmand, Ghandehar and Spin Buldak the prevailing wind direction is west. The wind directions in Delaram are complex with dominance east, west and northwest.

Farah and Ghandehar 2010-2016, Delaram and Spin Buldak 2010-2014, Helmand 2012, 36 sectors, with frequency in knot as a percentage of total winds.

Sometimes the location of low-pressure system lies on lower part as well and Sadobist Roozeh continues northerly direction in Sistan and effects some part of Baluchistan provinces on border of Iran and Pakistan.

Most of the effective wind directions clustered into the northeast at Khaf and Herat, north at Zohan, Asadabad, Nehbandan, Farah and Shindend, northwest at Zabol and Zahak, west (259-281°) at Helmand, Ghandehar and Spin Buldak and east (79-101°) at Delaram.

As seen in table 5.3, the prevailing wind above threshold in Zohan was N (349-11°) with a frequency 37% and secondary wind direction was S (169-191°) with a frequency 26%. In Zabol and Zahak, the dominant wind direction was NNW (304-349°) with a frequency 31% and secondary wind direction was NW (169-191°) with a frequency 22 and 16%, respectively. At Farah, the prevailing wind direction above threshold was N (349-11°) with frequency 6% and secondary wind direction was NNW (304-349°) with a frequency 4%. At Helmand, Ghandehar and Spin Buldak, the dominant wind direction was W (259-281°) with a frequency that ranged between 4 to 6% and secondary wind direction were WNW (281-304°) ENE (56-79°) and SSE (146-169°) with a frequency 2, 3 and 2%, respectively. The prevailing wind direction above threshold in Delaram was E (79-101°) with a frequency 4% and secondary wind direction was WNW (281-304°) with a frequency 9%.

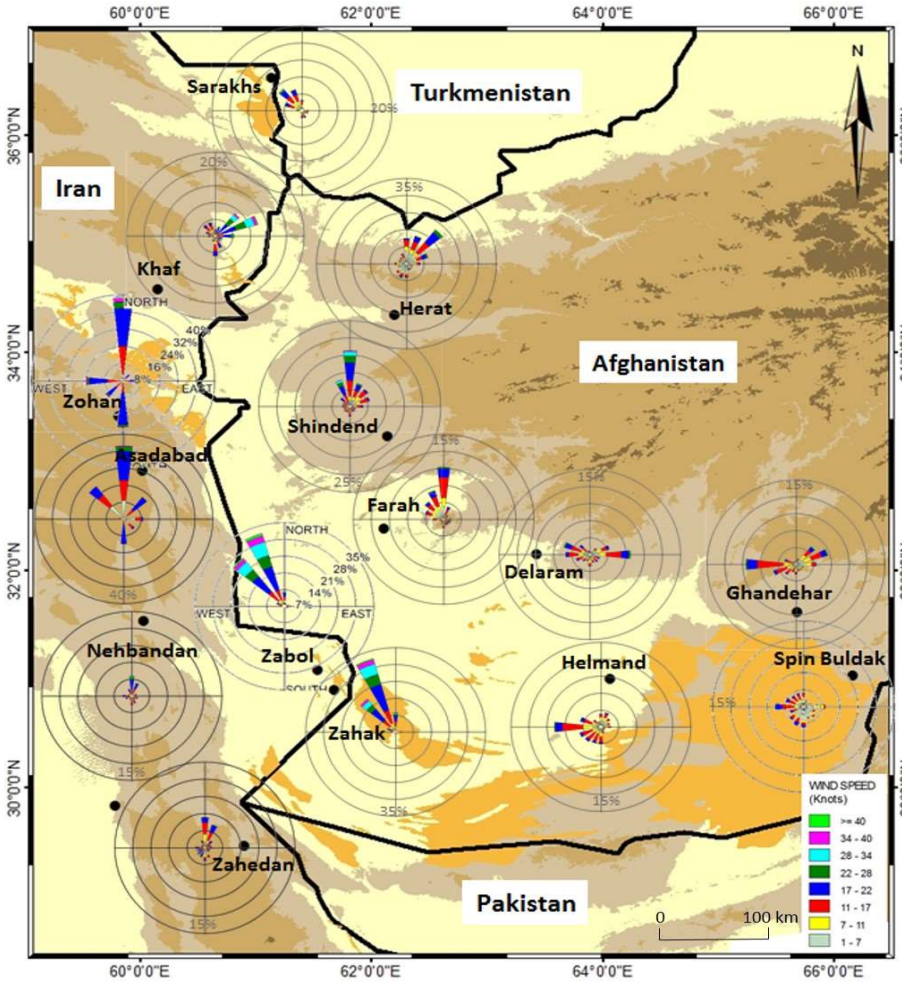

Fig. 5.4 Annual wind roses in Sadobist Roozeh wind domain; Duration of Iran Stations 1995-2016, (Source: Abbasi et al. 2018, p. 48)

Table 5.3 A summary of annual percentage of the two main wind direction with a velocity above threshold in Sistan and Registan desert. (Source: Abbasi et al. 2018, p.49)

Station	Prevailing wind		Second wind		sum
	Direction	%	Direction	%	
Zohan	N	37.0	S	25.8	62.8
Zabol	NNW	30.2	NW	21.7	51.9
Zahak	NNW	30.7	NW	15.6	46.3
Farah	N	6.3	NNW	3.8	10.1
Delaram	E	5.1	WNW	3.9	9
Helmand	W	4.0	WNW	1.8	5.8
Ghandehar	W	5.9	ENE	3.2	9.1
Spin Buldak	W	3.6	SSE	1.7	5.3

Table 5.4 Summary of annual mean of sand drift parameters in Sistan and Registan desert.

Station	Duration	DP (vu)	RDP	RDP/DP	RDD	Wind energy environment
Asadeyeh	1995-2010	286	174	0.6	184°	intermediate
Shindend	2010-2014	641	552	0.86	185°	high
Zohan	1995-2005	1023	289	0.3	112°	high
Zabol	1995-2016	2516	2447	0.97	121°	high
Zahak	1993-2012	1716	1638	0.95	119°	high
Farah	2010-2014	211	93	0.4	116°	intermediate
Delaram	2011-2012	188	25	0.1	107°	low
Helmand	2010-2016	140	69	0.5	73	low
Ghandehar	2011-2016	168	31	0.2	95	low
Spin Buldak	2010-2014	101	54	0.5	80	low

Duration of Iran Stations 1995-2016, Farah and Ghandehar 2010-2016, Delaram and Spin Buldak 2010-2014, Helmand 2012. DP: drift potential, RDP: resultant drift potential, RDD: resultant drift direction. (Source: Abbasi et al. 2018, p. 50)

5.5 Spatial variability of Sand transport

Drift potential (DP) is an index that shows the potential maximum of wind energy that could be moved sand in a region in a year (Lancaster, 2005; Pye and Tsoar, 1999). The distribution of erosive wind direction for the 16 compass directions is known as “sand rose diagram” (Fryberger and Dean, 1979) shows at Sadobist Roozeh wind domain in Fig. 5.5 Spatial variability of annual drift potential (Fig. 5.6) indicate that it varies spatially among the region, is mostly similar wind speed pattern. The maximum value was in Zabol (2516 vector unit), versus a minimum of 101 vector units (vu) at Spin Buldak which represented in table 6.4 for study area. From the point of view of wind energy, Sistan region classify into high energy and Registan desert into low energy environment. However, the current study result is much higher than the studies reported from different deserts such as 733 VU in Guaizi Lake Badain Jaran Desert (Zhang, et al. 2015), 621 VU in Umm-Amara Kuwait (Al-Awadhi et al., 2005), 399 VU in Ruoqiang Taklimakan, 358 VU in Shapotou station, 540 VU in Bahrain, 658 VU in Ghudamia Libya, 391 VU Simpson Australia, 489 VU in An Nafud Saudi Arabia, 948 VU in Bilma Niger, 111 VU in Peski Karakumy Kazakhstan and 520 in Upington south Africa (Fryberger and Dean, 1979). Although Tsoar (2005) reported 3999 VU for coastal dunes of Ijmuiden in Netherlands because the wind speed is faster on ocean than land Therefore It is one of the highest sand drift potential in inland desert in the world. Actually, Sadobist Roozeh wind accelerated in the lower parts of corridor in north of Sistan region where it enters into desert area.

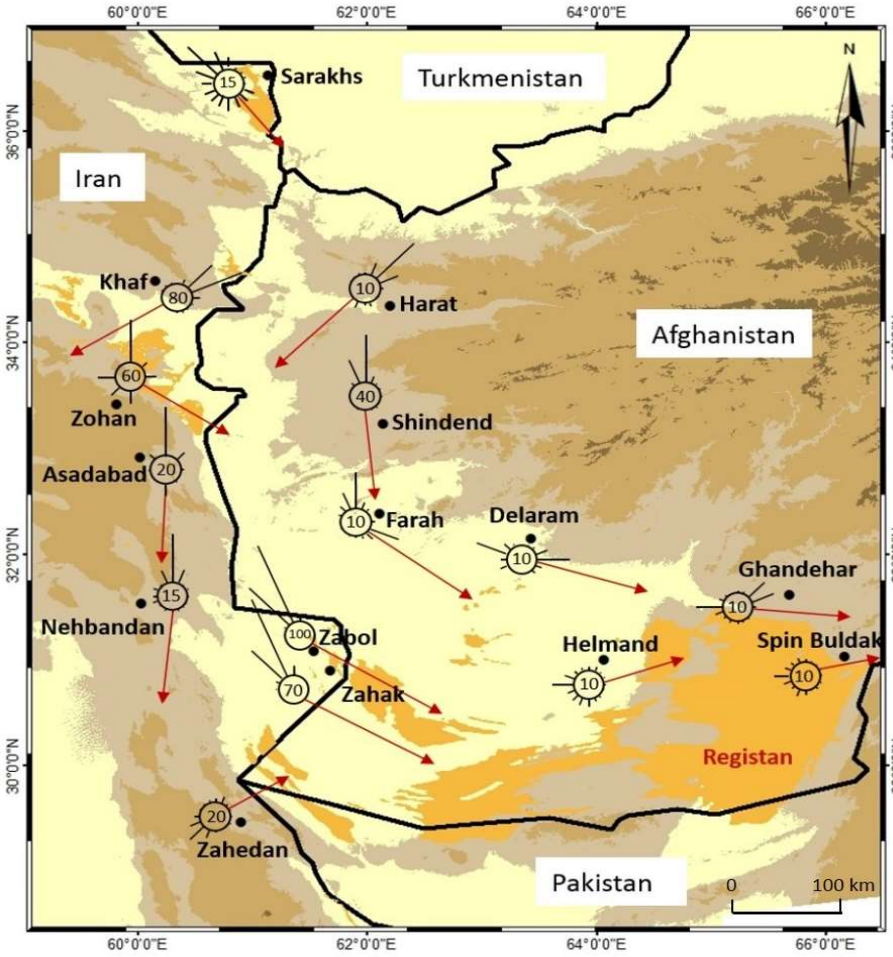

Fig. 5.5 Sand roses for the Sadobist Roozeh wind domain, during 1995-2016 for Iran stations and 2010-2016 for Afghanistan stations. Numbers into the roses are reduction factors for the adjacent sand rose of a given locality (criteria of Fryberger and Dean (1979). (Source: Abbasi et al. 2018, p. 50)

RDP were greatest at Zabol and Zahak with 2447 and 1638, respectively. These two stations also had the highest drift potential. RDP decreases gradually over Registan desert so that at Helmand, Ghandehar and spin Buldak reached to 69, 31 and 54, respectively. It is much higher than the studies reported from different inland deserts of world (Al-Awadhi et al. 2005; Fryberger and Dean, 1979; Livingstone et al. 2010; Zhang et al. 2015). The mean of Unidirectional index (RDP/DP) varies in study area from 0.97 to 0.1 at Zabol and Delaram. At Ghandehar and Spin Buldak, the values of UDI were 0.2 and 0.5, respectively. Totally, there is low variability (unimodal) wind at western part of study area (Sistan region) and intermediate to high variability direction (bimodal) at Eastern part of study area. This feature, unidirectional effective winds, were increased the dust process and shifting sediments on ephemeral lakes surface in Sistan region.

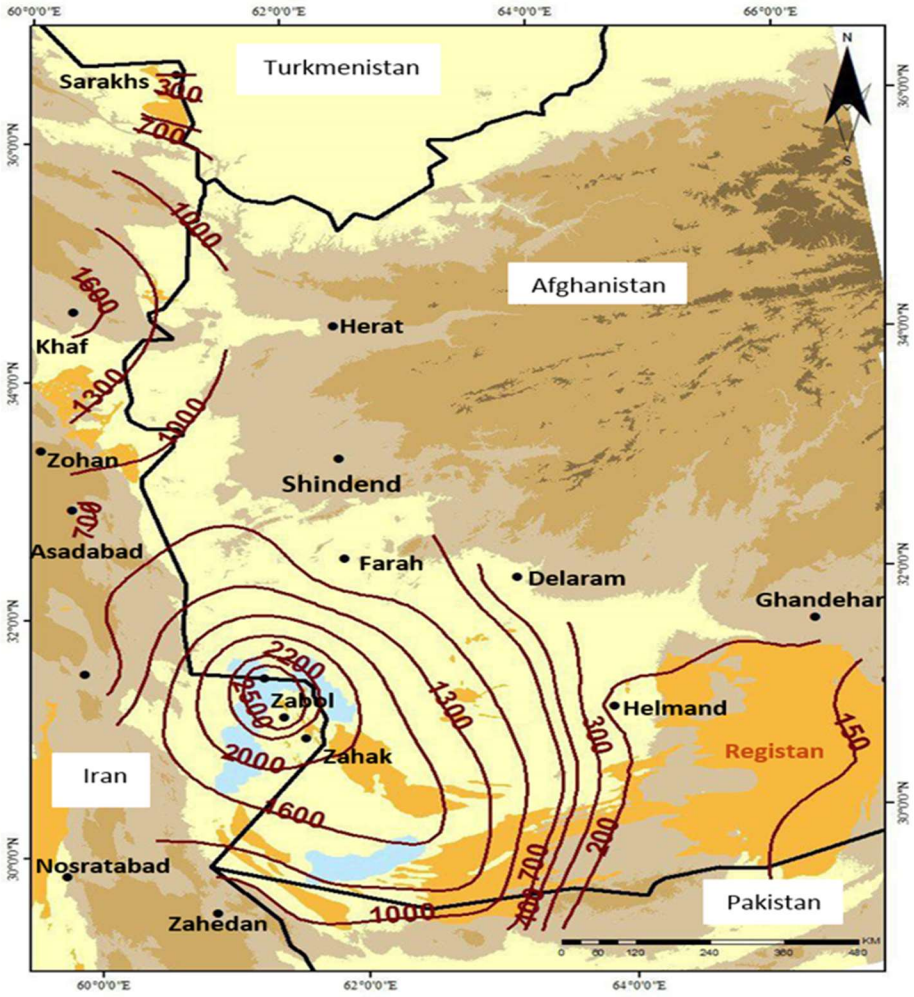

Fig. 5.6 The spatial distribution of DP in the Sadobist Roozeh wind domain. (Source: Abbasi et al. 2018, p. 51)

The angular direction of RDD, showing by red arrows in Fig. 5.5, varies with Sadobist Roozeh wind direction variability. It could be classified into three categories: 185° and 184° at Shindend and Asadeyeh, 121°, 119°, 116° and 107° at Zabol, Zahak, Farah and Delaram and 73°, 95° and 80° for Helmand, Ghandehar and Spin Buldak.

5.6 Temporal variability of Sand transport

The trends of annual DP, RDP, RDD and Unidirectional index (RDP/DP) provides at Fig. 5.7. The DP during 2000 -2016 in Sistan region shows considerable temporal variation so that it raised up to 4183 vector unit (vu), which is a record of drift potential in inland desert in the world, at Zabol station in 2001. Totally, DP were upper annual mean (2516 vector units) from 2000 to 2007 at Zabol but it experienced lower than from 2008 to 2016 as well as Zahak. The days with dust storm

also were showed a similar trend upper annual mean (185 days) from 2000 to 2007 and lower annual mean (170 days) between 2008 and 2015 in Zabol station.

Unfortunately, there is no wind data available before 2010 for eastern part of study area. At Helmand, Ghandehar, and Spin Buldak, DP were less than 200 between 2010 and 2016. In other hand, Registan in east of study area has low energy wind. DP fluctuated at Farah between 2010 and 2014 but it had an intermediate wind energy environment in most years because it is located on the leeward side of Hindu-Kush Mountains as well as Delaram.

The trend of RDD is matched by Sadobist Roozeh wind direction in Study area in most of year. At Zabol and Zahak ranged from 114˚ to 125˚; At Helmand ranged between 51˚ and 81˚ ; At Farah and Zohan ranged from 99˚ to 143˚; At Ghandehar and Spin Buldak generally ranged from 31˚ to 86˚.

The annual directional variability (RDP/DP) at Zabol and Zahak were constantly ranged between 0.95 and 0.98 in duration 2000-2016. It means that effective wind blows a narrow unimodal direction with low variability at Sistan in this period. At Zohan, Farah, Helmand, Spin Buldak and Ghandehar this ratio was mostly intermediate, with value between 0.3 and 0.8 exception: Farah at 2010 had low variability, Ghandehar had high variability in 2013 also Zohan in 2000, 2001 and 2002.

As seen in Fig. 5.8, the monthly of DP and RDP were high in July and August and low in September and January at Zabol and Zahak. Seventy percent of the average annual DP occurs between June and September (120 days) in these stations and it was greater than 400 vector units (vu) in July and August at Zabol. The RDD in all months was from NNW direction towards SSE, ranged from 118° to 124°, showed a very narrow unimodal direction in all seasons. The RDP/DP was near 1 in all months.

The monthly DP were high from February to August in Farah, Helmand, and Ghandehar and somewhat in Spin Buldak. RDD was consistently between 122° and 187° except March at Farah, between 47° and 89° at Helmand and between 40° and 139° at Spin Buldak. It is North-west direction with range of 38°–85° from SW direction for the period from March to November, while it varies slightly during December to February with a range of 225° to 253°.

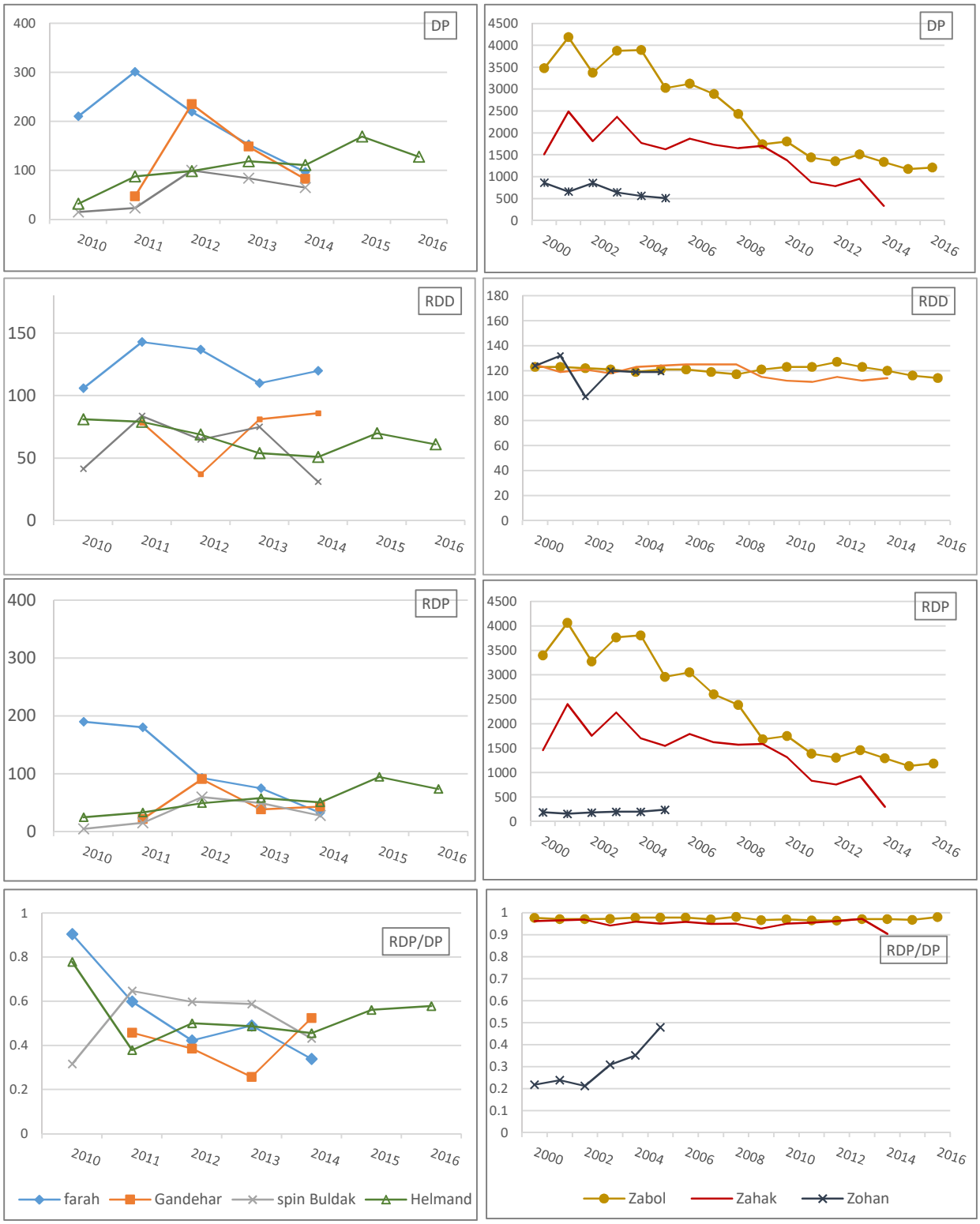

Fig. 5.7 Temporal variability of Sand transport characteristics in study area; DP: Drift Potential, RDD: Resultant drift direction, RDP: Resultant drift potential, RDP/DP: Unidirectional index. (Source: Abbasi et al. 2018, p. 52)

5.7 Morphology of dunes

The variety of dune shapes depend on wind regimes and sand availability as well as grain size of sediment (Bagnold, 1974; N Lancaster, 2005). McKee (1979) classified dunes on the basis of their shape and number of slip faces into crescentic, linear, reversing, star, and parabolic types which divided to varieties of simple, compound or complex. According this method, the morphology of sand dunes in Sistan and Registan was constructed based on visual interpretation of Landsat imagery supplemented with CNES/SPOT imagery via Google Earth in Fig. 5.9.

Totally, the most dune producing is associated with Sadobist Roozeh wind in Sistan and Registan sand sea therefore the most dunes type limited into the narrow unimodal wind regime and classified to crescentic shape. Garcia et al. (2016) shows that sand availability plays a major role on their formation and evolution transverse or barchan dunes in one wind direction regime. They show barchans shape in low sand availability, barchanoid ridge in medium availability and transverse dune in high sand availability were formed in laboratory condition. We considered these forms of dunes in the classification of dunes morphology in study area.

In Sistan, Single barchans transport into four erosive corridors linking sand source zones in Hamouns Lakes beds with depositional areas. The rate of barchans speed with 8-10 meter high into Sistan erosive corridor ranged 20-40 meter/year in field measurements in normal years. Sometimes, single barchans move alone from Sistan to Registan desert but in most cases, barchans joins and forms barchanoid ridges between Sistan region and Helmand province. Then, barchans and barchanoid ridges forms transverse dunes in Registan area, finally. In some area between Sistan and Registan, sand sheets formed as thin veneers of sand in transition area with rocky bed as reported by Kocurek and Nielson (1986). In addition, Zibar formed in some area that have sand thickness and roughly surface. Only in one case, star dunes created in a very small area near Delaram that the winds blew from many directions.

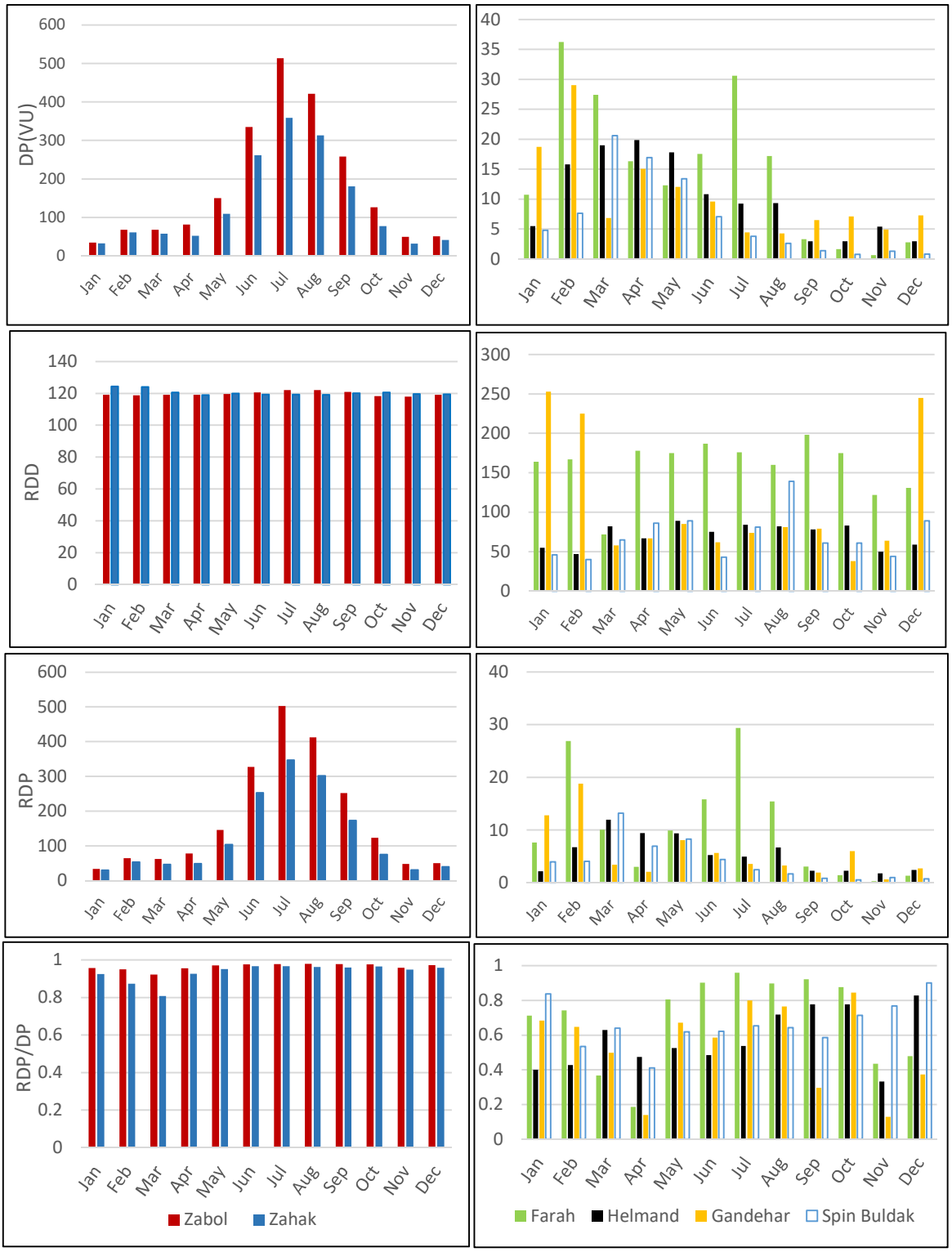

Fig. 5.8 Average monthly of DP, RDD, RDP and RDP/DP in the six stations around study area (Source: Abbasi et al. 2018, p. 53)

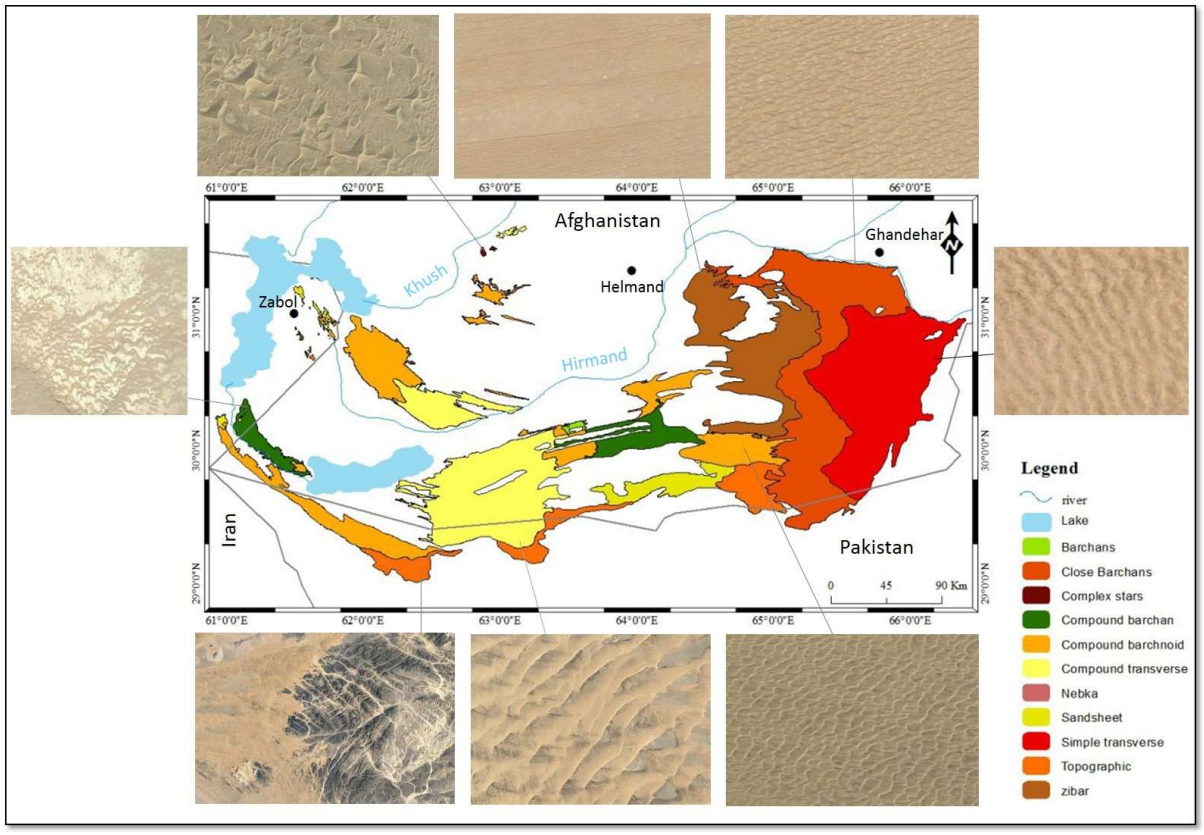

Fig. 5.9 Map of dune types in Sistan and Registan Sand Sea, with example Google earth images. (Source: Abbasi et al. 2018, p. 54)

5.8 Conclusion

The outcome of our study may help to understanding the wind regime specifications and moving sand control in Sistan and Registan. As previous mentioned, Sadobist Roozeh wind (wind of 120 days) accelerated due to local topography over the border of Iran and Afghanistan and intensified over Hamoun-e Sabari and Hamoun-e Baringak Lakes in Sistan region then it decreased gradually over Registan desert. In the context of wind energy environment according on Fryberger and Dean (1979) classification, Sistan region categorized into the high energy and Registan desert into intermediate to low energy. In addition, Drift potential is high in the western portion of study area and decreases gradually to east. The annual DP calculated in Sistan is one of the highest values (2516 vector units) in inland desert and categorized it into the windiest desert in the world. The trend of DP in Sistan indicated reduced considerable from 2000 to 2016 and the maximum annual sand DP is estimated to be 4183 vector units (vu) in 2001 (Fig. 5.7). Due to shortage data, the

variation of wind energy is not clear in Registan desert but there is no considerable variation from 2010 to 2016.

The most dune producing is associated with Sadobist Roozeh wind in Sistan and Registan sand sea characterized by a narrow range of wind directions. The direction of this wind is northwest in Sistan, west to southwest in Helmand and west direction in Registan. According on unidirectional of effective winds, crescentic dunes are the dominant form which depend on sand availability can be divided to barchans, barchanoid ridge and transverse dune.

Acknowledgment

The authors would like to thank the two anonymous reviewers. This work has also benefited from access the Meteorological Organization of Iran and Iowa State University database.

5.9 References

Al-Awadhi, J. M., Al-Helal, A., Al-Enezi, A. (2005). Sand drift potential in the desert of Kuwait. Journal of Arid Environments, 63(2), 425–438. https://doi.org/10.1016/j.jaridenv.2005.03.011

Alam, K., Qureshi, S., Blaschke, T. (2011). Monitoring spatio-temporal aerosol patterns over Pakistan based on MODIS, TOMS and MISR satellite data and a HYSPLIT model. Atmospheric Environment, 45, 4641–4651. https://doi.org/10.1016/j.atmosenv.2011.05.055

Alizadeh-Choobari, O., Zawar-Reza, P., Sturman, A. (2014). The "wind of 120days" and dust storm activity over the Sistan Basin. Atmospheric Research, 143, 328–341. https://doi.org/10.1016/j.atmosres.2014.02.001

Bagnold, R. A. (1974). The physics of blown sand and desert dunes. London: Methuen, 265 p.

Belly, P.Y. (1964). Sand movement by wind. United States Army Corps of Engineers. Coastal Engineering Research Center, Report, (1), 80.

Breed, C.S. and Grow, T., 1979. Morphology and distribution of dunes in sand seas observed by remote sensing. In: E.D. McKee (Editor), A Study of Global Sand Seas. Professional Paper. United States Geological Survey Professional Paper 1052, 253-304.

Bullard, J. E. (1997). A note on the use of the "Fryberger method" for evaluating potential sand transport by wind. Journal of Sedimentary, 67(3), 499–501.

Cooke, R. U., Warren, A., Goudie, A. S. (1993). Desert geomorphology. CRC Press limited, London, 526 p.

Ekhtesasi, M. R., Dadfar, S. (2014). Investigation on Relationship between Coastal Hurricanes and Sand Dunes Morphology in South of Iran. Physical Geography Research Quarterly, 45(4), 61–72. https://doi.org/10.22059/jphgr.2014.50072

Fryberger, S G, Ahlbrandt, T. S. (1979). Mechanisms for the formation of aeolian sand seas. Zeitschrift Für Geomorphologie, 23(4), 440–460.

Fryberger, S.G., Dean, G. (1979). Dune forms and wind regime. In McKee, E.D., ed. A study of global sand seas, US Government Printing Office Washington, Professional paper 1052, 137–169.

Garcia, A., Rodriguez, S., Valance, A., Narteau, C., Gao, X., Lucas, A. (2016). Genesis of dune fields under unidirectional wind with sand input flux control: an experimental approach, 8–10. https://doi.org/10.13140/RG.2.1.4237.4566

Goudie, A. S., Middleton, N. J. (2006). Desert dust in the global system. Springer Science Business Media, p.288.

Hamidianpour, M., Mofidi, A., Saligheh, M., Alijani, B. (2017). The role of topography on the simulation of Sistan wind structure in the east of Iranian Plateau. Scientific Journals Management System, 16(43), 25–53.

Jewell, P. W., Nicoll, K. (2011). Wind regimes and aeolian transport in the Great Basin, U.S.A. Geomorphology, 129(1–2), 1–13. https://doi.org/10.1016/j.geomorph.2011.01.005

Kaskaoutis, D., Rashki, A. Elias E. H., Aristides B., Philippe F., Michel L., Harry D. K. (2016). The Caspian Sea – Hindu Kush Index (CasHKI): definition, meteorological influences and Dust activities over southwest Asia. The First of International Conference on Dust, 2-4 March 2016, Shahid Chamran University, Ahvaz, Iran.

Kaviani, M.R., and Alijani, B. (2009). Principal Climatology, Samt, P.582. https://doi.org/http://samta.samt.ac.ir/content/9117/

Kocurek, G., Nielson, J. (1986). Conditions favourable for the formation of warm-climate aeolian sand sheets. Sedimentology, 33(6), 795–816.

Lancaster, N. (2005). Geomorphology of Desert Dunes. In second. Retrieved from file:///C:/Users/Asus/Downloads/9780203413128_googlepreview (1).pdf

Lettau, K., Lettau, H., 1978. Experimental and micrometeorological field studies of dune migration. In: Lettau, K., Lettau, H. (Eds.), Exploring the World's Driest Climate. University of Wisconsin, Madison, pp. 110–147.

Livingstone, I., Warren, A. (1996). Aeolian Geomorphology: An Introduction, Longman, p.210. http://nectar.northampton.ac.uk/5691/

Livingstone, I., Bristow, C., Bryant, R. G., Bullard, J., White, K., Wiggs, G. F. S., Thomas, D. S. G. (2010). The Namib Sand Sea digital database of aeolian dunes and key forcing variables. Aeolian Research, 2(2–3), 93–104. https://doi.org/10.1016/j.aeolia.2010.08.001

McKee, E. D. (1979). Introduction to a study of global sand seas. In A Study of Global Sand Seas, U.S. Geological Service, Washington, Professional Paper, 1052, pp. 3–19.

McMahan, H. (1906). Recent survey and exploration in Sistan. Geography, 28, 209–228.

Mesbahzadeh, T., Ahmadi, H. (2012). Investigation of sand drift potential (Case study: Yazd - Ardekan plain). Journal of Agricultural Science and Technology, 14(4), 919–928.

Nickling, W. G., Wolfe, S. A. (1994). The morphology and origin of Nebkhas, Region of Mopti, Mali, West Africa. Journal of Arid Environments, 28(1), 13–30. https://doi.org/10.1016/S0140-1963(05)80017-5

Peel, M. C., Finlayson, B. L., McMahon, T. A. (2007). Updated world map of the Köppen-Geiger climate classification. Hydrology and Earth System Sciences Discussions, 4(2), 439–473.

Pye, K., Tsoar, H. (1999). Aeolian sand and sand dunes. Springer Science Business Media, p.459. https://doi.org/10.1007/978-3-540-85910-9

Rashki, A. (2012). Seasonality and mineral, chemical and optical properties of dust storms in the Sistan region of Iran, and their influence on human health, Pretoria, University of Pretoria, Faculty of Natural and Agricultural Sciences, p.178.

Rashki, A., Kaskaoutis, D. G., Goudie, A. S., Kahn, R. A. (2013). Dryness of ephemeral lakes and consequences for dust activity: The case of the Hamoun drainage Basin, South-eastern Iran. Science of the Total Environment, 463–464, 552–564. https://doi.org/10.1016/j.scitotenv.2013.06.045

Thomas, D. S. G. (1986). Arid geomorphology. Progress in Physical Geography, 10(3), p 421-428.

Tsoar, H. (2005). Sand dunes mobility and stability in relation to climate. Physica A: Statistical Mechanics and Its Applications, 357(1), 50–56. https://doi.org/10.1016/j.physa.2005.05.067

Wang, X., Hasi, E., Zhou, Z., Liu, X. (2007). Significance of variations in the wind energy environment over the past 50 years with respect to dune activity and desertification in arid and semiarid northern China. Geomorphology, 86(3–4), 252–266. https://doi.org/10.1016/j.geomorph.2006.09.003

Wasson, R. J. (1984). Late Quaternary palaeoenvironments in the desert dunefields of Australia. J.C. Vogel (Ed.), Late Cainozoic Paleoclimates of the Southern Hemisphere, Balkema, Rotterdam, pp. 419-432.

Whitney, J.W. (2006). Geology, water, and wind in the lower Helmand Basin, southern Afghanistan, p. 40. https://pubs.usgs.gov/sir/2006/5182/.

WHO (2016). The 20 Most Polluted Cities in the World. https://doi.org/https://www.fabionodariphoto.com/en/most-polluted-cities-in-the-world/

Wilson, I. G. (1973). Ergs. Sedimentary Geology, 10(2), 77–106. https://doi.org/https://doi.org/10.1016/0037-0738(73)90001-8

Yang, Y. Y., Qu, Z. Q., Shi, P. J., Liu, L. Y., Zhang, G. M., Tang, Y., Sun, S. (2014). Wind regime and sand transport in the corridor between the Badain Jaran and Tengger deserts, Central Alxa Plateau, China. Aeolian Research, 12, 143–156. https://doi.org/10.1016/j.aeolia.2013.12.006

Zhang, Z., Dong, Z., Li, C. (2015). Wind regime and sand transport in China's Badain Jaran Desert. Aeolian Research, 17(JUNE), 1–13. https://doi.org/10.1016/j.aeolia.2015.01.004

6

Spatial and temporal variation of the aeolian sediment transport in the ephemeral Baringak Lake (Sistan Plain, Iran) using field measurements and geostatistical analyses[3]

Abstract

Wind erosion is one of the most serious problems in the Sistan region, located in the East of Iran and near the border of Afghanistan. During the dry and hot seasons, strong winds locally called the "Sadobist Roozeh", which means "120 windy days" blow from Northern and North-western directions to the Southeast. This wind entrains and transports dust and sand from the dry beds of ephemeral lakes, affecting the Sistan region in Iran, southern Afghanistan and northern Pakistan. In order to investigate the land surface sensitivity to aeolian transport, 74 graduated pins were embedded randomly in the ephemeral Baringak Lake bed and the aeolian transport rates were measured for three events in 2013 individually as well as for the total study period. The spatial and temporal variation of the aeolian transport was also mapped using GIS and geostatistics methods for these events and for the total duration of 103 days. The resulting variogram revealed a high spatial dependence of the different events and showed that geostatistical techniques are a valid tool for the mapping of aeolian sediment transport. The average transport rate in terms of the detected drift height on the dry lake bed was 1.93 cm or 31 kg/m between the 5th of August and the 17th of November in 2013.

Keywords: wind erosion, geostatistics, Sistan, Iran.

3 - Based on: Abbasi H.R., Opp C., Groll M., Rohipour H., Khosroshahi M., Khaksarian F. and Gohardoust A., in Zeitschrift für Geomorphologie - Volume 61/4 (2018), 315-326.

6.1 Introduction

Wind erosion is one of the main land degradation processes, affecting more than one third of the global land surface (Oldeman, 1992, Opp, 1998, Weinan and Fryrear, 1996) and also about 19.7 million hectares in Iran (Ahmadi, 1999). The sources of dust and sand storms are usually extensive and the land rehabilitation is extremely costly and time consuming. Thus, the identification of areas with a high sensitivity to wind erosion is a valuable tool for the selection of prioritized degradation areas for land management measures (Herrmann et al. 1999). The land cover vulnerabilities and wind erosion rates have been studied with different methods on different spatial and temporal scales (Belnap and Gillette 1998, Chepil 1945, Lancaster and Baas 1998, Li et al. 2005, Ravi et al. 2010, Reich et al. 1999, Wolfe and Nickling 1993). While Groll et al. (2013) and Opp et al. (2016) have analyzed the spatial and temporal differentiation of aeolian deposition with the help of deposition samplers around the Aral Kum in Central Asia, Hudson (1993) provided a review of the field measurement of soil erosion and runoff and explained the advantages and disadvantages of these methods as an instrument for getting a first approximation of the amount of erosion in a given situation. One of these reconnaissance methods is the widely used point or pin method (Casagli et al. 1999, Hadley and Lusby 1967, Haigh 1977, Hooke 1980, Takei et al. 1981, Wolman 1959), which is a very simple and cost effective method, requiring hardly any maintenance or staff training. Thus it allows for an extensive and long-term spatial measurement of aeolian transport processes. In recent years the method has been refined (e.g. in the form of photo-electronic erosion pins (Bertrand 2010, Horn and Lane 2006, Lawler 2001, McDermott and Sherman 2009). Combining the spatial array of erosion pins with probability theory based on geostatistical methods of interpolation (Burrough and McDonald 1986, Hengl 2009, Oliver et al 1989, Robinson and Metternicht 2006, Shi et al. 2003) allows the creation of reliable and detailed water and wind erosion rate maps, which can be important decision support tools for the land use management. Several studies have successfully used geostatistics approaches for mapping the spatial and temporal variation of the sediment transport rate (Chappell et al. 2003a, 2003b, Poortinga et al. 2015, Sterk and Stein 1997, Visser et al. 2004, Uzun et al. 2017), while so far there is no an indication of the application of such a combined approach in Iran.

The Sistan plain is located in the Eastern of Iran, near the border to Afghanistan. It is an alluvial plain in the lower reaches of the Hirmand River and is dominated by a group of six ephemeral lakes called “Hamoun Lakes” and characterized by a very strong wind during the hot season. This wind, locally called “Sadobist Roozeh” or “the 120 days of wind” is formed by a Siberian air stream flowing from Northern and North-western direction from the Hindu-Kush mountain range into the Sistan plain lowland between mid-May and mid-September (Alizadeh-Choobari et al. 2014). The water level of the six Hamoun Lakes varies largely and in times of prolonged droughts the lakes desiccate and dry up. When a strong wind blows during the hot and dry season it can easily mobilize the sediments of the dry lake beds, turning the Hamoun Lakes into important sources of dust and sand storms in the Southwest Asia (Goudie and Middleton 2006, Middleton 1986). A particular long drought began in 1999 and the number of dusty days has rapidly increased since

that year (Miri et al. 2010), negatively affecting not only the Sistan region but also Southern Afghanistan and Northern Pakistan.

In this study, the collected data of the aeolian sediment transport rate for the Sistan Baringak Lake has been analysed using a geostatistics approach in order to understand the temporal and spatial dust variation during a four months' period in 2013. The main objective of the study was to identify areas sensitive to the aeolian transport as a scientific base for the selection of prioritized areas for erosion mitigation measures.

6.2 Research Area

The Baringak Hamoun Lake is located in the Zabol county of the Sistan and Baluchistan Province (30.2°N-31.5°N; 61.0°E-62.2°E; average elevation: 500 m a. s. l.) in South-eastern part of Iran, the largest of the 31 provinces in the country. Zabol county borders to the Nimruz and Farah provinces in western Afghanistan and is close to the Chaghi district in the Baluchistan province in western Pakistan. The total area of the Zabol, Nimruz, Farah and Chaghi administrative units is 150,000 km², inhabited by approximately one million people.

Table 6.1 Area, average depth and location of the six Sistan Plain Lakes (UNEP 2006)

Sistan Plain Hamouns Lakes	Average depth (m)	Area (km²)	Area in Iran (%)	Area in Afghanistan (%)
Baringak	1	221.6	100	-
Chonge Sorkh	1	59.8	100	-
Hamoun Hirmand	2	2,388.8	100	-
Hamoun-e-Puzzak	2-3	1,514.4	5.2	94.8
Hamoun-e-Sabari	3	1,161.5	41	59
Gowd-e-Zareh	10	2,417.5	-	100

The annual precipitation in this region is 105 mm just near the Afghan border and 56 mm in the lower parts of the plain. The annual mean air temperature is relatively high with 21.6°C. The summers are hot and dry with averages temperatures of up to 35°C and the winters are mild (8°C) with an average monthly precipitation of 20 mm. This classifies the Sistan plain as a hot desert climate (BWh) after Köppen-Geiger (Peel et al. 2007).

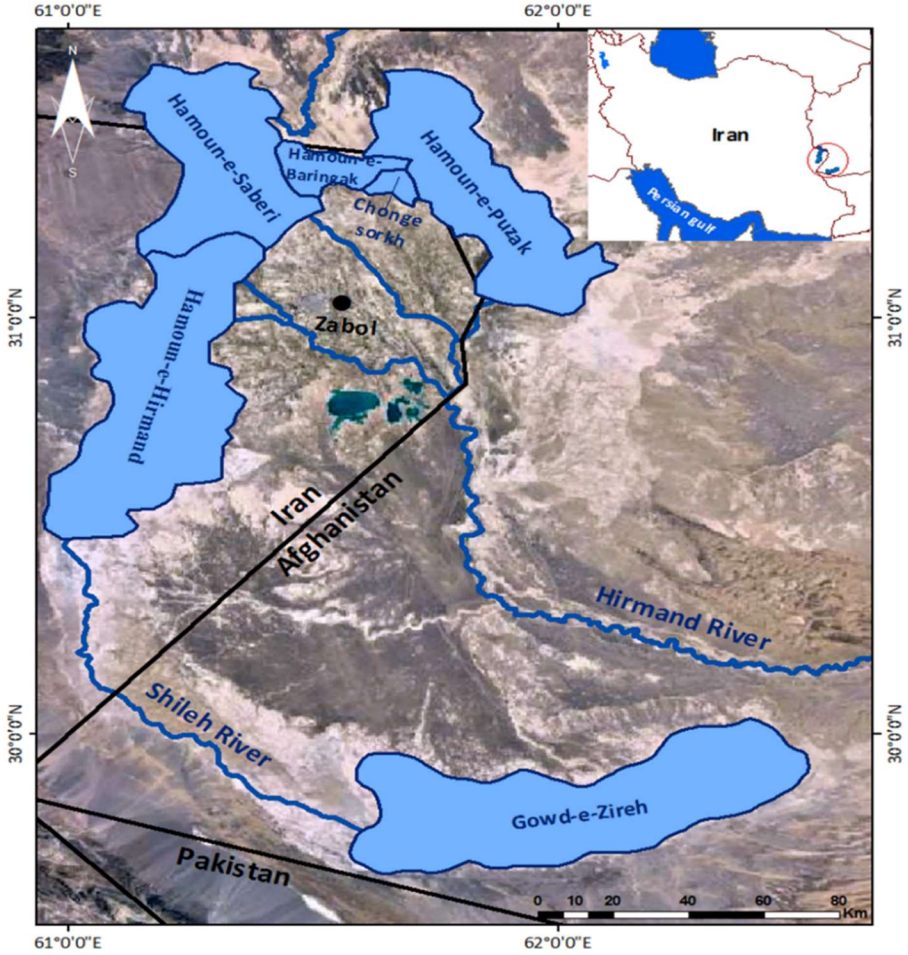

Fig. 6.1 Location of the Hamouns lakes in the Sistan plain (Source: Abbasi et al. 2018, p. 317)

The central element of the Sistan plain is a complex of six lakes (Fig. 6.1), which are in Persian called Hamoun Lakes, describing their ephemeral character. The Lakes of Hirmand, Chonge Sork, Baringak and some part of the Sabari and Puzzak Lakes are located in Iran while the other parts of the Sabari and Puzzak Lakes as well as the Gowd-e-Zareh Lake are located in Afghanistan (Table 6.1). The total area of the lakes is 7,763.6 km², 41.5% of which are located in Iran and 58.5% in Afghanistan (Vekerdy et al. 2006). The lake system is supplied by the Hirmand (or Helmand) River, which originates in the Kabul mountains in Afghanistan and flows into Iran. Its water is mainly used for irrigation farming in the Afghan part of the catchment. During the last 20 years, six dams have been constructed in the upper reaches, mainly for the irrigation water management, and as a result less water reaches the Hamoun Lakes. In combination with a severe drought, starting in

1999, the aeolian dust transport in the Sistan region has thus significantly increased in recent years (Rashki et al. 2013, Sharifikia 2013, Vekerdy et al. 2006).

The field measurement area selected for this study is the Hamoun-e-Baringak (31.2°N; 61.35°E), which is located between the Sabari and Puzzak Lakes near the Iran-Afghanistan border. It is a shallow lake with an area of 221.6 km² (Table 6.1). Water from the Hamoun-e-Puzzak flows into the Hamoun Sabari via the Baringak Lake during heavy flood events. The Hamoun-e-Baringak is a playa filled with quaternary lacustrine silts and clays, covered by Holocene fluvial sands, silts and clays (Whitney 2006). The dominant soils are Entisols or Aridisols (Aqusalids and Torriorthents). The soil texture (based on 48 soil samples) is composed of 24% sand, 43% silt and 33% clay. The topsoil bulk density is 1.6 gr/cm^3, the average electrical conductivity is 62 dS/m, and the average pH is 9.

6.3 Material and methods

For this study a combination of meteorological data, field measurements and geostatistical methods have been used. For the meteorological information, data from the Zabol station was adopted. This station is located 10 km south of the Baringak study area (31°02′N, 61°50′E, Fig. 6.1) at an elevation of 480 m. Wind speed and wind direction data recorded at 10 m above ground level were provided in three-hour intervals for the period from 1994 to 2013 by the IRIMO (I.R. Iran Meteorological Organization). Based on this high temporal resolution data, seasonal wind roses were created in 36 sectors using the frequency of different wind speeds as a percentage of the total winds (Fig. 6.4). In addition to this long-term analysis, the maximum daily wind speed data for the year 2013 was also plotted against the time (Fig. 6.5).

In order to monitor the aeolian sand and dust transport, a network of 74 graduated pins were embedded in the soil of Baringak study area (Fig. 6.2). This study area (20 km x 7 km) had been selected based on the interpretation of dust and sand storm satellite images (MODIS 2004) and on-site experiences, showing that the land could be a major sand and dust source in the region. The positions of the pins were determined randomly and then recorded with GPS (Fig. 6.3). All pins were embedded on the 5th of August 2013 and the aeolian transport rates were measured on the 28th of August, the 15th of September and the 17th of November in 2013.

The collected field data have been used for the generation of variograms in order to analyze the spatial and temporal dependencies of the aeolian transport rate. A variogram is a function describing the degree of spatial dependence of a random spatial random data field or within a stochastic process, and it is a useful tool for the interpretation of the causes of spatial variation (Webster and Oliver 2001). The variogram indicates the degree of similarity among the values of a variable when the samples are separated by sequential distance increments called lag distances, and what this distance is also spatially orientated (Akhavan 2010). The variogram analysis was

carried out in GS+ (version 10) for each event of sediment transport using a fitted model based on an ordinary kriging method. The mass transport rates were mapped using the geostatistical analysis extension in ArcGIS (version 9.3).

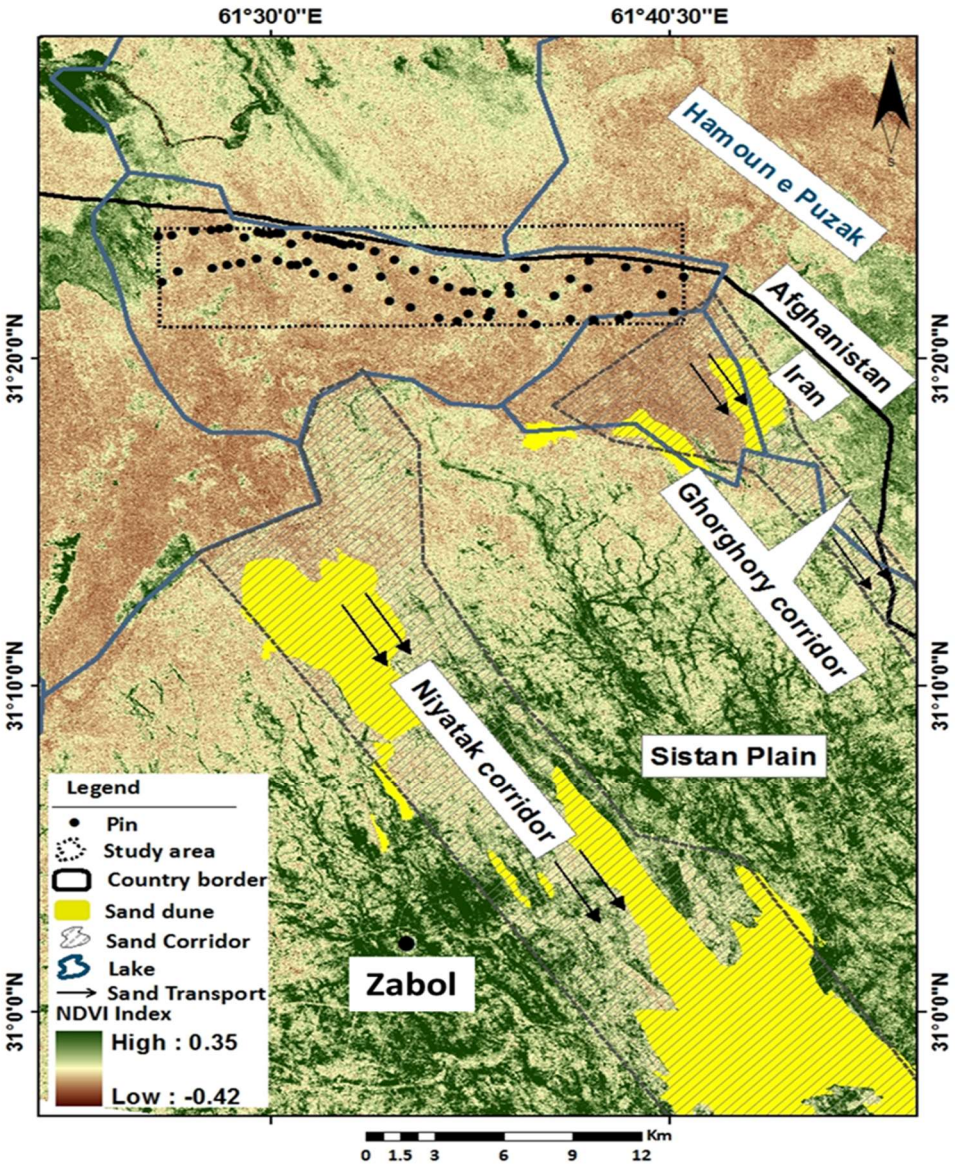

Fig. 6.2 NDVI for the Sistan Region derived from Landsat-8 ETM + images for the year 2013 and the locations of the installed erosion pins in the Hamoun-e-Baringak and study area, hachure parts show sand corridors. (Source: Abbasi et al. 2018, p. 319)

The mean absolute error (MAE), relative mean absolute error (RMAE), root-mean-square error (RMSE) were used in a second step to assess cross validated models. The best fitted model was

selected for the three events as well as for the whole duration, followed by an evaluation of the spatial variations of the aeolian transport rate. Ordinary kriging was used for the spatial interpolation and the results have been cross-validated in order to evaluate the variogram performance.

Fig. 6.3 Graduated erosion pin (left) and indicators of the wind energy in the Baringak Lake (right) (Source: Abbasi et al. 2018, p. 320)

6.4 Results and discussion

6.4.1 Wind data analysis and wind erosion events

The seasonal wind roses (Fig. 6.4) revealed prevailing winds blowing from northern and north-western directions throughout the year. The wind speed was characterized by strong day-to-day fluctuations of up to 20 m/s (Fig. 6.5). On average the highest speed winds were registered in spring and summer (6.75 m/s and 9.53 m/s) and were related to the “120 windy days”. During autumn and winter, on the other hand, the average wind velocities were much smaller (3.96 m/s and 3.81 m/s). The long-term (1995-2013) average wind speed was 11.96 m/s and the recorded maximum had been detected on June 13th in 2004 with 29 m/s.

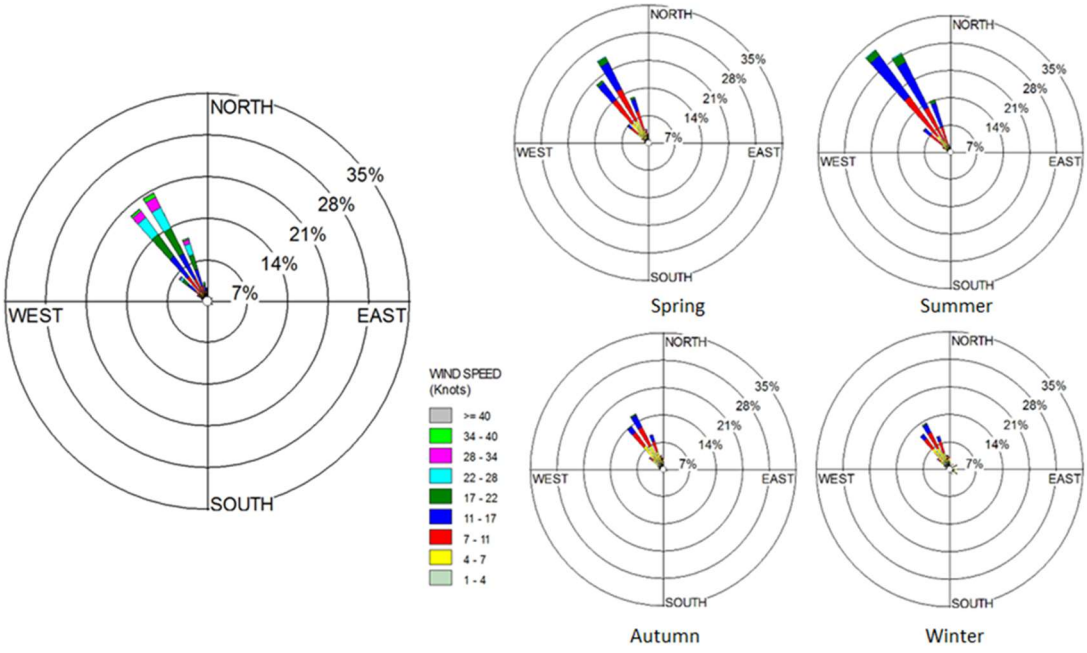

Fig. 6.4 Annual and seasonal wind roses for the Zabol Meteorological Station for 1995–2013; 36 sectors, with the frequency of different wind speeds as a percentage of the total winds (Source: Abbasi et al. 2018, p. 320)

Overall, the wind speed in the Sistan region is relatively high with 69 days (1,687 hours; 19% of all days) exceeding 10 m/s in 2013. Within the study period from the 5th of August to the 17th of November in 2013, this wind speed had been exceeded on 40 days (38% of the days).

The wind characteristics for the three measurement periods are given in Table 6.2. The highest wind speeds (up to 20 m/s, with an average of 10.3 m/s for all hours with a wind speed ≥7 m/s) were detected during the first period (05.08.-28.08.2013), which is still part of the "120 windy days". This first period was also characterized by the highest percentage of hours with an average wind speed of ≥7 m/s (61.3%). Over the course of the study period the maximum wind speed dropped considerably from 20 m/s to 15-17 m/s and the percentage of hours with a wind speed of ≥7 m/s steadily decreased from 61.3% to 48.6% during the second period and to 25.3% during the third period. This emphasizes the meteorological magnitude of the "120 windy days" and its potential for dust and sand mobilization. Throughout the whole period the dominant wind came from NNW, therefore the wind regime can be considered unimodal for this study, which increases the accuracy of the pin measurements.

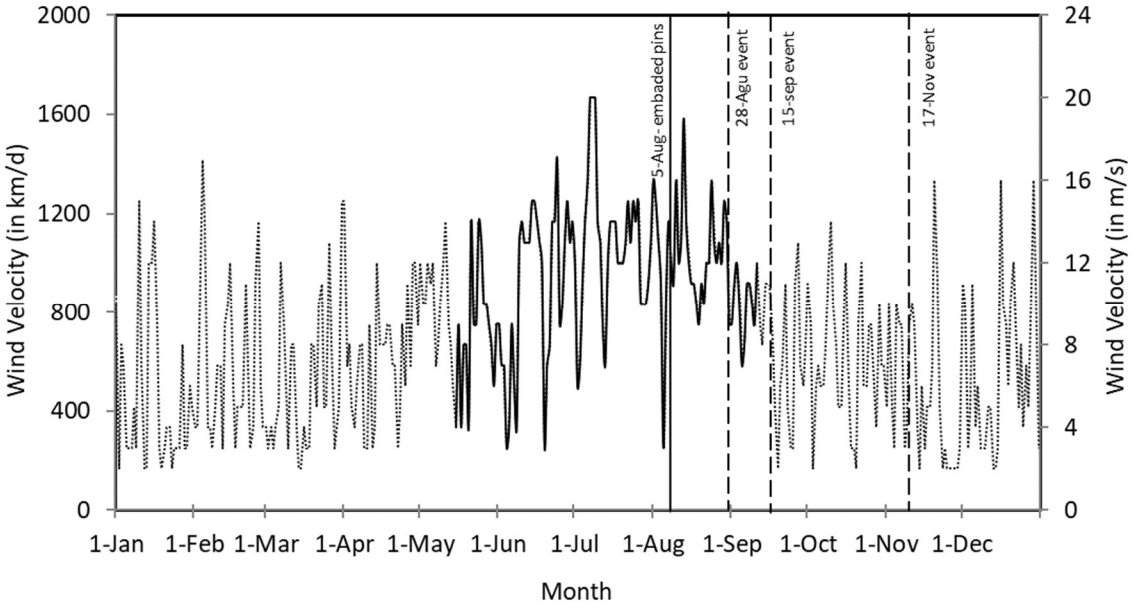

Fig. 6.5 Maximum daily wind speed at the Zabol meteorological station in 2013. The thicker black line section shows the duration of the wind of the 120 days; the black vertical line marks the embedding of the pins and the dashed vertical lines indicate the dates of the transport rate measurements. (Source: Abbasi et al. 2018, p. 321)

Table 6.2 General characteristics of wind erosion events between August and October 2013 in the Sistan region, based on data from the Zabol meteorological station

No	Event and Date	Maximum wind speed (m/s)	Average wind speed of all hours ≥7 m/s (m/s)	Wind duration ≥7 m/s (hours and % of the duration)	Dominant Wind direction
1	05.08.2013-28.08.2013	20	10.3	353 (61.3%)	NNW
2	29.08.2013-15.09.2013	15	9.6	210 (48.6%)	NNW
3	16.09.2013-17.11.2013	17	9.3	383 (25.3%)	NNW
4	Total duration	20	9.7	946 (37.5%)	NNW

(Source: Abbasi et al. 2018, p. 321)

6.4.2 Aeolian sediment transport

The meteorological data showed that the Sadobist Roozeh period during the summer months has a much higher potential for the dust and sand mobilization and long-distance transport than the autumn and winter seasons. This is also confirmed by the sediment erosion data gathered with the erosion pins. Several sediment transport metrics are provided in Table 6.3. During the first period (August 2013) both the variability and the mean erosion rate (0-64 kg/m and 17.94 kg/m on average) recorded in the Baringak study area have been much higher than during the following two periods.

Table 6.3 Summary statistics of the average transport rates in the Baringak study area.

Dates and events	No. of pins	Min-Max Range (kg/m)	Mean Transport		Median (kg/m)	Standard Deviation (kg/m)	Coefficient of Variation (%)	Kurtosis	Skewness
			kg/m	cm					
05.08.-28.08.2013	74	0-64	17.94	1.12	16	1.74	102	0.04	0.94
29.08.-15.09.2013	74	0-32	10.64	0.67	8	1.5	98	-0.57	0.75
16.09.-17.11.2013	66	0-16	2.54	0.16	0	0.99	153	2.58	1.7
Total	74	0-80	30.86	1.93	32	1.48	71	-0.65	0.36

(Source: Abbasi et al. 2018, p. 322)

The average erosion measured by the pins was 1.12 cm during the first period (Table 3) which equals an erosion rate of 0.53 mm/d. During the second and third period the recorded erosion rates were much lower (0.32 and 0.03 mm/d respectively). During the total duration of 103 days, 1.93 cm of soil was eroded from the Baringak Lake bed (30.86 kg/m). Based on this erosion rate it can be estimated that 6.84 million tons of lake bed sediments have been eroded from the 221.2 km² large Baringak Lake between August and November of 2013.

6.4.3 Geostatistical analysis

In order to give the point data collected with the erosion pins a spatial dimension, a geostatistical analysis of the erosion rate data was conducted. To reduce the skewness of the sample distribution, the data from the first two periods were transformed to square-root and for the third period data a natural logarithmic transformation (with zero values changed into 0.01 kg/m) was performed, since this increases the approximation of the sample distribution towards a Gaussian population.

The data set has been analyzed for spatial patterns using variograms for each of the three periods and for the total duration. The spherical and Gaussian models showed the best fit for the sediment transport during the different periods (Table 6.4) and thus were used for providing the needed spatial continuity. These models were selected based on the high spatial structure of the input data, and the good fit with the sill (C+Co) and nugget (Co) points used for the kriging. The range and sill parameters explain the structure of the spatial variation and estimate the unsampled locations with the kriging method (Chappell and Agnew 2001, Chappell and Oliver 1997). The spatial interrelation of the erosion data was assessed by C/(C+CO), which ranges 0-1 (where "1" stands for a suitable spatial interrelation and "0" stand for a weak spatial interrelation and high nugget effect).

All three sediment transport periods were characterized by high $C/(C+C_O)$ values as shown in Table 6.4. This shows that this geostatistical approach is a suitable tool for the estimation of the erodibility of land by aeolian processes.

The highest spatial interrelationship ($C/(C+C_O)$) was found for the periods 3 (0.99) and 1 (0.97), while for the period 2, as the transitional phase between the “120 windy days” and the winter season wind regime, showed a weaker (0.81) spatial pattern of the sediment transport data. This spatial variability is also apparent by the much larger nugget value for period 2. The geostatistical parameters calculated for the whole period from August to November also showed a weaker spatial interrelation, which emphasizes the importance of shorter time slices for the analysis of spatial patterns.

Table 6.4 Results of the cross variogram analysis and the fitted models for sediment transport for the three periods in 2013 at the Baringak Lake

Period	Model	MSE	Range	Spatially dependent variance C	Nugget Variance C_O	Sill ($C+C_O$)	$C/(C+C_O)$
1.:05.08.-28.08.2013	Spherical	1.33	1,698	7.17	0.16	7.33	0.97
2.:29.08.-15.09.2013	Gaussian	1.26	1,579	3.29	0.91	4.83	0.81
3.:16.09.-17.11.2013	Spherical	0.48	3,569	3.01	0.00	3.01	0.99
Total	Spherical	0.67	4,830	395.30	94.00	489.30	0.81

(Source: Abbasi et al. 2018, p. 322)

The data points and the fitted models are displayed in Fig. 6.6. This clearly shows that the sediment transport rates have changed between August and November of 2013.

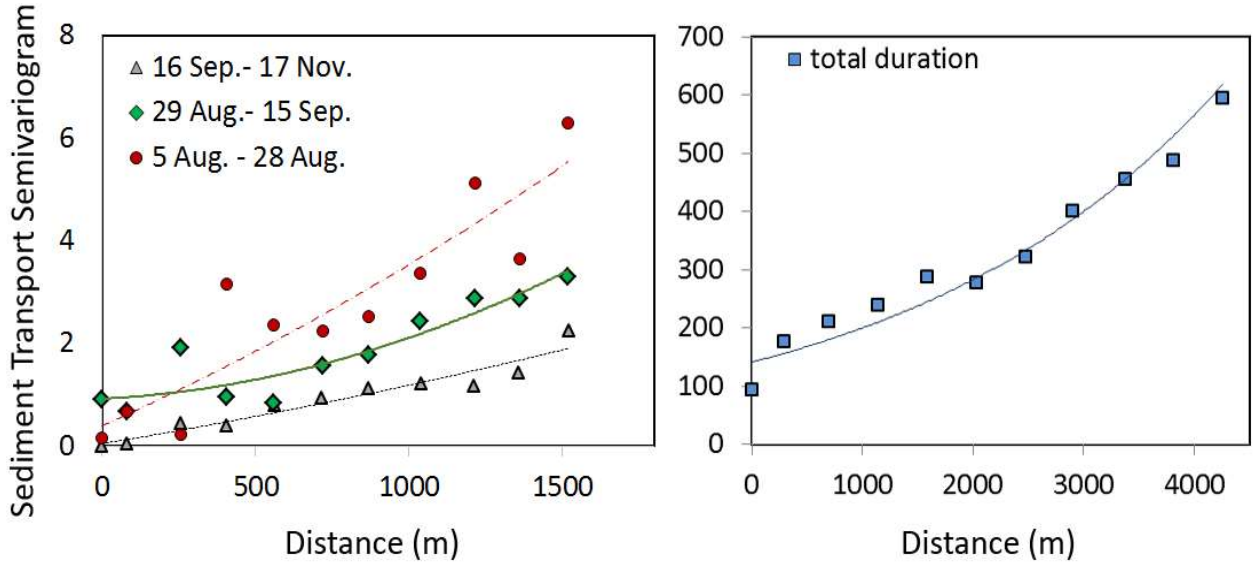

Fig. 6.6 Aeolian sediment transport rate variograms (point data) and fitted models (lines) for the three periods and the total duration for the Baringak Lake (Source: Abbasi et al. 2018, p. 323)

The results of the variogram analysis show that the sediment transport was characterized by a high spatial dependence during the different periods. Therefore, the assessment of the aeolian transport by combining the pin method with geostatistics models is acceptable in the Sistan region with its unimodal wind direction scheme during the Sadobist Roozeh wind period. The high spatial interrelation detected in this study (Table 6.4) is an indicator for less homogeneous natural conditions with regards to vegetation cover, soil crusting and land management. Other studies found much smaller spatial dependencies in a small cultivated field (60 m × 40 m) in Niger (Sterk and Stein 1997) and in three different geomorphic landscape units (valley, dune and degraded plot) in Burkina Faso (Visser et al. 2004).

The sediment transport rates recorded in the Baringak Lake showed a large range variability between the three periods (1,579 m – 3,566 m) and the range for the total duration was even greater (4,830 m). These ranges (and their variance) are much larger than the 676 to 2,344 m ranges (high spatial interrelation ratios) detected by Chappell et al. (2003) based on a 40 sampler campaign covering eight events in an Australian clay pan.

The results of the kriging interpolation of the sediment transport rate have been cross validated for all three periods and the total duration (Table 6.5). This validation focusses on the prediction issue, which evaluates the overall deviation of the predicted values from the observed values. This overall deviation is calculated by the mean absolute error (MAE) and the root-mean-square error (RMSE). The MAE indicates the accuracy of the fitted models and the resulting sediment transport maps. The MAE results show that the rate was smallest for the total study period (1.46%), while

the much higher rate for the second period (14.8%) represents transition time between summer and winter wind regimes.

Table 6.5 Validation of the kriging interpolation for the sediment transport rates

Date and event	No. of pins	Mean Absolute Error (MAE)		Root Mean Square Error (RMSE)	
		kg/m	%	kg/m	%
1.: 05.08.-28.08.2013	74	585.7	9.98	11.5	64.23
2.:29.08.-15.09.2013	74	484.7	14.84	8.8	82.79
3.:16.09.-17.11.2013	66	79.9	8.97	2.3	90.22
Total	74	703.7	1.46	12.5	40.49

(Source: Abbasi et al. 2018, p. 323)

6.4.4 Mapping of the aeolian sediment transport

The final results of the geostatistical analysis are the kriging maps of the sediment transport rates for each of the three periods as well as for the whole duration of this study (Fig. 6.7). As seen in these maps, the largest transport rate was detected during the first period, which was heavily influenced by the "120 windy days" wind regime. During this period, the highest sediment transport occurred in the south-eastern part of the study area, near the beginning of the Gorgoori and Niyatak corridors. These corridors are very active sand transport pathways from the Sistan plain into Afghanistan. During the second period, the area of the highest sediment transport activity shifted towards the south and the northwest. Towards the end of the study period the wind energy decreased and thus large areas of the lake's surface did not contribute significantly to the aeolian sediment transport. For the whole study duration from August to November two main centers of wind erosion activity were identified – one in the southeast of the Baringak Lake and the other one in the northwest.

These results show the high spatial variability of the wind erosion potential and emphasize the need for a high resolution ground based research approach when spatial decisions need to be made.

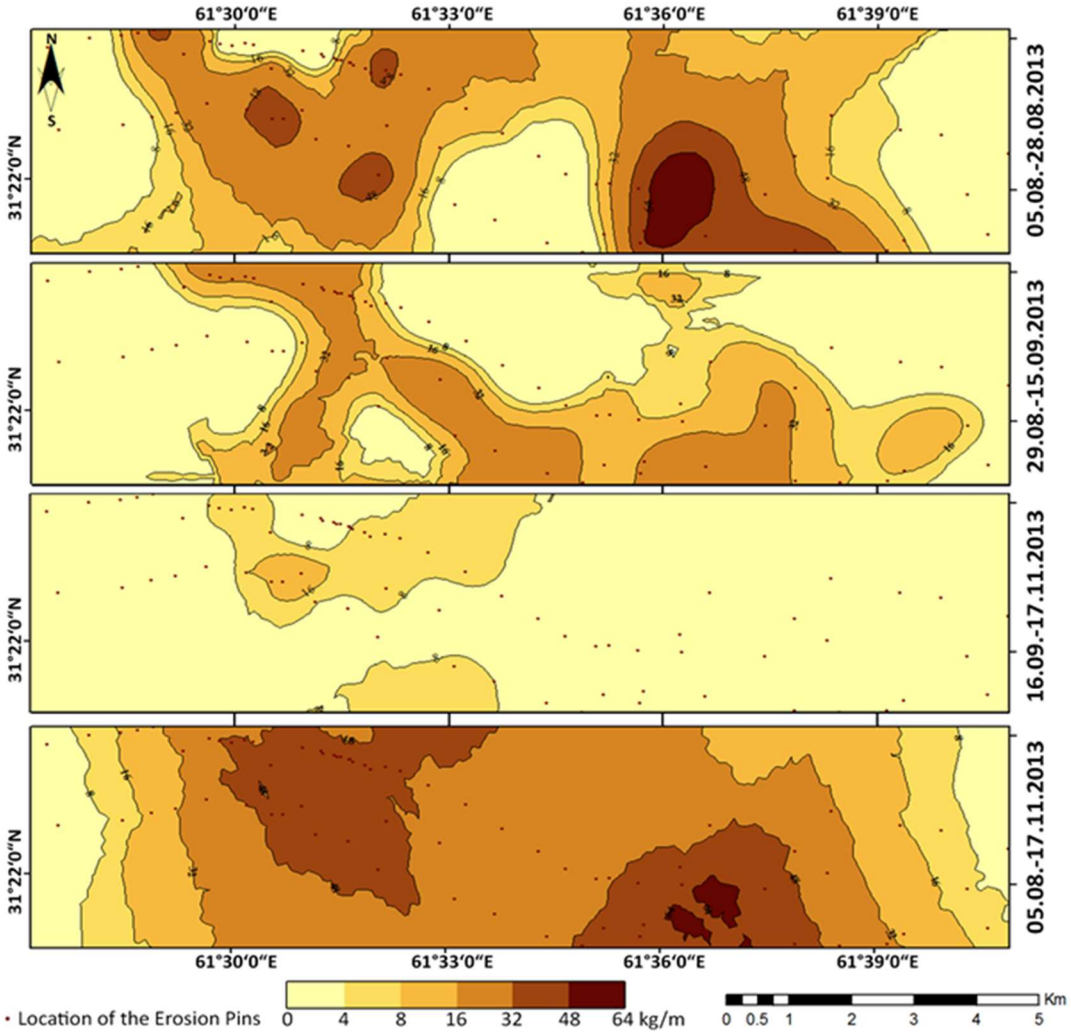

Fig. 6.7 Erosion pin locations and sediment transport rate (kg/m) in the Baringak Lake for the three periods and the total duration, estimated using ordinary kriging (Source: Abbasi et al. 2018, p. 324)

6.5 Conclusion

The application of the pin method for measuring the sediment transport rate and the mapping of the aeolian transport rate using a geostatistics model resulted in detailed data about the temporal and spatial distribution of the wind erosion activity in the Baringak Lake. The Hamoun Baringak Lake plays a very important role for the aeolian mobilization of sediments in the Sistan region because of the hydrological droughts, frequently affecting the lake since the construction of several dams in the upper Hirmand River catchment in Afghanistan, its higher elevation and thus shallow lake bed which is prone to falling dry early in the year, and the gradual decline of the wetland vegetation cover (Vekerdy et al. 2006). The results show that the aeolian transport rate

is highly variable both in time and space during the three time periods covered by this study. This study helped to identify the main sources of the aeolian sediment transport throughout the duration of measurements. The two most active areas should now be prioritized for land management measures in order to minimize the aeolian dust and sand transport in the future.

Furthermore, the results show the great spatial and temporal variability of the sediment fluxes – even in a region characterized by a unimodal wind regime. This highlights the importance of an indepth and high resolution research setup for any future studies.

6.6 References

Ahmadi, H. (2006). Applied Geomorphology, Desert and Wind Erosion, Vol.2, Tehran University publication, p. 716 (in Persian).

Akhavan, R. (2010). Spatial variability and estimation of tree attributes in a plantation forest in the Caspian region of Iran using geostatistical analysis. Caspian Journal of Environmental Sciences 8(2): 163-172.

Alizadeh-Choobari, O., Zawar-Reza, P, Sturman, A. (2014). The wind of 120 days and dust storm activity over the Sistan Basin. Atmospheric Research, 143: 328-341.

Belnap, J., Gillette, D.A. (1998). Vulnerability of desert biological soil crusts to wind erosion: the influences of crust development, soil texture, and disturbance. Journal of Arid Environments 39(2): 133-142.

Bertrand, F. (2010). Fluvial erosion measurements of streambank using Photo-Electronic Erosion Pins (PEEP): University of Iowa MS Thesis, accessed November 23, 2014, at http://ir.uiowa.edu/etd/642.

Burrough, P. A., and McDonnell, R. A. (1986). Spatial Analysis Using Continuous Fields. Principles of Geographical Information Systems, pp. 183–219. https://doi.org/10.1519/r-13104.1

Casagli, N., Rinaldi, M., Gargini, A, Curini, A. (1999). Pore water pressure and streambank stability: results from a monitoring site on the Sieve River, Italy. Earth Surface Processes and Landforms 24(12): 1095-1114.

Chappell, A, Agnew, C.T. (2001). Geostatistical analysis and numerical simulation of West African Sahel rainfall. Land Degradation, Springer. 58: 19-35.

Chappell, A., McTainsh, G., Leys, J, Strong, C. (2003a). Simulations to optimize sampling of aeolian sediment transport in space and time for mapping. Earth Surface Processes and Landforms 28(11): 1223-1241.

Chappell, A., McTainsh, G., Leys, J. and Strong, C. (2003b). Using geostatistics to elucidate temporal change in the spatial variation of aeolian sediment transport. Earth Surface Processes and Landforms 28(6): 567-585. doi: 10.1002/esp.463.

Chappell, A., and Oliver, M. (1997). Geostatistical analysis of soil redistribution in SW Niger, West Africa. Quantitative Geology and Geostatistics 8(2): 961-972.

Chepil, W. (1945). Dynamics of wind erosion: I. Nature of movement of soil by wind. Soil Science 60(4): 305-320.

Goudie, A., and Middleton, N.J. (2006). Desert dust in the global system. Springer Science and Business Media: 288.pp.

Groll, M., Opp, C., Aslanov, L. (2013). Spatial and temporal distribution of the dust deposition in Central Asia, results from a long term monitoring program. Aeolian Research 9: 49-62.

Hadley, R.F., and Lusby, G.C. (1967). Runoff and hillslope erosion resulting from a high-intensity thunderstorm near Mack, western Colorado. Water Resources Research 3(1): 139-143.

Haigh, M. (1977). The use of erosion pins in the study of slope evolution. British Geomorphological Research Group Technical Bulletin 18: 31-49.

Hengl, T. (2009). A practical guide to geostatistical mapping. Second Edition, University of Amsterdam. 291 p.

Herrmann, L., Stahr, K., Jahn R. (1999). The importance of source region identification and their properties for soil-derived dust: The case of Hrmattan dust sources for eastern west Africa. Contributions to atmospheric physics, 72(2): 141-150.

Hooke, J. (1980). Magnitude and distribution of rates of river bank erosion. Earth surface processes 5(2): 143-157.

Horn, D.P., Lane, S.P. (2006). Measurement of high-frequency bed level changes in the swash zone using Photo-Electronic Erosion Pins (PEEPS). Coastal Engineering Conference, World Scientific: 2591p.

Lancaster, N., Baas, A. (1998). Influence of vegetation cover on sand transport by wind: field studies at Owens Lake, California. Earth Surface Processes and Landforms 23(1): 69-82.

Lawler, D.M. (2001). The photo-electronic erosion pin (PEEP) automatic erosion monitoring system: principles and applications. 7th Federal Interagency Sedimentation Conference on Sediment: Monitoring, Modelling and Managing, Nevada, USA, 1: 56-P59.

Li, F.R., Kang, L.F., Zhang, H., Zhao, L.Y., Shirato, Y., Taniyama, I. (2005). Changes in intensity of wind erosion at different stages of degradation development in grasslands of Inner Mongolia, China. Journal of Arid Environments 62(4): 567-585.

McDermott, J.P, Sherman, D.J. (2009). Using photo-electronic erosion pins for measuring bed elevation changes in the swash zone. Journal of Coastal Research 25(3): 788-792.

Middleton, N.J. (1986). Dust storms in the Middle East. Journal of Arid Environments, 10(2): 83-96.

Miri, A., Moghaddamnia, A., Pahlavanravi, A, Panjehkeh, N. (2010). Dust storm frequency after the 1999 drought in the Sistan region, Iran. Climate Research, 41(1): 83-90.

Oldemann, L.R. (1992). Global extent of soil degradation. ISRIC Bi-Annual Report 1991–1992, International Soil Reference and Information Centre (ISRIC), Wageningen, Netherlands, 19–36.

Oliver, M., Webster, R, Gerrard, J. (1989). Geostatistics in physical geography. Part II: applications. Transactions of the Institute of British Geographers, 14(3): 270-286.

Opp, C. (1998). Geographische Beiträge zur Analyse von Bodendegradationen und ihrer Diagnose in der Landschaft. Leipziger Geowissenschaften 8, Leipzig: 187 pp.

Opp, C., Groll, M., Aslanov, I., Lotz, T., Vewreshagina, N. (2016). Aeolian dust deposition in the southern Aral Sea region (Uzbekistan): Ground-based monitoring results from the LUCA project. Quaternary International (2016), http://dx.doi.org/10.1016/j.quaint.2015.12.103.

Peel, M.C., Finlayson, B.L, McMahon, T.A. (2007). Updated world map of the Köppen-Geiger climate classification. Hydrology and earth system sciences discussions 4(2): 439-473.

Poortinga, A., Keijsers, J., Visser, S., Riksen, M, Baas, A. (2015). Temporal and spatial variability in event scale aeolian transport on Ameland, Netherlands. Geo. Res. J., 5: 23-35.

Rashki, A., Kaskaoutis, D., Goudie, A, Kahn, R. (2013). Dryness of ephemeral lakes and consequences for dust activity: the case of the Hamoun drainage Basin, south-eastern Iran. Science of the Total Environment, 463: 552-564.

Ravi, S., Breshears, D.D., Huxman, T.E, D'Odorico, P. (2010). Land degradation in drylands: Interactions among hydrologic, aeolian erosion and vegetation dynamics. Geomorphology 116(3): 236-245.

Reich, P., Eswaran, H, Beinroth, F. (1999). Global dimensions of vulnerability to wind and water erosion, In: Sustaining the global farm, edited by: Stott, D. E., Mohtar, R. H., and Steinhardt, G. C., Selected papers from the 10th International Soil Conservation Organization Meeting at the Purdue University and the USDAARS National Soil Erosion Research Laboratory, West Lafayette, USA, 24–29 May: 838–846.

Robinson, T, Metternicht, G. (2006). Testing the performance of spatial interpolation techniques for mapping soil properties. Computers and Electronics in Agriculture, 50(2): 97-108.

Sharifikia, M. (2013). Environmental challenges and drought hazard assessment of Hamoun Desert Lake in Sistan region, Iran, based on the time series of satellite imagery. Natural hazards, 65(1): 201-217.

Shi, W., Fisher, P, Goodchild, M.F. (2003). Spatial data quality. CRC Press, Boca Raton: 340 pp.

Sterk, G, Stein, A. (1997). Mapping wind-blown mass transport by modelling variability in space and time. Soil Science Society of America Journal, 61(1): 232-239.

Takei, A., Kobashi, S, Fukushima, Y. (1981). Erosion and sediment transport measurement in a weathered granite mountain area. Publ. IAHS, 133: 493–501

Uzun, O., S. Kaplan, Basaran, M., Deviren Saygın, S., Youssef, F., Nouri, A., Ozcan, A. U., Erpul G. (2017). Spatial distribution of wind-driven sediment transport rate in a fallow plot in Central Anatolia, Turkey. Arid Land Research and Management, 31(2): 125-139.

Vekerdy, Z., Dost, R., Reinink, G, Partow, H. (2006). History of environmental change in the Sistan Basin based on satellite image analysis: 1976–2005. Report, United Nations Environmental Programme (UNEP) and ITC, 60 pp. http://postconflict.unep.ch/publications/sistan.pdf

Visser, S.M., Sterk, G, Snepvangers, J.J. (2004). Spatial variation in wind-blown sediment transport in geomorphic units in northern Burkina Faso using geostatistical mapping. Geoderma 120 (1): 95-107.

Webster, R, Oliver, M.A. (2001). Geostatistics for Environmental Scientists. Statistics in Practice. Wiley, Chichester: 265 pp.

Weinan, C, Fryrear, D.W. (1996). Grain-size distributions of wind-eroded material above a flat bare soil. Physical Geography, 17(6): 554-584.

Whitney, J.W. (2006). Geology, water, and wind in the lower Helmand Basin, Southern Afghanistan. US Geological Survey Scientific Investigation Report: 5182. 40 pp.

Wolfe, S.A, Nickling, W.G. (1993). The protective role of sparse vegetation in wind erosion. Progress in Physical Geography 17: 50-50.

Wolman, M.G. (1959). Factors influencing erosion of a cohesive river bank. American Journal of Science, 257(3): 204-216.

7
Final Conclusion

7.1 Conclusion

The following conclusion provides an overview of the main findings of the present thesis which is associated with three key objectives, while the conclusions of the individual core chapters 4–6 were already discussed comprehensively within the individual chapters.

The first key objective of the thesis was the investigation of the spatial variations of DP, the simulation and comparison current used sand dunes activity models and development of a new model regarding Iran dunes conditions. This objective set out to improve the accuracy by which the new model of sand dunes activity in the whole of Iran using climatological and field data. Accordingly, the identification of areas with active dunes is of paramount importance in prioritizing the monitoring and stabilization efforts. These data will be extremely useful for policymakers and national planners to mitigate significant shifting dunes hazards. Kelley et al. (2015) expect drier and potentially dustier situations in the Middle East in the 21st Century. In fact, with improved future SDS scenarios and accurately defined wind erosion source areas and fully active dunes, these results will help to reduce and to mitigate hazard.

Regarding wind energy variations based on DP, there are great spatial variations across Iran's deserts. High wind energy environment occurs, with 39% of desert area, in the eastern and southern Lut desert, Sistan, the northern and central part of Dasht-e Kavir desert, the western of Jazmorian, some parts of Yazd and Khuzestan provinces. According to results, the east of Iran experienced one of the highest wind energy among inner deserts in the world. Whereas moderate wind energy environment covers most of Iran's deserts with 39% of desert area e.g. the central-west part of Dasht-e Kavir desert, the western and south-western parts of the Lut desert, the south-eastern and western parts of the Khuzestan province and whole of the Oman Sea coast.

A low energy wind environment with 22% of desert area can be found in the southwest of Dasht-e Kavir desert (Kashan and Aran), the eastern part of Jazmorian, Sarakhs, Ferdous, Booshroyeh, Gonabad and the central and northern parts of Khuzestan province and Neyshabor region.

The results of estimated DP and other key parameters in relation to wind energy based on Fryberger and Dean (1979) method in national scale showed that it provides realistic and practical results but the collection and analysis of data can be time-consuming and expensive although the new automatic models are coming out e.g. the ERA-Interim project which integrates surface wind data and satellite images data to simulate speed and direction of winds (Dee et al. 2011; Largeron et al. 2015; Radebaugh et al. 2017). To the knowledge of the author, this model can be able to simulate effective wind characteristics. Further development and application of methods for assessing effective winds in relation to wind erosion and sand transport at the landscape scale will improve our capacity for monitoring and modelling land degradation processes in remote desert environments.

In the following, three more commonly used dune activity models, Lancaster mobility index (LMI), Tsoar mobility index(TMI) and Yizhaq model (YMI) were evaluated in Iran's deserts. The analysis of the indices showed that the dunes activity was characterized by big spatial variations across Iran's deserts. All three models identified fully active dunes in the Sistan plain, the whole of the Lut desert, as well as in the Zirkuh Qaien and Deyhook regions, while the dunes in the northern part of Rig Boland, Booshroyeh and in the Neyshabor dunefields were categorized as stabilized dunes. For other dunes, the models show a less unified activity classification, with the Lancaster and Yizhaq models having more similar results while the Tsoar model stands more apart. One of the different parameters used in the models is the wind power parameter. It is in LMI the percentage of times of winds above the transport threshold (W%), while the TMI and YMI used DP. DP reflects the quantity (frequency) and quality (intensity) of the wind power, but W% only shows its quantity (frequency of winds above the transport threshold). According to this, DP is used in the LMI instead of W% and a new model which named modified Lancaster mobility index (MLI) was developed based on DP, precipitation and potential evapotranspiration. The results of MLI show a large spatial variations of dunes activity due to the high variations of the wind energy, precipitation and potential evapotranspiration in Iran's desert areas. The MLI classified dunes in Sistan plain, whole of Lut desert, Zirkuh Qaien and Deyhook as fully active and in the northern part of Rig Boland, Booshroyeh and Neyshabor dunefields as stabilized dunes. The results of MLI are more realistic with field observations in comparison with other models. The highest similarities were found between the LMI and MLI, followed by the Yizhaq model.

Out of the four mobility indexes, fully active dunes area was noticeably higher in LMI, at 66%, in MLI, at nearly 64%, in YMI, at 42%, and in TMI near 31%. Proportion of the area of semi-active dunes was highest in YMI, at 43%, while were significantly lower in LMI and MLI with 34 and 33%, respectively. As mentioned in chapter 4, there is no semi-active class in TMI. It can be seen that the stabilized dunes have great different area in four indexes so that TMI has the largest

percentages of area, at nearly 66%, then YMI, at 15%, and LMI and MLI just over 1 and 3% respectively.

The scientific community has focused on climate change, global warming and the impact of natural and anthropogenic sources of air pollution on Earth's weather and climate systems in recent years. The International Panel on Climate Change (IPCC) has clearly reported that global warming is likely to reach 1.5°C between 2030 and 2052 (IPCC, 2018) and even "hothouse earth" outlook has been raised recently (Steffen et al. 2018). In fact, climate models project robust differences in regional climate characteristics between present-day and global warming of 1.5°C, and between 1.5°C and 2°C. According IPCC report (2018), these differences include increases in: mean temperature in most land and ocean regions (high confidence), hot extremes in most inhabited regions (high confidence), heavy precipitation in several regions (medium confidence), and the probability of drought and precipitation deficits in some regions (medium confidence).

Both global climate change and overgrazing of dune system in Iran cause substantially environmental and economic damages. Available evidence indicates that dune reactivation can be driven by changes in aridity, increased wind speed, fire, biogenic disturbance, human disturbance, or a combination of the previous (Barchyn and Hugenholtz, 2013). It seems that further studies are needed to consider different climate change scenarios to predict sand dunes activity. This thesis provided a database including the most important associated information about the climatological data that can predict the climate change impacts on reactivation dunes in Iran's arid and semi-arid areas. In fact, beyond this database, the data produced in this investigation can be used to support several future research opportunities in relation to climate change and sand dune activities.

The advantage of a new model (MLI) is that it can show climate change impacts on dunes activity because the PET and DP parameters are used together that none of the other models express. This model is able to show the trend of temperature and consequently the PET in different scenarios of climate change. Holdridge (1967) showed that each degree of temperature corresponds with 59 mm year–1 of PET according to the Thornthwaite method. According IPCC scenarios, an increase of 1.5°C and 2°C, PET will increase 90 and 118 mm year–1, respectively. The increasing PET will reactivate some sand dunes even if the precipitation and wind energy remain constant in future.

As the meteorological stations are not homogeneously distributed across Iran's deserts, and they are far away from the dune fields e.g. in the central part of the Lut and the Dasht-e Kavir, the assessment of the dune activity requires complementary field observations, as it already was pointed out by Bullard et al. (1997). In order to accurately simulate effective winds in Iran, especially for the mountainous corridors that accelerated winds, it is necessary to create a closer station network which guaranties a better representation of the surface.

The second key objective of the thesis was an investigation of wind regime and sand transport. The outcome may help to understand the wind regime specifications and shifting-sand control in Sistan plain and Registan sand sea. In order to obtain objective, three decisive parameters sand transport, wind speed, duration, and direction were estimated in the Sadobist Roozeh wind domain.

Due to prolonged droughts in Sistan (Kaskaoutis et al. 2015; Sharifikia, 2013) and dams' construction in Afghanistan (Bazrkar et al. 2013: Ahlers et al. 2014), less water reach to the complex Hamouns Lakes. The Sadobist Roozeh wind lifted sediment into the atmosphere easily (Hickey and Goudie, 2007). The Sadobist Roozeh wind became accelerated due to local topography over and along the border of Iran and Afghanistan. This wind has been blowing intensively over Hamoun-e Sabari and Hamoun-e Baringak Lakes in Sistan region, then it decreased gradually over Registan desert. In the context of wind energy environment according to Fryberger and Dean (1979) classification, Sistan region was categorized into high energy and Registan desert into intermediate to low energy. In addition, Drift potential is high in the western portion of the study area and decreases gradually in eastern direction. The annual DP calculated in Sistan is one of the highest values (2516 vector units) in inland deserts, therefore the study area is categorized into the windiest desert in the world.

Being a narrow corridor with north-south direction between the Hindu-Kush Mountains in Afghanistan and southern Khorasan mountains in Iran, the Sadobist Roozeh wind accelerates into it. This corridor was named as "East Wind Corridor" because it is located on the east border of Iran in which a high potential for utilization of wind energy occurs. The resulting annual mean wind velocity of 5.5 m s-1 in the Sistan area is much higher than in the Registan desert. The annual mean days with dust storms were estimated: 174 days from 2000 to 2015 in Zabol, whereas Alizadeh Choobari et al. (2014) reported an average of 167 dusty days per year, and Middleton (1986) reported more than 30 dust storms per year originating from Sistan.

The Sadobist Roozeh wind blowing from Northern to south along the border of Iran and Afghanistan, which turns from north-western to southeast directions in Sistan region and finally, it turns to west-east directions in Registan in south-western directions in Afghanistan. The monthly effective winds of Sadobist Roozeh started to in May, reach the maximum DP and RDP in July, and dropped low again in October at Sistan. Mofidi et al. (2014) believed that the average period of the Sadobist Roozeh wind blowing increased from 120 to 165 days during the period 1972-2012 which is apparently longer than the period which has been estimated by former researchers. According to Zabol weather station data, about 70% of the average annual DP occurs between June and September (120 days), and it was higher than 400 vector units (vu) in July and August at Zabol. The resultant drift direction (RDD) during all months has a NNW direction, ranged from 118° to 124°, showing a very narrow unimodal direction in all seasons. The RDP/DP was 0.97 during all months in Sistan plain that shows a high impact on sand movement.

In Registan, the monthly wind energy based on DP were high from February to August which showed that there is other effective wind in that region. The sand rose diagram of Ghandehar illustrated that effective winds transported sand in W and NE major directions. RDD was consistently between 122° and 187° except March at Farah, between 47° and 89° at Helmand and between 40° and 139° at Spin Buldak.

There has been considerable temporal variability of DP between 2000 and 2016 in Sistan region. It raised up to 4,183 vector units (vu), which is a record of drift potential in inland desert in the world, at Zabol station in 2001. Totally, DP were upper annual mean (2,516 vector units) from 2000 to 2007 at Zabol but it experienced lower than from 2008 to 2016 as well as Zahak. The days with dust storm also showed a similar trend upper annual mean (185 days) from 2000 to 2007 and lower annual mean (170 days) between 2008 and 2015 in Zabol station. Kaskaoutis et al. (2015) showed that 356 dust-storms with less than 1 Km visibility were happened during the summer months (June–September) in the period 2001 to 2012.

Unfortunately, there is no wind data available before 2010 for eastern part of study area. At Helmand, Ghandehar, and Spin Buldak, DP were less than 200 between 2010 and 2016. In other hand, Registan in east of study area has low energy wind. DP fluctuated at Farah between 2010 and 2014 but it had an intermediate wind energy environment in most years because it is located on the leeward side of Hindu-Kush Mountains as well as Delaram.

The trend of RDD is matched by the Sadobist Roozeh wind direction in the study area during the year. At Sistan it ranged from 114˚ to 125˚; between Sistan and Registan ranged between 51˚ and 81˚ ; at Registan generally it ranged from 31˚ to 86˚.

The annual directional variability (RDP/DP) at Sistan constantly ranged between 0.95 and 0.98 in duration 2000-2016. It means that effective wind blows in a narrow unimodal direction with low variability in this period. At Registan, this ratio is mostly intermediate, with value between 0.3 and 0.8 with the exception of Ghandehar, which had a high variability in 2013.

The morphology of dunes is associated with the Sadobist Roozeh wind which has a narrow range of directions in Sistan and Registan sand sea. Unidirectional winds form crescentic dunes. They are the dominant form which depends on sand availability. It can be divided into barchans, barchanoid ridges and transverse dunes. Predominant dune types are compound barchans and barchanoid in Sistan, compound transvers and barchanoid in Dasht-e Margo, and close barchans and simple transvers in Registan. The south-western part of Afghanistan is a high plateau, located between Sistan depression and Registan with around 300 m height difference. It shows that sand dunes move up a sloping and rough plateau and always change in form and shape due to topography, till finally reach to Registan sand sea.

In addition, Chaghi mountains which are located between the border of Baluchistan province of Pakistan and Helmand province of Afghanistan, act as a topographic obstacle, induce separation

of airflow and dunes developed in front of cliffs. Therefore, the dunes are developed into climbing dunes in the western and north Chaghi mountain facieses.

The last key objective of the thesis was the measurement of the aeolian sediment transport in the ephemeral Baringak Lake using field measurements and geostatistical analyses. Recent studies have described how climatic parameters control dust production from the Sistan region (D. G. Kaskaoutis et al., 2015; A. Rashki et al., 2012). Several regional-scale dust storms occur in the Hirmand Basin per year and reduce visibility and air quality in the most populated regions of Sistan and south Afghanistan. Using satellite images over a multiyear time period, the Hamoun-e Baringak Lake plays a very important role for the aeolian mobilization of sediments in the Sistan region because of the hydrological droughts, frequently affecting the lake since the construction of several dams in the upper Hirmand River catchment in Afghanistan. Its higher elevation than other ephemeral lakes and thus shallow lake bed which is prone to falling dry early in the year. In fact, Baringak Lake is a wide canal linked Hamoun-e Puzzak to Hamoun-e Sabari. It acts as one of the major dust and sand source which suffered to more than 200 rural areas in Sistan and two main sand transport corridors, Niyatak and Gorgori-Puzzak, starts from it.

Separate approaches can be applied to assess wind erosion at different scales and different land management. Practices pin method is useful to assess wind erosion directly under field conditions, which is widely-used and a cost effective method. It consists of driving a pin into the soil, that the top of the pin gives a datum from which changes in the soil surface level can be measured (Hudson, 1993). It allows an extensive and long-term spatial measurement of aeolian transport processes based on event or period. Measurements of the amount of aeolian deflation rate (e.g. kg m-1 year-1) in point are required to interpolate a map to improve a fitted model on regional scale. Combining the spatial array of erosion pins with the probability theory based on geostatistical methods of interpolation (Burrough and McDonnell, 1986; Hengl, 2009; Oliver, et al. 1989) allows the creation of reliable and detailed water and wind erosion rate maps, which can function as important decision support tools for land use management.

Several studies have successfully used geostatistics approaches for mapping the spatial and temporal variation of the sediment transport rate (Chappell and Oliver, 1997; Chappell et al. 2003; Poortinga, et al. 2015; Visser et al. 2004). The application of the pin method for measuring the sediment transport rate and the mapping of the aeolian transport rate using a geostatistics model resulted in detailed data about the temporal and spatial distribution of the wind erosion activity in the Baringak Lake.

The results show the average sediment transport rate in terms of the detected drift height on the dry lake bed was 1.93 cm or 31 kg/m2 between the 5th of August and the 17th of November in 2013. The aeolian transport rate is highly variable both in time and space during the time period covered by this study. The great spatial and temporal variability of the sediment fluxes even in a region characterized by a unimodal wind regime. This highlights the importance of an indepth and high resolution research setup in landscape scale for any future studies.

This study helped to identify the main sources of the aeolian sediment transport throughout the duration of measurements. The two most active areas should now be prioritized for land management measures in order to minimize the aeolian dust and sand transport in the future. In addition, further studies are needed for a better understanding of mechanism of aggravation of erosion in dried lakes. Land managers should consider the hydroclimatic setting of the region as well as the surface and soil characteristics of the geomorphological units for rehabilitation planning. Sediment carries by dry-wash rivers and saline soils do have a high erodibility according to wind erosion as pointed by Hahnenberger and Nicoll (2014) and Tadhg (2008).

7.2 References

Alizadeh-Choobari, O., Zawar-Reza, P, Sturman, A. (2014). The wind of 120 days and dust storm activity over the Sistan Basin. Atmospheric Research, 143: 328-341.

Ahlers, R., Brandimarte, L., Kleemans, I., Hashmat Sadat, S. (2014) Ambitious development on fragile foundations: Criticalities of current large dam construction in Afghanistan. Geoforum, 54: 49-58. https://doi.org/10.1016/j.geoforum.2014.03.004

Barchyn, T.E., and Hugenholtz, C.H. (2013). Reactivation of supply-limited dune fields from blowouts: A conceptual framework for state characterization. Geomorphology, 201, 172–182. https://doi.org/10.1016/j.geomorph.2013.06.019

Bazrkar, M. H., Nabavi, E., and Eslamian, S. (2013). System dynamic approach to hydro-politics in Hirmand transboundary river basin from sustainability perspective, International Journal of Hydrology Science and Technology, 3(4): 378–398. https://doi.org/10.1504/IJHST.2013.060338

Bullard, J. E., Thomas, D. S. G., Livingstone, I., Wiggs, G. F. S. (1997). Dunefield activity and interactions with climatic variability in the southwest Kalahari Desert. Earth Surface Processes and Landforms, 22(2), 165–174. https://doi.org/10.1002/(SICI)1096-9837(199702)22:2<165::AID-ESP687>3.0.CO;2-9

Burrough, P. A., and McDonnell, R. A. (1986). Spatial Analysis Using Continuous Fields. Principles of Geographical Information Systems, pp. 183–219. https://doi.org/10.1519/r-13104.1

Chappell, A, and Oliver, M. A. (1997). Geostatistical analysis of soil redistribution in SW Niger, West Africa. Quantitative Geology and Geostatistics, 8(2), 961–972.

Chappell, Adrian, McTainsh, G., Leys, J., and Strong, C. (2003). Using geostatistics to elucidate temporal change in the spatial variation of aeolian sediment transport. Earth Surface Processes and Landforms, 28(6), 567–585. https://doi.org/10.1002/esp.463

Dee, DP, Uppala S.M., Simmons, A.J., Berrisford, P., Poli, P., Kobayashi, S., Andrae, U., Balmaseda, M.A., Balsamo, G., Bauer. P., Bechtold, P., Beljaars, A.C.M., van de Berg, L., Bidlot, J., Bormann, N., Delsol, C., Dragani, R., Fuentes, M., Geer, A.J., Haimberger, L., Healy, S.B., Hersbach, H., H'olm, E.V., Isaksen. L., K˝allberg, P., K˙ohler, M., Matricardi, M., McNally, A.P., Monge-Sanz, B.M., Morcrette, J-J., Park, B-K., Peubey, C., de Rosnay, P., Tavolato, C., Th´epaut, J-N., Vitart, F. (2011). The ERA-Interim reanalysis: configuration and performance of the data assimilation system. Q. J. R. Meteorol. Soc.137: 553 – 597. DOI:10.1002/qj.828

Fryberger, S. G, Dean, G. (1979). Dune forms and wind regime. In: McKee, E.D. (Ed.), A study of global sand seas. Professional Paper 1052, United State Geological Survey, US Government Printing Office, Washington, pp. 137–169.

Hahnenberger, M., and Nicoll, K. (2014). Geomorphic and land cover identification of dust sources in the eastern Great Basin of Utah, U.S.A. Geomorphology, 204, 657–672. https://doi.org/10.1016/j.geomorph.2013.09.013

Hengl, T. (2007). A Practical guide to geostatistical mapping. EUR – scientific and technical research reports. Luxembourg: Office for Official Publications of the European Communities. pp. 272.

Hickey, B. and A.S. Goudie, 2007: The use of TOMS and MODIS to identify dust storm source areas: The Tokar delta (Sudan) and the Seistan basin (south west Asia), in Geomorphological Variations, A.S. Goudie and J. Kalvoda (Eds), 37–57, P3K, Prague, Czech Republic.

Holdridge, L. R. (1967). Life zone ecology. Life Zone Ecology., Tropical Science Center, pp.206.

Hudson, N. (1993). Field measurement of soil erosion and runoff. FAO, 68, pp.141.

IPCC. (2018). Summary for Policymakers. In: Global Warming of 1.5°C. An IPCC Special Report on the impacts of global warming of 1.5°C above pre-industrial levels and related global greenhouse gas emission pathways, in the context of strengthening the global response to, pp.24. https://www.ipcc.ch/site/assets/uploads/sites/2/2019/05/SR15_SPM_version_report_LR.pdf

Kaskaoutis, D. G., Rashki, A., Houssos, E. E., Mofidi, A., Goto, D., Bartzokas, A., Legrand, M. (2015). Meteorological aspects associated with dust storms in the Sistan region, south-eastern Iran. Climate Dynamics, 45(1–2), 407–424. https://doi.org/10.1007/s00382-014-2208-3

Kelley, C. P., Mohtadi, S., Cane, M. A., Seager, R., and Kushnir, Y. (2015). Climate change in the Fertile Crescent and implications of the recent Syrian drought. Proceedings of the National Academy of Sciences, 112(11), 3241–3246. https://doi.org/10.1073/pnas.1421533112

Largeron, Y., Guichard, F., Bouniol, D., Couvreux, F., Kergoat, L., and Marticorena, B. (2015). Can we use surface wind fields from meteorological reanalyses for Sahelian dust emission simulations? Geophysical Research Letters, 42(7), 2490–2499. https://doi.org/10.1002/2014GL062938

Middleton, N.J. (1986). Dust storms in the Middle East. Journal of Arid Environments, 10(2): 83-96.

Mofidi, A., HamidianPour, M., Saligheh, M., Alijani, B. (2014). Determination of the Onset, Withdrawal and Duration of Sistan wind using a Change Point Approach. Geography and Environmental Hazards, 2(8), 87–112. https://doi.org/https://doi.org/10.22067/geo.v0i0.25026

Oliver, M., Webster, R., and Gerrard, J. (2019). Geostatistics in Physical Geography. 238(4827), 625–631.

Poortinga, A., Keijsers, J. G. S., Visser, S. M., Riksen, M. J. P. M., and Baas, A. C. W. (2015). Temporal and spatial variability in event scale aeolian transport on Ameland, The Netherlands. GeoResJ, 5, 23–35. https://doi.org/10.1016/j.grj.2014.11.003

Radebaugh J., Kerber, L., Narteau, C., Rodriguez, S. and Gao, X. (2017). Yardangs and Dunes of Iran's Lut Desert Reveal Winds on Planetary Surfaces. Lunar and Planetary Science XLVIII.

Rashki, A., Kaskaoutis, D. G., Rautenbach, C. J. d. W., Eriksson, P. G., Qiang, M., and Gupta, P. (2012). Dust storms and their horizontal dust loading in the Sistan region, Iran. Aeolian Research, 5, 51–62. https://doi.org/10.1016/j.aeolia.2011.12.001

Sharifikia, M. (2013). Environmental challenges and drought hazard assessment of Hamoun Desert Lake in Sistan region, Iran, based on the time series of satellite imagery. Natural Hazards, 65(1), 201–217. https://doi.org/10.1007/s11069-012-0353-8

Steffen, W., Rockström, J., Richardson, K., Lenton, T. M., Folke, C., Liverman, D., Schellnhuber, H. J. (2018). Trajectories of the Earth System in the Anthropocene. Proceedings of the National Academy of Sciences, 115(33), 8252–8259. https://doi.org/10.1073/pnas.1810141115

Tadhg, B. (2008). Dust Storms in the Lake Eyre Basin: Evaluation of their Sources, their Frequency and their Content. A thesis in School of Geography an Environmental Science Monash University, pp.478.

Visser, S. M., Sterk, G., Judith, and Snepvangers, J.J.J.C. (2004). Spatial variation in wind-blown sediment transport in geomorphic units in northern Burkina Faso using geostatistical mapping. Geoderma, 120(1–2), 95–107. https://doi.org/10.1016/j.geoderma.2003.09.003

Appendix A:

Summary of wind records for meteorological stations in this study

No.	Provinces	Weather stations	Period	Calm %	Mean wind Speed (m/s)	Rain (mm)	PET (mm/year)
1	Alborz	Karaj	1985-2016	32	2.4	248	896
2		Hashtgerd	2006-2017	19	2.7	338	854
3	Bushehr	Bandar dayer	1995-2013	39	3.4	226	2499
4		Bandar-e-Deylam	2001-2013	20	3.2	329	1975
5		Borazjan	2008-2014	30	2.0	200	4924
6		Bushehr	1995-2013	36	2.9	267	1761
7		Kangan JAM	1995-2013	31	2.9	188	1631
8	Esfahan	Kabootar Abad	1992-2010	44	1.5	113	843
9		Anarak	1985-1987	11	3.6	82	1657
10		Aran Bidgol	2007-2015	75	0.9	128	1212
11		Ardestan	1992-2010	18	3.8	127	1131
12		Chopanan	2006-2010	21	2.5	80	1685
13		Daran	1992-2010	63	1.8	330	662
14		Esfahan	1992-2010	57	1.6	125	872
15		Fereydoon	2003-2010	36	2.0	543	689
16		Golpaygan	1992-2010	33	2.6	274	792
17		Jangalbani-badroud	1958-2015	20	4.1	195	1491
18		Jangalbani Zavareh	1985- 2012	14	2.4	127	1131
19		Siman Sepahan	1985-1987	1	3.6	125	872
20		Kashan	1971-2010	67	0.6	136	1173
21		Khansar	2005-2011	18	3.2	390	761
22		Biyabanak and Khor	1992-2010	62	1.3	84	1389
23		Meimeh	2000-2010	14	4.0	164	710
24		MORCHEHKHORT	2007-2010	17	3.4	125	1035
25		Naien	1992-2010	17	3.6	98	921
26		Najaf Abad	2003-2010	13	3.2	151	802
27		Natanz	1992-2010	28	2.2	195	1491
28		Semirom	1992-2010	30	2.8	488	761
29		Shahreza	1993-2011	42	2.6	142	795
30		Esfahan E	1976-2011	31	2.9	106	839
31		Varzaneh	2007-2011	17	3.4	85	1164
32		Zarin Shahr	2005-2010	30	2.1	148	1068
33	Fars	Abadeh	1977-2014	47	2.4	115	771
34		Bavanat	2004-2013	19	3.6	206	853
35		Darz va Sayeban	1997-2010	49	1.4	198	2434
36		Lamerd	2010-2014	21	2.7	217	2104
37		lar	1995-2013	47	1.8	208	2237
38		Neyriz	2006-2013	30	2.5	184	1300
39		Safashahr	2006-2013	18	3.5	194	804
40		Zarindasht	2008-2013	30	2.0	217	2418
41	Khorasan North	Bojnurd	1995-2013	57	2.4	268	755
42		Esfrayen	2006-2013	31	2.6	192	961
43		Jajarm	2006-2013	13	5.1	125	983
44		Maneh-va-Samanqan	2006-2013	28	2.4	284	946

Summary of wind records for meteorological stations in this study

No.	Provinces	Weather stations	Period	Calm %	Mean wind Speed (m/s)	Rain (mm)	PET (mm/year)
45	Kerman	Anar	1995-2013	35	2.7	67	1313
46		Azizabad-bam	1996-2010	67	1.3	55	1574
47		Baft	1995-2013	40	3.0	221	796
48		Bam	1985-2013	36	3.1	55	1574
49		Daheseyf Ziyaratgah	1997-2011	61	2.1	31	3805
50		Jiroft	2008-2014	45	1.8	168	2868
51		Kahnouj	1990-2013	39	3.5	168	2836
52		Kerman	1990-2013	40	2.8	148	841
53		Kuhbanan	2004-2009	9	4.8	148	1192
54		Lalehzar	2003-2013	5	4.4	210	676
55		Rafsanjan	2012-2014	41	2.6	90	1016
56		Rahmatabad Rigan	1995-1996	10	5.3	58	1574
57		Ravar	2004-2011	33	2.1	42	1192
58		Rayen Bam	1997-2010	2	4.1	55	1574
59		Shahdad	2003-2013	17	3.3	31	3805
60		Shahr Babak	1995-2013	43	2.8	147	827
61		Sirjan	1995-2013	52	2.6	133	927
62		Zarand	1995-2013	18	3.3	140	1192
63	Khorasan Razavi	Arask	2001-2011	35	2.1	82	1534
64		Asadabad Torbat	1995-2011	13	3.9	206	805
65		Bejestan	1995-2010	6	4.8	120	981
66		Booshroyeh	1995-2013	36	1.5	97	1204
67		Dargaz	2008-2013	21	2.4	229	1107
68		Fariman	2006-2013	7	4.7	248	706
69		Golmakan	1995-2013	18	3.3	208	759
70		Gonabad	1990-2013	48	2.0	137	981
71		Kalateh Mazinan	1996-2010	42	3.0	187	1012
76		Kashmar	1997-2013	55	1.5	186	1013
77		Khaf	2006-2013	8	5.4	120	1232
78		Mashhad	1995-2013	26	2.7	252	800
79		Neyshabor	1995-2013	62	1.5	238	797
80		Sabzevar	1995-2013	25	3.4	187	1012
81		Sarakhs	1992-2013	40	2.2	185	1029
82		Taybad	2001-2004	49	1.2	173	870
83		Torbat Hidareyh	1995-2013	44	2.4	268	805
84		Torbat-jam	1995-2013	27	4.1	173	870
85	Khuzestan	Dezful Airport	1995-2013	65	1.4	393	1992
86		Abadan	1995-2013	33	3.1	154	2389
87		Ahvaz	1995-2013	31	2.5	220	2965
88		Bandar-e- Mahshahr	1995-2013	27	3.7	197	2346
89		Behbahan	1995-2013	57	1.6	317	2158
90		Bostan	1995-2013	15	3.6	198	1908
91		Gotvand	2009-2013	31	1.7	353	3614
92		Hendijan	2000-2013	7	4.5	205	2380
93		Hoseyniyeh	2005-2013	4	4.5	376	4248
94		Izeh	1995-2013	30	2.1	634	1294
95		Masjedsoleyman	1995-2013	59	1.7	440	2555
96		Omidiyeh (Aghajari)	1995-2013	44	3.0	259	2572
97		Safiabad Dezful	1995-2013	57	1.4	328	1876
98		Shadegan	2008-2013	10	3.9	141	3887
99		shush	2009-2013	28	1.9	213	3969
100		Shushtar	1995-2013	29	2.5	298	3048

Summary of wind records for meteorological stations in this study

No.	provinces	Weather stations	Period	Calm %	Mean wind Speed (m/s)	Rain (mm)	PET (mm/year)
101	Qom	Kahak	2004-2013	4	4.5	153	1066
102		Kooshk Nosrat	2011-2012	18	4.7	92	1520
103		Qom	1997-2013	28	2.9	148	784
104	Semnan	Ahmadabad	1997-2015	45	2.7	128	926
105		Amirieh	2005-2015	14	1.8	116	970
106		Baghestan	1994-2015	39	2.3	106	1017
107		Biarjmand	1992-2010	34	2.8	128	926
108		Damghan	2002-2010	30	3.8	116	970
109		Dastgerd Shahrood	2001-2005	29	4.0	128	926
110		Foromad	1991-2013	23	3.6	118	789
111		Garmsar	1986-2010	48	2.2	121	1142
112		Hosseinan	1986-2015	14	4.3	93	1380
113		Kavire Karvansarayeh	1986-1997	0	4.5	98	1354
114		kouhan	1986-2015	8	3.8	106	1017
115		Meyameh	1986-1997	0	3.2	106	1017
116		Semnan	1992-2010	45	2.0	141	1091
126		Shahrmirzad	1965-2010	53	1.5	230	785
127		Shahroud	1951-2010	30	2.0	153	824
128		Torood	1990-2006	1	4.9	230	785
130	Sistan and Baluchistan	Bahookalat	1986-1996	3	3.7	111	2243
131		Bampoor	1998-2011	1	3.3	110	2806
132		Chabahar	1990-2013	19	3.2	118	1802
133		Goharkouh	2002-2011	0	7.5	151	1120
134		Iranshahr	1990-2013	31	2.8	112	2806
135		Jonabad	2007-2011	0	3.3	151	1120
136		Karvandar	1996-2003	0	4.8	151	1120
137		Khash	1990-2013	34	2.7	151	1120
138		Konarak	1990-2013	31	3.2	97	2005
139		Mirjaveh	2006-2013	8	3.5	96	2925
140		Mohammadabad Koorin	1995-1999	3	4.4	89	985
141		Nikshahr	2006-2013	18	2.8	219	2970
142		Nosratabad	1995-2011	0	5.9	103	1234
143		Rask	2006-2013	17	2.2	131	4662
144		Saravan	1990-2013	34	2.9	107	1359
145		Sarbaz	1995-2011	1	3.6	174	1120
146		Zabol	1995-2013	19	6.0	58	1556
147		Zahak	1995-2013	17	5.0	53	1608
148		Zahedan	1997-2013	32	3.0	89	985
149	South Khorasan	Asadabad Birjand	1995-2010	3	4.5	169	892
150		Birjand	1990-2013	41	2.5	169	892
151		Fathabad Ferdous	1998-2011	42	2.2	147	966
152		Khusf	1995-2001	0	4.6	103	1197
153		Nehbandan	1999-2013	0	2.6	131	1230
154		Qaien	1990-2013	39	2.2	164	784
155		Sedeh Birjand	1995-2010	0	4.4	164	784
156		Zohan	1995-2005	1	6.6	170	762
157	Tehran	Abali	1997-2013	36	2.5	532	587
158		Chitgar	1997-2013	31	1.8	270	990
159		Damavand	2008-2013	25	2.1	385	783
160		Dowshan Tappeh	1997-2013	49	1.7	265	1046
161		Firuzkuh	1997-2013	30	2.6	288	607
162		Shahriyar	2008-2013	15	3.6	173	1065
163		Tehran (Airport)	1997-2013	30	2.8	233	999
164		Tehran (Shemiran)	1997-2013	70	1.0	415	886
165		Varamin	2008-2013	28	2.5	118	1368

Summary of wind records for meteorological stations in this study

No.	provinces	Weather stations	Period	Calm %	Mean wind Speed (m/s)	Rain (mm)	PET mm/year)
166	Yazd	Abarkuh	2000-2013	24	2.9	60	1225
167		Ardekan	2000-2011	72	1.1	58	1276
168		Bafg	1997-2013	33	2.7	42	1357
169		Bahadoran	1998-2010	14	2.8	61	1518
170		Chadormalu	1995-2011	16	2.3	111	1722
171		Deyhook	2010-2011	25	5.1	102	1543
172		Kavir Sieyakuh	2005-2010	30	2.3	58	1297
173		Madan parvadeh	2003-2011	31	2.7	82	1534
174		Mehriz	2003-2013	16	2.9	58	1287
175		Meybod	2002-2013	9	3.8	59	1225
176		Nadoshan	1998-2011	13	3.5	91	1463
177		Robat Posht Badam	1992-2010	15	3.1	110	1104
178		Sabzdasht	2003-2011	70	1.4	42	1347
179		Tabas	1995-2013	55	1.6	82	1534
180		Yazd	1995-2013	22	2.7	46	1284
181	Hormozgan	Bandar Langhe	1995-2013	14	3.4	137	2171
182		Bandar Abas	1995-2013	16	3.2	176	2310
183		Hajiabad	1998-2013	35	2.5	179	1617
184		Jask	1990-2013	10	4.4	139	2002
185		Minab	1995-2013	51	1.4	197	2491
186		Rudan	2003-2013	23	3.0	223	4734
187		Abkhan Mousian	2008-2014	48	2.7	180	2807
188		Darreh Shahr	2002-2016	37	2.0	435	1483
190		Dehloran	1990-2016	33	2.5	290	2807
191	Ilam	Eyvan	1999-2016	18	3.6	671	934
192		Ilam	1999-2016	32	2.5	578	939
193		Mehran	2004-2016	25	3.8	205	2171
194		Pahleh Zarinabad	2002-2015	34	1.6	354	713
195		Mehran	2004-2016	25	3.8	205	2171